DISCERNING THE ROLE OF DENITRIFICATION, ANAMMOX, AND N_2O PRODUCTION IN AQUATIC SYSTEMS

By

Kateri Rose Salk-Gundersen

A DISSERTATION

Submitted to
Michigan State University
in partial fulfillment of the requirements
for the degree of

Integrative Biology—Doctor of Philosophy

2017

ABSTRACT

DISCERNING THE ROLE OF DENITRIFICATION, ANAMMOX, AND N_2O PRODUCTION IN AQUATIC SYSTEMS

By

Kateri Rose Salk-Gundersen

This dissertation investigates (1) the magnitude and relative importance of denitrification and anammox in aquatic nitrogen (N) loss, (2) microbial pathways of nitrous oxide (N_2O) production, (3) impact of ecosystem restoration on N loss and export, and (4) linkages of N loss with harmful algal blooms (HABs). Study ecosystems included a mesotrophic lake, a wetland undergoing restoration, an embayment of Lake Erie, and a coastal seagrass bed. A variety of stable isotopic techniques were employed to achieve these research objectives.

Chapter one focuses on Muskegon Lake, a Great Lakes Area of Concern that is targeted for water quality improvements. This system experiences seasonal hypolimnetic hypoxia that is driven by water column stratification and respiration enhanced by high rates of epilimnetic primary production. Hypoxic conditions were associated with production of N_2O, which was produced predominantly by nitrification as evidenced by site preference, the difference in $\delta^{15}N$ between the central and outer N atoms in N_2O. Upon seasonal water column mixing, atmospheric N_2O emissions from Muskegon Lake were among the highest reported in estuarine and lacustrine environments, suggesting that lakes are an underappreciated source of N_2O.

Chapter two evaluates the role of restoration activities on N loss in a floodplain wetland upstream of Muskegon Lake. Current restoration efforts of this former agricultural field include dredging of organic-rich sediment and hydrologic reconnection to adjacent Bear Creek. ^{15}N tracer incubations and modeling via the isotope pairing technique (IPT) indicate that restoration activities will likely result in a twofold reduction in denitrification rate in wetland sediments,

which are driven largely by a decrease in coupled nitrification-denitrification. Despite a decrease in the N loss capacity of the wetland sediments, hydrologic reconnection has the capacity to decrease the downstream N load by as much as 10 %. However, a reduction in N availability under restoration conditions resulted in a threefold increase in N_2O:N_2 yield, potentially increasing the N_2O footprint of this Great Lakes Area of Concern following restoration.

Chapter three highlights the development and empirical testing of a new revision to the IPT that accounts for the activity of dissimilatory NO_3^- reduction to NH_4^+ (DNRA) as well as denitrification and anammox. This work, conducted in eastern Australia, provides the first complete accounting of NO_3^- reduction in a seagrass environment. Without employing the revised IPT, denitrification in this system would have been overestimated by as much as 600 %. DNRA outcompeted denitrification for NO_3^-, indicating that this high C:N system functions to recycle and retain N rather than facilitate its loss. Furthermore, the suppression of denitrification allowed anammox to dominate N loss, an unexpected result in comparison to other coastal systems and suggests anammox may be important in other seagrass systems.

Chapter four evaluates the drivers of dramatic shifts in nutrient abundance and N cycling in Sandusky Bay, Lake Erie, and the impact of these transitions on HAB formation. Isotope tracer assays quantified rates of N loss and N fixation. Denitrification and anammox were found to drive large swings in N:phosphorus ratios from > 10,000 to < 16, the threshold for N limitation. N limitation stimulated N fixation, which indirectly supported the development of a HAB in the late summer. Denitrification and nitrification contributed equally to N_2O production, and emissions of N_2O were highest when N supply was greatest. Climate change is expected to increase the frequency of episodic rain events, which will likely (1) enhance N_2O emissions and nitrate export from Sandusky Bay and (2) stimulate offshore HABs in Lake Erie.

This dissertation is dedicated to Knute,
who has supported my work in countless ways.

ACKNOWLEDGEMENTS

The completion of this dissertation was made possible by the efforts of many. In particular, I wish to extend my gratitude to the following people:

My doctoral advisor, Nathaniel Ostrom, whose expertise and guidance allowed me to progress immensely as a scientist. Your criticism, encouragement, and trust have given me countless opportunities to develop my conceptual expertise, analytical skills, writing, grantsmanship, and network of scientific peers. Thank you for helping me join the small but mighty band of isotope biogeochemists.

My graduate committee, Peggy Ostrom, Al Steinman, Bopi Biddanda, and Steve Hamilton. Each of you have brought unique expertise and insight into my graduate work. The products of this dissertation (including myself) are richer as a result of your efforts. Thank you for your edits, questions, and support.

Scientists who have welcomed me into their research groups, showing me the value of strong collaboration. Thank you to Bopi Biddanda, Al Steinman, Dirk Erler, Brad Eyre, George Bullerjahn, Mike McKay, Mark McCarthy, and Silvia Newell.

My various coauthors and helpers in the field and laboratory: Anthony Weinke, Leon Gereaux, Adam McMillan, Alex Dutcher, James Smit, Maggie Oudsema, Mary Ogdahl, Natasha Carlson-Perret, Jamie David, Iain Alexander, Matheus Carvalho, Taylor Tuttle, and Emily Davenport. Without your assistance, this work would not have been pushed forward with such force as it was. Most of all, thank you to Hasand Gandhi, whose knowledge of instrumentation and patience in training an eager student know no limits.

My family and friends, who have enthusiastically supported my work but have also

shown me the value of a good laugh, a good adventure, and a good beer. Thank you to my parents, who have encouraged my fascination for lakes and academics from the very beginning. Thank you to my companions at Michigan State, who will no doubt become lifelong friends. Lastly, thank you to my husband, Knute Gundersen, who continuously motivates me to do my best work. Thank you for your unconditional support and celebration of my accomplishments.

This dissertation was supported by the NSF Graduate Research Fellowship [No. DGE1424871], EPA Great Lakes Restoration Initiative [No. GL00E00460-1], NSF/AAS East Asia and Pacific Summer Institutes [No. IIA-1414842], ARC Grants [DP160100248, LP110200975, and LP150100519], Michigan State University (MSU) Water Research Initiation Grant, MSU College of Natural Science Doctoral Recruiting Fellowship, MSU Department of Integrative Biology John R. Shaver Research Fellowship, MSU Rose Graduate Fellowship in Water Research, MSU College of Natural Science Marvin Hensley Endowed Fellowship, and an Annis Water Resources Institute research grant. Any opinions, findings, and conclusions or recommendations expressed in this material are those of the author and do not necessarily reflect the views of the Environmental Protection Agency, the National Science Foundation, or the Australian Research Council.

TABLE OF CONTENTS

LIST OF TABLES

LIST OF FIGURES

CHAPTER 1

ECOSYSTEM METABOLISM AND GREENHOUSE GAS PRODUCTION IN A MESOTROPHIC NORTHERN TEMPERATE LAKE EXPERIENCING SEASONAL HYPOXIA

ABSTRACT

Many lacustrine systems, despite management efforts to control eutrophication, are hypoxic during stratified periods. Hypoxia is a major concern, not only for its impact on aquatic life but also for its potential to stimulate production of the greenhouse gases, methane (CH_4) and nitrous oxide (N_2O). We investigated the drivers of hypoxia in Muskegon Lake, a temperate dimictic freshwater estuary that experiences frequent hypolimnetic mixing due to atmospheric forces, riverine inputs, and intrusion of oxic water from coastal upwelling in Lake Michigan. Primary production (GPP) and respiration (R) rates obtained from a $\delta^{18}O$ mass balance model were similar to other mesotrophic environments (0.56-26.31 and 0.57-13.15 mmol O_2 m^{-3} d^{-1}, respectively), although high P/R (≥ 2 in mid-summer) indicated there is sufficient autochthonous production to support hypoxia development and persistence. The isotopic enrichment factor for respiration (ε_{obs}) varied markedly and was least negative in August of both sampling years, consistent with high R rates. Hypoxic conditions were associated with accumulation of N_2O but not CH_4, and emissions of N_2O are among the highest reported from lakes. The average N_2O site preference (SP) value of 25.4‰ indicates that the majority of N_2O was produced by nitrification via hydroxylamine oxidation, despite the presence of resilient hypoxia. While it has been hypothesized that denitrification acts as a sink for N_2O in hypoxic lakes, it is clear that Muskegon Lake functions as a strong source of N_2O via nitrification. Further considerations of lakes as global sources of N_2O thus warrant a closer evaluation of nitrification-fueled N_2O production.

INTRODUCTION

Hypoxia is a major water quality concern for inland waters and is often accompanied by nuisance algal blooms, declines in fisheries, and decreased recreational value (Diaz and Rosenberg 2008). The development of hypoxia is primarily a product of several physical and biological factors in lakes and coastal oceans: (1) a stratified water column, (2) basin shape, and (3) respiration (R) in excess of O_2 supply. Stratification occurs as surface waters become warmer than bottom waters, and a thermocline isolates the cooler lower water column (hypolimnion) from wind-driven mixing with the atmosphere. When stratification minimizes the influx of O_2 to the hypolimnion, sinking primary production or sediment organic matter drives respiratory O_2 demand. This leads to a depletion of O_2 to hypoxic levels (<63 μM) (CENR 2000). Nutrient-rich agricultural runoff stimulates primary production (GPP) and subsequent R in lakes and coastal environments, which has led to an increase in the extent, intensity, and duration of hypoxia in aquatic systems worldwide (Livingstone and Imboden 1996; Jankowski et al. 2006; Diaz and Rosenberg 2008; Rabalais et al. 2010; Friedrich et al. 2014). Lake Erie and the Gulf of Mexico are examples of two systems in which hypoxia is enhanced when the water column is stratified in the shallow portions of their basins and GPP is high (Rabalais et al. 2010; Scavia et al. 2014). Ecosystem metabolism, often characterized by the ratio of GPP to R (P/R), can thus be an important indicator of the propensity of a system to develop hypoxia (Hanson et al. 2003; Williamson et al. 2008). Systems with high P/R generally display a high degree of eutrophy (del Giorgio and Peters 1994), and given requisite physical conditions, are prone to hypoxia.

Changes in land use and nonpoint source pollution have resulted in increases in the incidence of hypoxia in freshwaters, raising concerns about the production of greenhouse gases, particularly CH_4 and N_2O (Kaushal et al. 2014). Because both CH_4 and N_2O have anaerobic

production pathways, there is potential for these gases to accumulate in the hypoxic or anoxic hypolimnia of stratified lakes and be emitted rapidly during storm-driven or seasonal periods of mixing (Michmerhuizen et al. 1996; Riera et al. 1999; Bastviken et al. 2004). CH_4 and N_2O have global warming potentials that are 25 and 298 times higher than CO_2 over a period of 100 years, respectively (IPCC 2007). Thus, small increases in the atmospheric emissions of one or both of these gases could have a dramatic impact on the greenhouse gas budget from lakes. Despite this possibility, CH_4 and N_2O emissions from lakes are markedly understudied relative to CO_2 (Seitzinger et al. 2006; IPCC 2013). Measurements of the rates of atmospheric N_2O emissions from lakes are particularly sparse, with fewer than ten published studies (Lemon and Lemon 1981; Huttunen et al. 2003; Wang et al. 2006; Whitfield et al. 2011; Miettinen et al. 2015; Yang et al. 2015). However, N_2O emissions from lakes have the potential to rival those from reservoirs, rivers, streams, and wetlands (Whitfield et al. 2011; Morse et al. 2012; Audet et al. 2014; Beaulieu et al. 2014), which merits a closer examination of the role of lakes in the global N_2O budget.

Determining the N_2O budget from lakes depends on an understanding of the microbial pathway by which it is produced. N_2O is produced via three microbial processes that occur under a range of redox conditions: denitrification, nitrifier-denitrification, and hydroxylamine oxidation (Wrage et al. 2001). Denitrification is generally restricted to very low O_2 levels, and as a heterotrophic process, requires a carbon supply (Knowles 1982). The microbial denitrification pathway involves a stepwise reduction of nitrate (NO_3^-) to N_2 gas, in which nitrite (NO_2^-), nitric oxide (NO) and N_2O are produced as intermediates. It is estimated that 7-16% of nitrogen applied to the terrestrial biosphere is denitrified in lakes (Seitzinger et al. 2006), of which a small yet variable portion (typically 0.1-6.0%) is not completely reduced to N_2 and released as N_2O

(Seitzinger and Kroeze 1998). Nitrifiers reduce NO_2^- by the same pathway as denitrifiers (nitrifier-denitrification), producing N_2O as an intermediate product (Poth and Focht 1985; Wrage et al. 2001). In the third pathway, nitrifiers produce N_2O as a product of the decomposition of hydroxylamine (NH_2OH; Wrage et al. 2001). This process is autotrophic and, in contrast to denitrification, can occur in oxic environments. In pure cultures of nitrifiers, the production of N_2O is maximized as O_2 declines, although production ceases under anoxic conditions (Goreau et al. 1980; Frame and Casciotti 2010). Therefore, hypoxia provides the ideal conditions for maximal N_2O production, although the precise microbial production mechanism involved is often uncertain.

Stable isotope analyses of N_2O are used to distinguish N_2O production mechanisms (Ostrom and Ostrom 2011). The relative abundance of a stable isotope within a particular material or reservoir is reported in standard delta notation:

$$\delta = \frac{R_{sam} - R_{std}}{R_{std}} \times 1000 \quad (1)$$

where R_{sam} is the isotope ratio of the sample, R_{std} is the isotope ratio of the standard, and δ is reported as per mil (‰). Because N_2O is a linear asymmetric molecule, the isotopic composition of the N atom in the central position (α) and the N atom in the outer position (β) may be distinct. The difference between $\delta^{15}N^{\alpha}$ and $\delta^{15}N^{\beta}$ in N_2O is referred to as site preference (SP). In contrast to bulk $\delta^{15}N$ and $\delta^{18}O$ values, SP is a conservative tracer of microbial N_2O production mechanisms that is independent of the substrate isotopic composition (Sutka et al. 2003; Toyoda et al. 2005; Sutka et al. 2006; Sutka et al. 2008). In general, denitrification and nitrifier-denitrification produce N_2O with constant SP values of -10 to 0 ‰, whereas hydroxylamine oxidation produces N_2O with a SP value of 33 to 37 ‰ (Toyoda et al. 2005; Sutka et al. 2006; Frame and Casciotti 2010; Ostrom and Ostrom, 2011). N_2O derived from denitrification and

nitrifier-denitrification is indistinguishable on the basis of SP, likely because the enzymes catalyzing these processes are identical (Stein 2011). Therefore, production of N_2O from denitrification and nitrifier-denitrification will henceforth be referred to collectively as denitrification. Fractionation in SP has been demonstrated with a purified fungal nitric oxide reductase enzyme but not within microbial culture which likely reflects maintenance of NO in cells at low concentration and steady state (Yang et al. 2014). Therefore, SP is expected to hold as a conservative, non-fractionating measure of N_2O production mechanism under *in situ* environmental conditions. SP analysis has been demonstrated as an effective approach for distinguishing microbial N_2O production from denitrification vs. hydroxylamine oxidation in a variety of terrestrial and aquatic environments (e.g., Westley et al. 2006; Yamagishi et al. 2007; Opdyke et al. 2009; Sasaki et al. 2011).

In this study, we examined the relationships among ecosystem metabolism, hypoxia, and greenhouse gas production and atmospheric emissions in Muskegon Lake, MI. The relationship between P/R, the oxygen isotopic enrichment factor for respiration (ε_{obs}), and the development of hypoxia was also determined. In addition, we evaluated the influence of hypoxia and water column mixing on the production and atmospheric fluxes of CH_4 and N_2O. Further, we determined the microbial pathway of N_2O production in Muskegon Lake through SP analysis and related biogeochemical indicators.

METHODS

Study site

Muskegon Lake is a 17 km^2 drowned river-mouth lake in western Michigan with a mean depth of 7 m and a maximum depth of 23 m (Freedman et al. 1979; Carter et al. 2006). The lake

drains the Muskegon River Watershed, a 7,032 km^2 basin comprised mainly of forest and agricultural land (Tang et al. 2005), and discharges directly into Lake Michigan by means of a narrow shipping channel (Figure 1). The hydraulic residence time of Muskegon Lake is highly dependent on the rate of water inflow from the Muskegon River, ranging from 14 to 70 days with a mean of 23 days (Freedman et al. 1979; Carter et al. 2006). Historical nutrient loading led to eutrophication and water quality degradation of Muskegon Lake, and as a consequence it was designated a Great Lakes Area of Concern in 1985 (Steinman et al. 2008; U.S. EPA 2013). There has been subsequent improvement in water quality, but Muskegon Lake remains characterized by relatively high nutrient concentrations, periodic nuisance algal blooms, and summer hypoxia in the hypolimnion (Steinman et al. 2008; Biddanda 2012).

Buoy observatory measurements

Time series data for water temperature (2, 4, 6, 7, 9, and 11 m), dissolved O_2, pH, chlorophyll *a* fluorescence (2, 5, 8, and 11 m), and wind speed (1 m above water) were obtained for the period of May to November in 2012 and 2013 from the Muskegon Lake Observatory (MLO). The MLO buoy was deployed in the central part of the lake (Figure 1) and collected water and meteorological data during the ice-free periods. The water depth at the MLO was approximately 12 m and 11.25 m in 2012 and 2013, respectively, due to differences in lake water level between the two years. Water sensors at the MLO collected data every 15 to 30 min, and meteorological sensors collected data every 5 min. Additional information on the MLO can be found in Biddanda (2012), McNair et al. (2013), and Vail et al. (2015).

Figure 1. Muskegon Lake. Inset shows the location of Muskegon Lake (star) and its watershed (light gray) within the state of Michigan, USA. The white circle in the middle of the lake represents the location of the Muskegon Lake Observatory Buoy (MLO; www.gvsu.edu/buoy/).

Field sampling procedure

Water samples for nutrient, P/R, and greenhouse gas analysis were collected at the MLO (Figure 1) between 9:00 am and 12:00 noon on an approximately monthly basis from May to September in 2012 and 2013. In addition, intense temporal sampling was conducted three times over a four-day period in August 2013. Water samples were taken by Niskin bottle (General

Oceanics, Inc., Miami, FL) at 2, 5, 8, and 11 m (2012) or 10.25 m (2013) depth. For nutrient analysis, water was filtered (0.45 μm) and frozen upon return to the lab. Water for determination of $\delta^{18}O$-O_2 and greenhouse gas analyses was transferred into 250 mL glass serum bottles and sealed without headspace with butyl rubber septa. Biological activity was halted by adding 1 mL of saturated $HgCl_2$ solution to each bottle. Water column profiles of temperature, dissolved O_2, pH, and chlorophyll *a* fluorescence were taken using a YSI 6600 sonde (Yellow Springs Instruments, Inc., Yellow Springs, OH).

Ecosystem metabolism measurements

Respiration rates were determined from lake water collected at 2 m using a Niskin bottle. Water from the Niskin bottle was placed into a 20 L carboy and subsequently dispensed into 300 mL acid-washed BOD bottles that were sealed with glass stoppers without headspace. The BOD bottles were incubated in the dark at *in situ* temperature. Dissolved O_2 concentrations were then measured in triplicate each day for four days from sacrificed bottles. O_2 concentration was measured via Winkler autotitration using a Radiometer Analytical Titralab 650 with platinum combined Ag/AgCl reference electrode (Weinke et al. 2014).

The $\delta^{18}O$ of dissolved O_2 was determined using water from 2, 5, 8, and 11 m into which $HgCl_2$ was added at the time of collection (2012) or from water at 2 m that was preserved with $HgCl_2$ at the same time points as the BOD bottles (2013). Water was transferred from BOD bottles into pre-evacuated 200 mL glass vessels fitted with high vacuum stopcocks according to Emerson et al. (1991) and Roberts et al. (2000). The vessels were stored at room temperature for at least 4 h to allow the water and headspace to come to equilibrium. The headspace was then introduced to an evacuated 3 mL sampling loop and then onto a 5 m packed molecular sieve (5

Å) column (Alltech, Inc., Deerfield, IL) using He carrier gas within a gas chromatograph (HP-5980, Hewlett Packard, Ramsey, MN) interfaced to an Isoprime isotope ratio mass spectrometer (Elementar Americas, Inc., Mount Laurel, NJ) for determination of the $\delta^{18}O$ of O_2. Analytical reproducibility of standards was 0.3 ‰.

The oxygen isotopic enrichment factor for respiration, ε_{obs}, was determined using a Rayleigh model from two sets of data, (1) *in situ* observations of $\delta^{18}O$-O_2 by depth in 2012 and (2) four-day bottle incubations from which $\delta^{18}O$-O_2 was measured in 2013:

$$\varepsilon_{obs} = \frac{\delta_{so} - \delta_s}{ln(O_2Sat)} \quad (2)$$

Where and δ_s is the *in situ* $\delta^{18}O$-O_2 value or the $\delta^{18}O$-O_2 value at a given time point in a bottle incubation, δ_{so} is the initial $\delta^{18}O$-O_2 value, and O_2Sat is the fractional saturation of O_2 (Mariotti et al. 1981; Ostrom et al. 2014). When $ln(O_2Sat)$ is regressed against δ_s, the slope is equivalent to ε_{obs}.

Rates of GPP, R, and P/R ratios in the epilimnion were estimated using a steady-state, mass balance model (hereafter the ^{18}O model; Bocaniov et al. 2012):

$$GPP = \left(\frac{F}{Z_m}\right) \cdot \frac{O_2\left(\alpha_g \cdot {}^{18:16}O - \alpha_r \cdot {}^{18:16}O\right) - O_{2s}(\alpha_g \cdot \alpha_s \cdot {}^{18:16}O_a - \alpha_r \cdot {}^{18:16}O)}{\alpha_p \cdot {}^{18:16}O_w - \alpha_r \cdot {}^{18:16}O} \quad (3)$$

$$R = \left(\frac{F}{Z_m}\right) \cdot \frac{O_2\left(\alpha_g \cdot {}^{18:16}O - \alpha_p \cdot {}^{18:16}O_w\right) - O_{2s}(\alpha_g \cdot \alpha_s \cdot {}^{18:16}O_a - \alpha_p \cdot {}^{18:16}O_w)}{\alpha_p \cdot {}^{18:16}O_w - \alpha_r \cdot {}^{18:16}O} \quad (4)$$

where Z_m is the depth of the mixed layer, O_2 is the measured concentration of dissolved O_2, O_{2s} is the concentration of O_2 at atmospheric saturation, $^{18:16}O$ is the measured oxygen isotope ratio of dissolved O_2, $^{18:16}O_w$ is the measured oxygen isotope ratio of H_2O, and $^{18:16}O_a$ is the isotopic ratio of atmospheric oxygen (23.5 ‰). α_g, α_s, α_p, and α_r are the fractionation factors associated with gas transfer (0.9972), gas solubility in water (Benson and Krause 1984), photosynthetic

reaction rates of ^{18}O-H_2O to ^{16}O-H_2O (1.000), and respiration ($1 + \varepsilon_{obs}/1000$), respectively. $\delta^{18}O$-H_2O was determined by off-axis integrated cavity output spectroscopy using a Los Gatos Research Liquid Water Isotope Analyzer (Lis et al. 2008). Analytical reproducibility of standards was 0.2 ‰. When direct measurements of $\delta^{18}O$-H_2O were not available, mean values from the remainder of the sampling period were used.

The oxygen gas transfer rate (F) was calculated according to Wanninkhof (1992):

$$F = k_w(C_w - C_a) \quad (5)$$

where C_w is the dissolved O_2 concentration at the surface (measured at 2 m depth) and C_a is the calculated dissolved O_2 concentration in equilibrium with the atmosphere (Wanninkhof 1992; Walker et al. 2010). The gas transfer coefficient (k_w, in m s^{-1}) is calculated as:

$$k_w = 0.31U_{10}^2\left(\frac{Sc}{600}\right)^{-1/2} \quad (6)$$

where Sc is the Schmidt number for O_2 determined by the kinematic viscosity of freshwater divided by the diffusion coefficient of O_2 (Wanninkhof 1992) and U_{10} is the wind speed 10 m above the surface determined using the measured wind speed 1 m above the surface and the power law relationship outlined in Walker et al. (2010). Wind speed was measured by the MLO and averaged over the dissolved O_2 residence time in the mixed layer (2-5 d). Because buoy data were not available on 6 May 2013, wind speed data were obtained from instruments at the Muskegon County Airport (8 km from MLO) and adjusted by the roughness lengths of flat land and water (World Meteorological Organization 2008).

Nutrient concentrations and trace gas analysis

Samples collected in 2013 were analyzed for the concentration of nitrate + nitrite (NO_3^-), ammonium (NH_4^+), and soluble reactive phosphorus (SRP). All nutrient analyses were

performed according to Standard Methods (APHA 2005). SRP was analyzed spectrophotometrically using the ascorbic acid method, NO_3^- was determined colorimetrically after cadmium reduction, and NH_4^+ was analyzed using the phenate method. NO_3^- and NH_4^+ were analyzed using a wet chemistry continuous flow analyzer (Skalar Analytical B.V., Breda, the Netherlands).

Water samples for CH_4 and N_2O concentration analysis were introduced by syringe injection at atmospheric pressure into glass serum bottles that had been flushed with He prior to sample introduction. The water sample was equilibrated with the remaining headspace overnight by gentle shaking. The headspace was then analyzed by GC-ECD-FID (Shimadzu Greenhouse Gas Analyzer GC-2014, Shimadzu Scientific Instruments, Columbia, MD) for N_2O and CH_4 concentration. The dissolved concentration was calculated based on the headspace equilibrium concentration (Hamilton and Ostrom 2007). Diffusive atmospheric emissions of CH_4 and N_2O (F) were calculated by equations 5 and 6, substituting the measured concentration, saturation concentration, and Schmidt number of CH_4 and N_2O for those of dissolved O_2.

The isotopic composition of N_2O was analyzed upon introduction of sample water into an enclosed 0.75 L glass vessel that was previously purged of atmospheric air using a gentle flow of He. Dissolved gases were subsequently stripped from the water by sparging the sample with He (Sansone et al. 1997), which carried sample gases into a Trace Gas sample introduction system interfaced to an Isoprime isotope ratio mass spectrometer (Elementar Americas, Inc., Mount Laurel, NJ). Analytical reproducibility for replicate samples was 0.5 ‰ for bulk $\delta^{15}N$ and $\delta^{18}O$, 0.75 ‰ for $\delta^{15}N_\alpha$ $\delta^{15}N_\beta$, and 1.3 ‰ for SP.

The microbial origin of N_2O produced in Muskegon Lake was evaluated by several approaches. First, a Keeling plot was employed to calculate the isotopic composition of

microbially-produced N_2O (end-member) by regressing the isotopic ratios of N_2O vs. the inverse concentration of N_2O in measured samples and the atmospheric end-member (Pataki et al. 2003; Yamagishi et al. 2007). Second, apparent oxygen utilization (AOU; $O_{2saturation} - O_{2measured}$) and ΔN_2O ($N_2O_{measured} - N_2O_{saturation}$) were compared to provide evidence for nitrification-fueled N_2O production (Yoshinari 1976; Nevison et al. 2003; Bange et al. 2010). Third, $\Delta^{18}O$ ($\delta^{18}O\text{-}N_2O$ - $\delta^{18}O\text{-}O_2$) was calculated to evaluate the relative contributions of hydroxylamine oxidation and denitrification (Ostrom et al. 2000).

Statistical analyses

All statistical analyses were conducted using R statistical software (version 3.0.2). Principal component analysis was performed on 2013 data to analyze correlation among temperature, pH, greenhouse gas concentrations, dissolved O_2, nutrient concentrations, and chlorophyll *a* fluorescence (Appendix). Prior to principal component analysis, each variable was standardized to equalize variance across variables. Differences in N_2O isotopic composition between the epilimnion and hypolimnion were evaluated by Welch 2-sample t-tests following tests for distribution normality and equal variance. The relationship between AOU and ΔN_2O was evaluated by linear regression.

RESULTS

Muskegon Lake displays a dimictic stratification pattern, with periods in the spring and fall of homogenous temperature and O_2 concentration throughout the water column (Figure 2). The summer period is characterized by higher surface water temperatures than in the spring and fall and low concentrations of O_2 in the hypolimnion. When the water column is stratified, the

thermocline is located between 6 and 8 m. A weak to strong thermocline was present on all sampling dates except 6 June 2012, 20 September 2012, and 11 June 2013 (Figures 3a, 3e). June sampling dates coincided with wind-driven episodic mixing events, and 20 September 2012 coincided with the fall mixing period. O_2 concentrations in the hypolimnion during stratified periods regularly decreased to hypoxic levels (Figures 2, 3b, 3f).

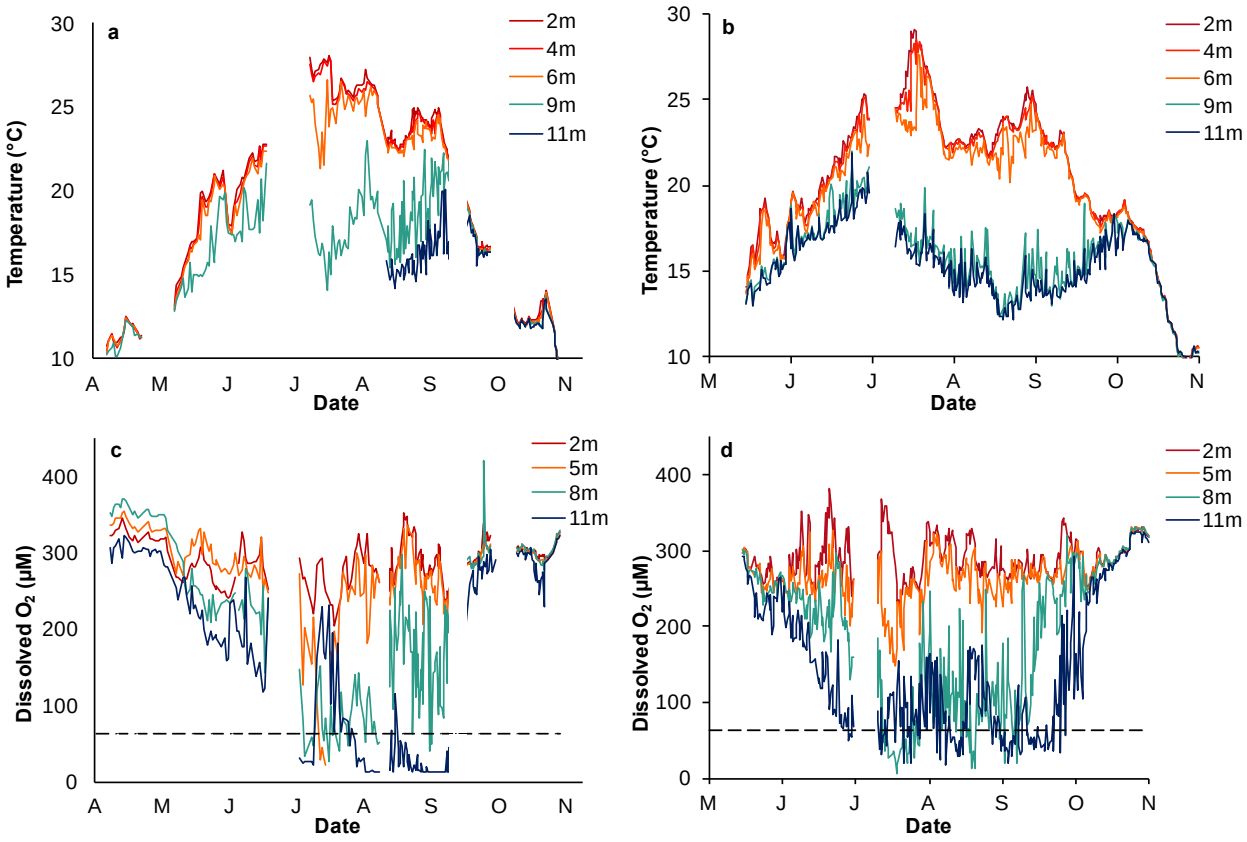

Figure 2. (a-b) Temperature and (c-d) dissolved O_2 concentration from April to November in 2012 (left panel) and 2013 (right panel). Data were collected by the MLO sensors placed at various depths in the water column. Hypoxia (dissolved O_2 <63 µM) is indicated by a dotted line.

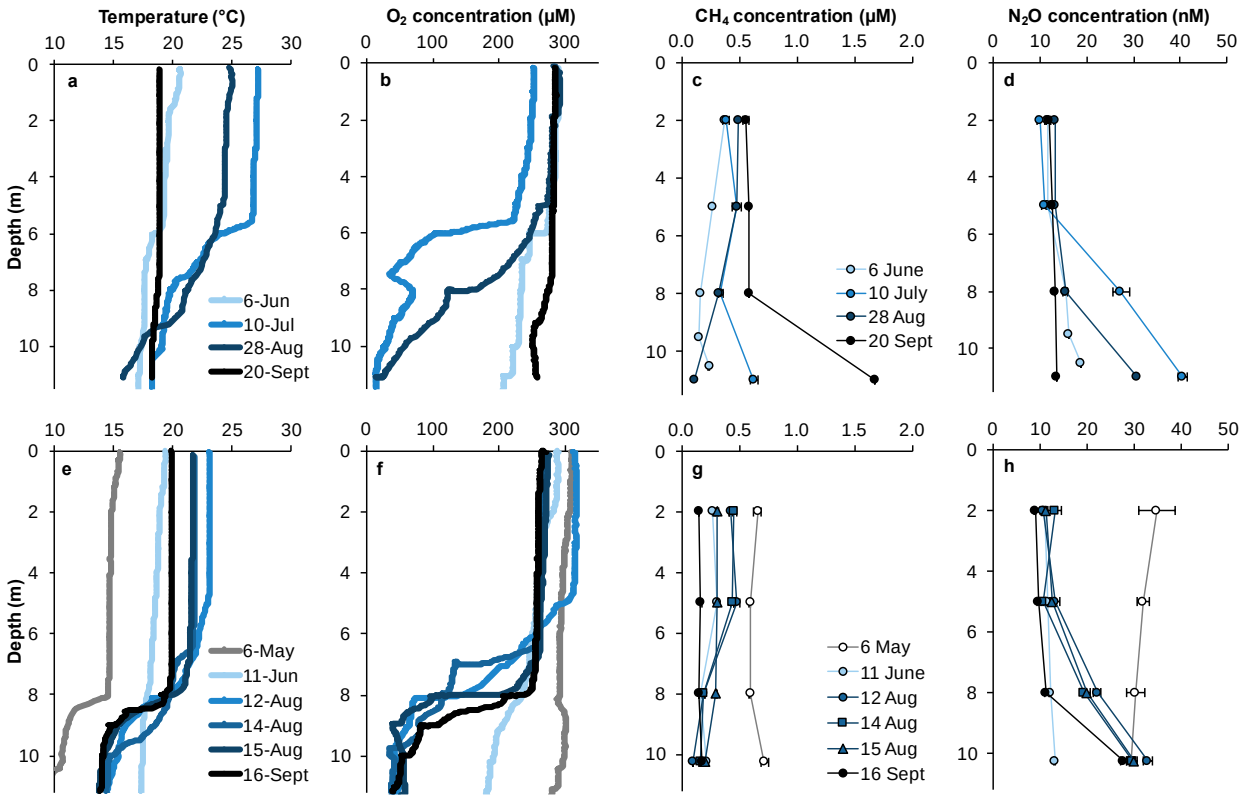

Figure 3. Water column profiles at the MLO in (a-d) 2012 and (e-h) 2013. Temperature and dissolved O_2 concentration were measured continuously throughout the water column on each sampling date. CH_4 and N_2O concentrations were measured at four depths on each sampling date. Error bars represent standard error.

Epilimnetic GPP and R rates obtained by the ^{18}O model ranged from 0.56 - 26.31 mmol O_2 m^{-3} d^{-1} and 0.57 - 13.15 mmol O_2 m^{-3} d^{-1}, respectively (Figure 4). The lowest GPP and R rates occurred during September 2012 and May 2013. The highest GPP rate occurred in August of both years, and the highest R rate occurred in August 2012 and September 2013. P/R ranged from 0.79 - 2.36, with the highest ratios occurring in August in each year and the lowest ratios occurring during May, June, and September (Figure 4).

The isotopic enrichment factor for respiration, ε_{obs}, varied by over 10 ‰ within each sampling season (Table 1). ε_{obs} was most negative in June 2012, May 2013, and September 2013. ε_{obs} was least negative in August of both years. The range in ε_{obs} values was less negative in 2012 when the *in situ* method was used than in 2013 when the bottle incubation was used.

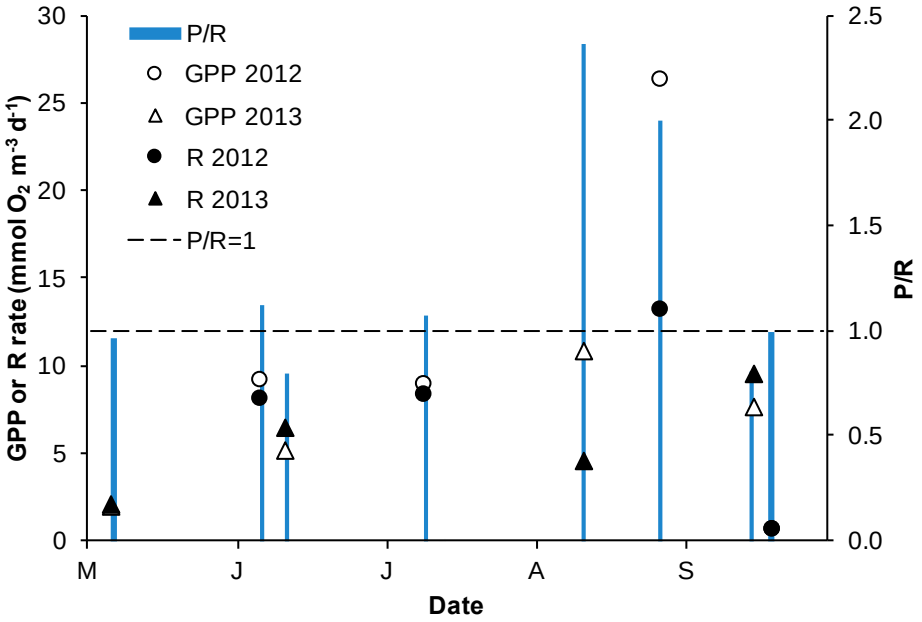

Figure 4. Primary production (GPP), respiration (R), and P/R in Muskegon Lake in 2012 and 2013. P and R rates (open and closed symbols, respectively) were calculated according to Bocaniov et al. (2012) on four occasions each year from May through September. P/R ratios (bars) were calculated by dividing P by R. The horizontal line represents P/R=1.

Table 1. ε_{obs} values in Muskegon Lake measured by the *in situ* (2012) and bottle incubation (2013) methods.

Date	ε_{obs} (‰)	Method
6-Jun-12	-16.1	*In situ*
10-Jul-12	-7.9	*In situ*
28-Aug-12	-2.3	*In situ*
20-Sep-12	-4.1	*In situ*
6-May-13	-21.1	Bottle incubation
12-Aug-13	-11.3	Bottle incubation
16-Sep-13	-23.7	Bottle incubation

NH_4^+, NO_3^-, and SRP concentrations ranged from 2.3 - 44.5 μg L^{-1}, 163.3 - 373.7 μg L^{-1}, and 0.8 - 17.5 μg L^{-1}, respectively (Appendix Figure A1). NH_4^+, NO_3^-, and SRP concentrations were negatively correlated with O_2 concentration and chlorophyll *a* fluorescence (Appendix Figure A2), indicating an accumulation of nutrients in the hypolimnion.

CH_4 and N_2O were supersaturated in the water column at all times (1.1 - 4.8 and 3,700 - 30,000 times atmospheric equilibration concentration, respectively). CH_4 was fairly homogeneous throughout the water column on each sampling date with the exception of a single extremely high concentration at the lowest sampling depth in September 2012 (Figure 3c). Excluding this point, the highest concentrations of CH_4 throughout the water column occurred in May 2013 (Figure 3g). N_2O concentrations were also high throughout the water column in May 2013 (Figure 3h). Hypolimnetic N_2O concentration were negatively associated with O_2 concentration, displaying accumulation in the hypolimnion during hypoxic periods (Figure 3).

CH_4 and N_2O atmospheric emissions by diffusive evasion were low yet variable throughout the majority of sampling dates in both years with the exception of two dates during which emissions were 10 - 100 times higher than other sampling dates (Figure 5a). The first period of high emissions occurred in September 2012 during a period of strong wind, and the second occurred in May 2013 when concentrations of both gases were high throughout the water column. When converted to CO_2 equivalents by multiplying emissions by 298 and 25 for N_2O and CH_4, respectively (IPCC 2007), the radiative forcing of CH_4 emission was 2.1 - 22.9 times that of N_2O (Figure 5b).

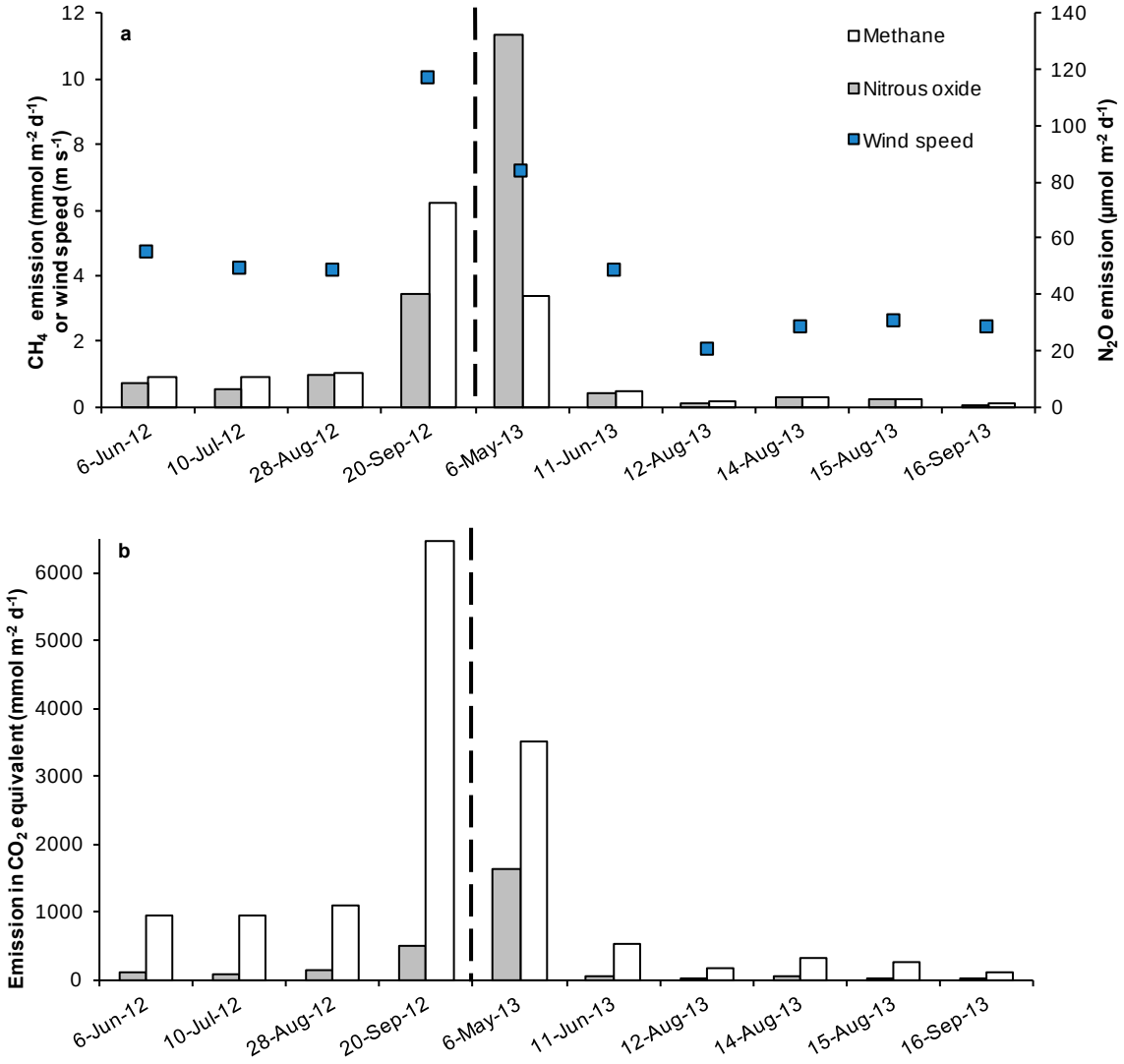

Figure 5. (a) CH_4 and N_2O emissions and wind speeds for each sampling date in 2012 and 2013 and (b) CH_4 and N_2O emissions converted to CO_2 equivalent for each date. Wind speed was measured by the MLO. CH_4 and N_2O emissions were multiplied by their radiative forcing to obtain CO_2 equivalents (IPCC 2007). The vertical dashed line represents the division between the two sampling years.

The isotopic composition of N_2O (mean ± SD) in the epilimnion and mixed water column ($\delta^{15}N$: 4.5 ± 0.7 ‰, $\delta^{18}O$: 50.1 ± 1.9 ‰, SP: 20.0 ± 2.4 ‰) and hypolimnion ($\delta^{15}N$: 0.0 ± 0.3 ‰, $\delta^{18}O$: 54.3 ± 0.9 ‰, SP: 23.1 ± 1.8 ‰) were distinct (Table 2). Relative to the epilimnion and mixed water column, Welch 2 sample t-tests indicated that hypolimnetic $\delta^{15}N$-N_2O values

were significantly lower ($t = 15.02$, $df = 9.9$, $p < 0.0001$), $\delta^{18}O$-N_2O values were significantly higher ($t = -5.5$, $df = 10.4$, $p < 0.0001$), and SP values were significantly higher ($t = -2.59$, $df = 10.3$, $p < 0.01$). The $\delta^{15}N$, $\delta^{18}O$, and SP of microbially-produced N_2O in Muskegon Lake, determined by the y-intercepts of the Keeling plot, were -3.2 ‰, 58.8 ‰, and 25.4 ‰, respectively (Figure 6). AOU was positively correlated with ΔN_2O (Appendix Figure A3; linear regression, $R^2 = 0.58$, $t = 6.97$, $df = 35$, $p < 0.0001$). The mean $\Delta^{18}O$ value for N_2O was 22.1 ± 6.0 ‰.

Table 2. Isotopic composition of N_2O in the troposphere (Yoshida and Toyoda 2000), epilimnion/mixed water column in Muskegon Lake, and hypolimnion of Muskegon Lake.

Date	Depth m	O_2 uM	N_2O nM	$\delta^{18}O$-N_2O ‰	$\delta^{15}N$-N_2O ‰	$\delta^{15}N_\alpha$-N_2O ‰	$\delta^{15}N_\beta$-N_2O ‰	N_2O SP ‰
Tropospheric N_2O				43.7 ± 0.9	7.0 ± 0.6			18.7 ± 2.2
Epilimnion/Mixed water column								
11-Jun-13	2	281	10.96	47.9	5.4	14.4	-3.7	18.1
11-Jun-13	5	259	11.47	48.6	4.8	12.7	-3.1	15.8
11-Jun-13	10.25	188	13.05	51.3	3.5	13.8	-6.7	20.6
12-Aug-13	2	317	10.61	48.4	5.1	14.8	-4.6	19.4
12-Aug-13	5	297	13.09	50.3	4.5	16.4	-7.4	23.8
14-Aug-13	2	264	13.11	53.6	5.2	16.2	-5.9	22.0
14-Aug-13	5	262	10.47	49.7	4.1	14.1	-5.9	20.0
16-Sep-13	8	209	11.42	51.0	3.4	13.5	-6.7	20.2
Mean		**260**	**11.77**	**50.1**	**4.5**	**14.5**	**-5.5**	**20.0**
SD		**43**	**1.14**	**1.9**	**0.7**	**1.3**	**1.5**	**2.4**
Hypolimnion								
12-Aug-13	8	146	22.10	54.9	-0.1	11.0	-12.6	25.0
14-Aug-13	10.25	42	29.80	54.7	-0.4	11.2	-11.9	23.1
15-Aug-13	8	99	20.09	55.2	0.3	12.1	-11.5	23.6
15-Aug-13	10.25	57	29.91	53.4	-0.3	11.5	-12.1	23.6
16-Sep-13	10.25	53	27.66	53.4	0.2	10.2	-9.8	20.0
Mean		**79**	**25.91**	**54.3**	**0.0**	**11.2**	**-11.6**	**23.1**
SD		**43**	**4.54**	**0.9**	**0.3**	**0.7**	**1.0**	**1.8**

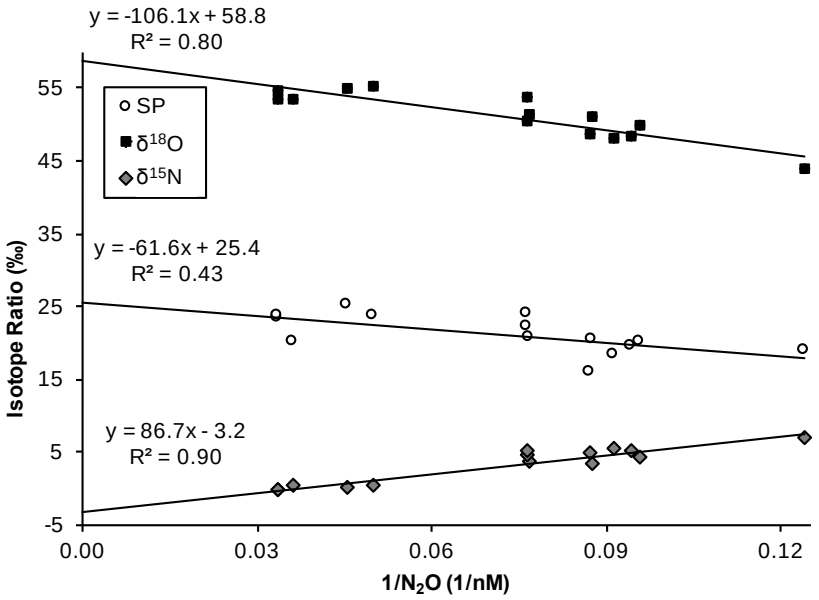

Figure 6. Linear regression of SP, $\delta^{18}O$, and $\delta^{15}N$ of measured N_2O with the inverse concentration of N_2O at each sampling point. *In situ* N_2O concentrations and isotopic values are plotted with the atmospheric N_2O concentration and isotopic composition (rightmost value; Yoshida and Toyoda 2000). The isotopic composition of microbially produced N_2O is represented as the y-intercept value (Yamagishi et al. 2007).

DISCUSSION

Hypoxia development and ecosystem metabolism

Hypoxia is a consequence of extensive nutrient loading, requires the development of stratification, and is predominant in lakes with shallow hypolimnia. In Muskegon Lake, hypoxia was first documented during a period of extensive nutrient loading the late 1970s (Freedman 1979), but hypoxia may be a natural phenomenon in this system. The water column is stratified from June through September or October, but episodic intrusion of oxygenated Lake Michigan water during westerly seiches is demonstrated by increases in hypolimnetic O_2 concentrations by as much as 150 μM on daily to weekly timescales (Figure 2; B. Biddanda, A. Weinke, S. Kendall, and D. Koopmans, personal communication). The observed decline of hypolimnetic temperature from the onset of stratification to early August, an unusual trend in stratified

systems, provides additional evidence of upwelling-induced intrusion of cold Lake Michigan water into Muskegon Lake. Following such hypolimnetic oxygenation events, O_2 concentrations decline rapidly (often within 12 h) to hypoxic conditions (Figure 2). Thus, hypoxia exhibits resilience in Muskegon Lake despite a short hydraulic residence time and evidence of the episodic intrusion of cold, oxic water. The persistence of hypoxia in Muskegon Lake points to a strong driving factor for O_2 consumption in the hypolimnion.

The balance of GPP and R and its seasonal variation provides insight into the development of hypoxia. Although rates of GPP and R are lower than many hypoxic systems (Ostrom et al. 2005; Bocaniov et al. 2012), observations of P/R in Muskegon Lake suggest there is sufficient excess primary production to fuel hypolimnetic respiration and hypoxia development. P/R in the epilimnion was ≥ 1 throughout the majority of the sampling period (Figure 4), demonstrating net autotrophy during the growing season between May and September. Two earlier studies of pelagic metabolism in Muskegon Lake similarly demonstrated a consistent trend of $P/R > 1$ during this time period as well (Weinke et al. 2014; Dila and Biddanda, 2015). In particular, GPP was two-fold higher than R in August of both sampling years (2.00 and 2.36 in 2012 and 2013, respectively). A portion of this surplus production from the epilimnion likely sinks into the hypolimnion and fuels water column or sediment respiration in subsequent days to years. Thus, despite evidence of episodic intrusion of oxic water into the hypolimnion, high P/R values indicate a supply of organic matter that reaches the hypolimnion to fuel strong O_2 consumption and persistent hypoxia.

While water column respiration has been demonstrated as the primary driver of hypoxia in systems such as Lake Erie and the Gulf of Mexico (Conroy et al. 2011; McCarthy et al. 2013; Ostrom et al. 2014), respiration in organic matter-rich sediments can enable hypoxia to establish

at more moderate nutrient loading than would be expected (Turner et al. 2008). A combination of water column and sediment respiration thus likely fuels hypoxia establishment and resilience in Muskegon Lake. While water quality indicators have neared or exceeded remedial action plan targets for reducing eutrophication (Michigan DEQ 2011), summer hypoxic conditions have persisted and will likely persist for many years. Two potential explanations are that (1) remediation of eutrophication in Muskegon Lake is insufficient to reduce hypoxia or (2) hypoxia is a natural feature of this system.

Seasonal variation in ε_{obs}

The magnitude of isotopic fractionation of O_2 during respiration, ε_{obs}, is generally assumed to be a constant, but substantial variation has been observed in this study and other estuarine and coastal marine ecosystems (Quiñones-Rivera et al. 2007; Lehman et al. 2009; Fry and Boyd 2010; Ostrom et al. 2014). Isotopic fractionation during respiration takes place when O_2 is consumed by oxidative respiratory enzymes such as cytochrome oxidase (Feldman et al. 1959). If diffusion limits the supply of O_2 to the respiratory enzyme, then the expression of isotopic fractionation by the enzyme is reduced (Ostrom et al. 2014). For instance, isotopic discrimination approaching 0 ‰ has been observed for respiration in sediments where diffusion is expected to be slow, limiting the movement of O_2 into the cell (Brandes and Devol 1997). In contrast, isotopic discrimination in the water column is generally quite large and assumed to be constant (e.g., -21.2 ‰), because diffusion is not expected to limit the supply of O_2 to the respiratory enzyme (Quiñones-Rivera et al. 2007; Fry and Boyd 2010). In Muskegon Lake, ε_{obs} was evaluated by two approaches: bottle incubation and the *in situ* method. ε_{obs} values obtained by bottle incubation reflect only water column respiration, whereas ε_{obs} values obtained by the *in*

situ method reflect both water column and sediment respiration. Indeed, the ε_{obs} values obtained from the *in situ* method were less negative than those obtained from the bottle incubation method (Table 1), likely reflecting a greater influence of sediment respiration on the ε_{obs} values than in the bottle method. Nonetheless, values for ε_{obs} obtained by the bottle incubation method varied by over 10 ‰, even in the absence of sediment respiration and were least negative during the summer stratified period in Muskegon Lake. This is in agreement with Ostrom et al. (2014), who proposed that ε_{obs} in the water column might in fact approach 0 ‰ when R rates are high and that ε_{obs} may correlate with rates of total respiration beneath the thermocline (water column and sediment respiration). Low ε_{obs} values in August are thus indicative of high R, supported by the highest water column R observed at this time in 2012 (Figure 4).

The observation of marked seasonal variation in ε_{obs} indicates that ε_{obs} in the water column should not be assumed to be constant, as is often the case. For example, if an ε_{obs} value of -21.2 ‰ had been incorporated into the ^{18}O model rather than the measured value of -11.3 ‰ in August 2013, the GPP and R rates for Muskegon Lake would have been overestimated by factors of 2.0 and 3.3, respectively. Further, the subsequent calculation of P/R would have yielded a value of 1.41 rather than 2.36. Accurate assessments of ecosystem metabolism by models that utilize ε_{obs} thus require that variation in ε_{obs} be incorporated into P/R models.

Greenhouse gas concentrations and emissions

On a global basis, freshwater ecosystems support a variety of microbial processes that emit CH_4 and N_2O, important greenhouse gases (IPCC, 2007). Fluxes of greenhouse gases arising from the lower water column and sediments vary as a function of wind mixing and with the development and deterioration of thermal stratification (e.g., Fallon et al. 1980). In many

systems, CH_4 accumulates in anoxic waters beneath the thermocline as a result of anaerobic methanogenesis in both the water column and sediments (Bastviken et al. 2004). This suggests that O_2 and CH_4 should be negatively correlated. Contrary to observations in other temperate dimictic lakes (Fallon et al. 1980; Striegl and Michmerhuizen 1998), profiles of CH_4 in Muskegon Lake revealed no apparent connection between hypoxic conditions and high CH_4 concentrations (Figure 3). With the exception of one date that occurred during a seasonal mixing event near the sediment-water interface (20 September 2012), accumulation of CH_4 within the hypolimnion was not observed in Muskegon Lake. This lack of hypolimnetic accumulation could relate to low CH_4 production, elevated oxidation of CH_4, or evolution of CH_4 to upper water column and atmosphere (Fallon et al. 1980; Striegl and Michmerhuizen 1998; Huttunen et al. 2006).

Despite the lack of hypolimnetic accumulation, diffusive CH_4 emissions from Muskegon Lake were comparable in magnitude and range to those in other lakes of similar size (Bastviken et al. 2004; Ortiz-Llorente and Alvarez-Cobelas, 2012). Owing to strong winds and high epilimnetic concentrations, high emissions of CH_4 were observed in September 2012 and May 2013 (Figures 3c, 3g, 5a). While CH_4 emissions were measured at a single location in Muskegon Lake and thus provide limited ability to extrapolate to the lake as a whole, our results indicate that sampling on a seasonal basis is important to capture variability in CH_4 emissions from lakes.

In contrast to CH_4, hypolimnetic production of N_2O was evident by a negative correlation between N_2O and O_2 (Appendix Figure A2), indicating that periods of hypoxia and water column turnover could be strong regulators of N_2O emissions from this system. Indeed, N_2O was markedly supersaturated in the hypoxic hypolimnion, potentially setting the stage for high emissions to the atmosphere during periods of water column turnover. Diffusive emissions of

N_2O measured at the MLO were lowest during stratified periods and highest during the development or breakdown of stratification. Periods of exceptionally high emissions, up to two orders of magnitude greater than those during the stratified period, are among the highest reported for natural lakes (Lemon and Lemon 1981; Huttunen et al. 2003; Wang et al. 2006; Whitfield et al., 2011; Miettinen et al. 2015; Yang et al. 2015). In fact, only one study has reported higher atmospheric fluxes of N_2O than those observed in Muskegon Lake (Wang et al. 2006). While limited spatial sampling restricts the ability to evaluate the absolute N_2O emissions from Muskegon Lake, our results illustrate wide variation in N_2O fluxes on seasonal time scales. Total annual fluxes may thus be dominated by a few brief periods of high emissions during mixing events following hypolimnetic accumulation (Figure 5a), emphasizing the importance of temporal sampling to capture important periods of N_2O emissions from lakes.

When diffusive emissions of CH_4 and N_2O are converted into CO_2 equivalents (IPCC 2007), the radiative forcing of CH_4 always exceeded that of N_2O in Muskegon Lake (Figure 5b). However, the radiative forcing of N_2O in this study closely approached that of CH_4 on several occasions, indicating that N_2O is an important contributor to total greenhouse gas emissions from this environment. Nonetheless, the number of publications reporting lacustrine CH_4 emissions is over six-fold greater than those reporting N_2O emissions (Whitfield et al. 2011; Ortiz-Llorente and Alvarez-Cobelas 2012), reflecting a need for greater attention to N_2O in studies that measure greenhouse gas emissions.

Determination of microbial origin of N_2O

The marked differences in the $\delta^{15}N$, $\delta^{18}O$, and SP of N_2O between epilimnetic/mixed water column samples and hypolimnetic samples point to distinct sources, namely atmospheric

exchange and microbial N_2O production, respectively (Table 2). It is therefore expected that the isotope composition of N_2O samples collected from Muskegon Lake reflects a mixture between atmospheric and microbially derived N_2O, with microbial production stimulated by hypoxic conditions in the hypolimnion (Goreau et al. 1980; Knowles 1982). Treating the atmospheric isotopic composition (Table 2; Yoshida and Toyoda 2000) and the microbial isotopic N_2O composition (unknown) as isotopic end members in Muskegon Lake, regressing the isotopic composition of measured N_2O by the inverse N_2O concentration yields the isotope composition of microbially-produced N_2O as the y-intercept (Figure 6; Pataki et al. 2003; Yamagishi et al. 2007). While $\delta^{15}N$-N_2O (-3.2 ‰) and $\delta^{18}O$-N_2O (58.8 ‰) values obtained from the mixing model are heavily dependent on the isotopic composition of source material, SP (25.4 ‰) has been shown to be a conservative tracer, enabling the distinction of production from hydroxylamine oxidation (nitrification) from that by denitrification (Ostrom and Ostrom 2011). SP was therefore used as the primary indicator of the microbial N_2O production mechanism in this study. When SP values of 33 ‰ and -10 to 0 ‰ are considered as end-members for N_2O production via hydroxylamine oxidation and denitrification, respectively (Sutka et al. 2006; Frame and Casciotti 2010), the observed SP of 25.4 ‰ indicates that 77-82% of *in situ* production of N_2O is derived from hydroxylamine oxidation.

Because reduction of N_2O by denitrification is likely under low-oxygen conditions and has a marked fractionation effect on its isotopic composition (Popp et al. 2002; Westley et al. 2006; Ostrom et al. 2007; Yamagishi et al. 2007), reduction must be considered as a possible influence on SP in Muskegon Lake that may bias interpretations of microbial sources. If substantial reduction occurs, $\delta^{15}N$ and $\delta^{18}O$ values of N_2O tend to positively correlate because the conversion of N_2O to N_2 preferentially leaves ^{15}N and ^{18}O in the residual N_2O. Similarly,N_2O

reduction results in elevated SP values in the residual N_2O pool because the isotopic discrimination is more pronounced in the α than the β position (Westley et al. 2006). However, a negative correlation was found between $\delta^{15}N\text{-}N_2O$ and $\delta^{18}O\text{-}N_2O$ in Muskegon Lake (Appendix Figure A4a; linear regression, $R^2 = 0.68$, $t = 4.87$, $df = 11$, $p < 0.001$), which suggests that N_2O reduction is not an important process. Moreover, while the $\delta^{18}O\text{-}N_2O$ and SP values were positively correlated, the observed slope of 0.78 differed substantially from the expected slope of 0.45 arising from the fractionation of N_2O during reduction (Appendix Figure A4b; Ostrom et al. 2007; Opdyke et al. 2009). Therefore, we conclude on the basis of stable isotopic indicators that N_2O reduction was not important in removing N_2O from Muskegon Lake, supporting our interpretation of hydroxylamine oxidation as the predominant N_2O production pathway on the basis of SP. Further, while it has been posited that lakes may act as sinks for N_2O under anoxic conditions (Lemon and Lemon 1981; Beaulieu et al. 2014; 2015), N_2O reduction was not demonstrated as an appreciable pathway in Muskegon Lake. A potential explanation for the absence of appreciable N_2O reduction is the evidence of intrusion of oxic water into the hypolimnion; although hypoxia reestablishes quickly in this system, complete anoxia does not develop for long periods, which could inhibit the complete reduction of N_2O by denitrification.

Stoichiometric relationships can also be examined to determine N_2O production pathways. A positive relationship between AOU and ΔN_2O has been attributed to N_2O production by nitrification, as AOU is a tracer of organic matter remineralization that produces the substrates for nitrification (Yoshinari 1976; Nevison et al. 2003; Bange et al. 2010). Indeed, AOU was positively correlated with ΔN_2O, and NO_3^- and NH_4^+ concentrations increased in the hypolimnion throughout the stratified period (Appendix Figure A1, A2), providing a further

indication that nitrification is the primary N_2O production mechanism under hypoxic conditions in Muskegon Lake.

Additional insight into the microbial origin of N_2O can be provided by its $\delta^{18}O$ composition. The oxidation of NH_4^+ to hydroxylamine incorporates an initial oxygen atom from O_2, and further oxidation to NO_3^- derives oxygen from H_2O (Dua et al., 1979; Hollocher et al., 1981; Andersson and Hooper, 1983; Kumar et al., 1983). N_2O production by hydroxylamine oxidation therefore reflects the isotopic composition of O_2, whereas denitrification produces N_2O with a $\delta^{18}O$ value influenced both by O_2 and H_2O. Given that O_2 is generally enriched in ^{18}O by at least 23.5 ‰ relative to H_2O, $\Delta^{18}O$ values are high when hydroxylamine oxidation dominates and are lower when denitrification dominates. For example, Ostrom et al. (2000) observed a shift in $\Delta^{18}O$ values from approximately 23 ‰ at the surface to approximately 13 ‰ at 300 m depth in the Pacific Ocean that was interpreted as a transition in N_2O production from hydroxylamine oxidation to denitrification. Similarly, Muskegon Lake $\Delta^{18}O$ values **(**22.1 ± 6.0 ‰) are consistent with production via hydroxylamine oxidation.

The microbial origin of N_2O from hydroxylamine oxidation was confirmed by multiple lines of isotopic and stoichiometric evidence, demonstrating that Muskegon Lake is as a nitrification-driven source of N_2O to the atmosphere. Previous studies have shown that denitrification can dominate N_2O production in some eutrophic lakes (Lemon and Lemon 1981; Wang et al. 2006) and that increased availability of organic carbon and nutrients has the capacity to stimulate denitrification (Taylor and Townsend 2010). Further, Beaulieu et al. (2014; 2015) have demonstrated that reservoirs have the capacity to alternate between a source and a sink of N_2O depending on the degree of hypolimnetic anoxia and the timing of water column turnover. Our results conversely indicate the capacity for ample supplies of organic matter and nutrients to

fuel N_2O production via denitrification lakes is not ubiquitous. Together, this body of work demonstrates that N_2O dynamics in lakes are more complicated than previously thought, and constraining the role of lakes in the global N_2O budget will entail (1) distinguishing between nitrification and denitrification pathways of N_2O production, (2) evaluating N_2O reduction as a potential sink for N_2O, and (3) investigating water column turnover events as opportunities for brief yet intense periods of N_2O emissions.

Conclusion

Hypoxia persists in Muskegon Lake despite episodic intrusions of oxic water from Lake Michigan into the hypolimnion. We demonstrate net autotrophy in the epilimnion and substantial variation in ε_{obs} in late summer, consistent with delivery of autotrophic material to the hypolimnion followed by high rates of respiration. The presence of hypoxia in Muskegon Lake not only supports N_2O production via nitrification but also results in exceptionally high N_2O emissions to the atmosphere, among the highest reported from lakes, during seasonal water column mixing events. A complete understanding of the impact of hypoxic lakes on the global greenhouse budget will rely on quantification of atmospheric fluxes, particularly during seasonal transitions in stratification. This study adds to the emerging narrative of inland waters as sources of globally significant greenhouse gas emissions to the atmosphere.

APPENDIX

Principal component analysis was performed on 2013 data (N_2O and CH_4 concentration, temperature, dissolved O_2 concentration, pH, chlorophyll *a* concentration, and nutrient concentrations (NO_3^-, NH_4^+, and SRP) to identify principal components (PCs) that maximize the correlation among measured variables. Observations were separated by date and depth. Data were standardized to eliminate scale differences. The loadings for each variable were calculated as the correlation of the original variable with each PC, and the scores for each observation were calculated by multiplying by the eigenvector for each PC.

Principal component analysis revealed that two PCs explained 74% of the variance in the dataset (Fig. A2). N_2O concentration was positively associated with PC1 and PC2, whereas CH_4 was positively associated with PC2 only. The loadings for chlorophyll *a* and dissolved O_2 concentration were similar in magnitude and direction, indicating these two variables were closely related in Muskegon Lake. Similarly, temperature and pH were also closely related to one another. Nutrient variables (NO_3^-, NH_4^+, and SRP) were all positively correlated to PC1 but were not strongly correlated with PC2. When plotted by their scores for the two PCs, observations sorted into four apparent groupings: (1) all depths on 6 May, characterized by high greenhouse gas concentrations, low temperature and nutrient concentrations, and high dissolved O_2 concentrations; (2) epilimnion samples, characterized by low greenhouse gas concentrations and high temperature, pH, chlorophyll, and dissolved O_2 concentrations; (3) hypolimnion samples during the stratified period, characterized by high N_2O concentrations, high nutrient concentrations, and low chlorophyll and dissolved O_2 concentrations; and (4) metalimnion samples, characterized by intermediate characteristics between epilimnion and hypolimnion samples.

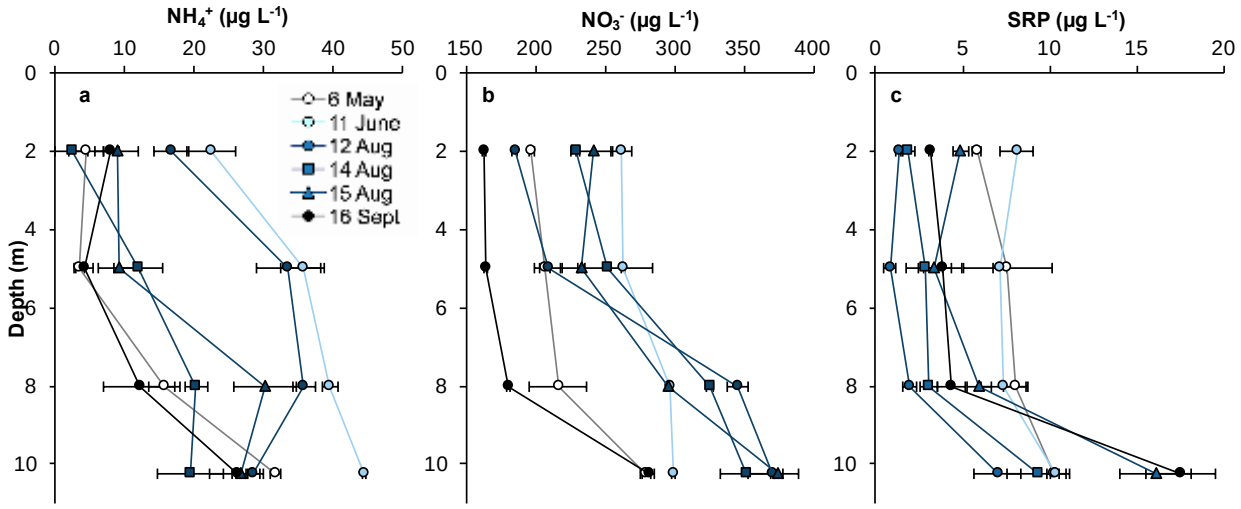

Figure A1. Nutrient concentrations in 2013. (a) NH_4^+, (b) NO_3^-, and (c) SRP concentrations were measured at four depths on each sampling date.

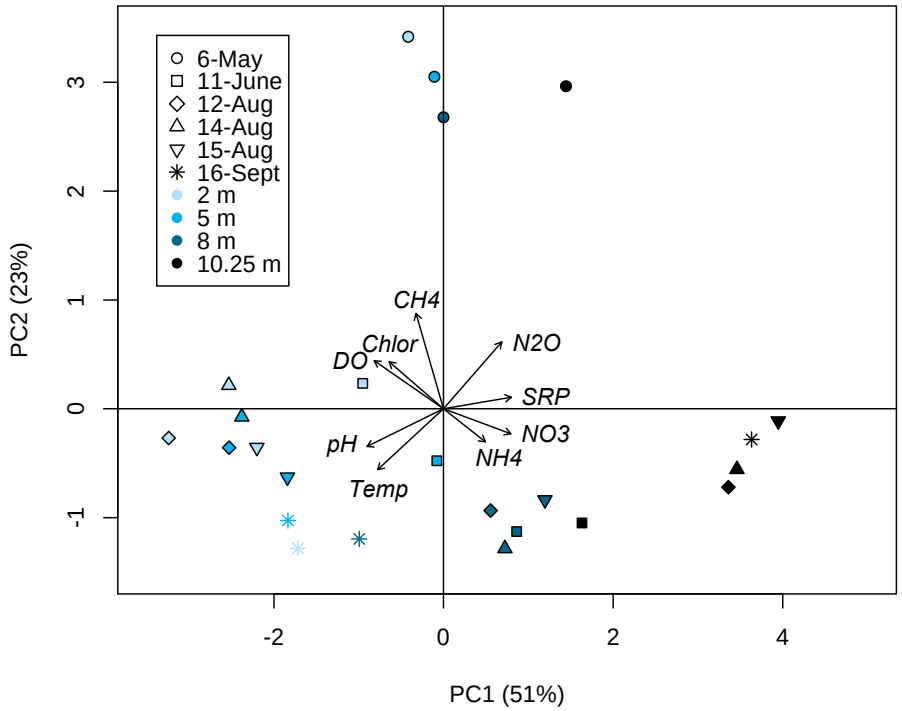

Figure A2. Principal component analysis for 2013 data. Points represent principal component scores for each sampling depth on a given date. Vectors represent loadings for each variable on a scale of zero to one and are plotted for illustrative purposes only. CH4 = CH_4 concentration, N2O = N_2O concentration, Temp = temperature, DO = dissolved O_2, pH = pH, Chlor = chlorophyll *a* fluorescence, NO3 = NO_x concentration, NH4 = NH_4^+ concentration, SRP = soluble reactive phosphorus concentration.

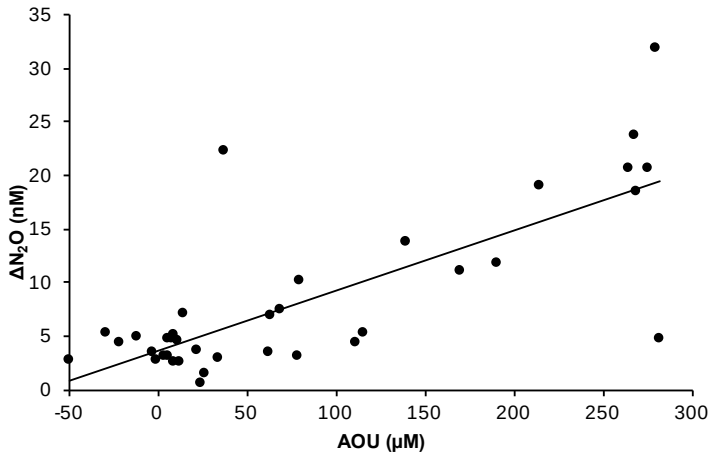

Figure A3. Relationship between ΔN_2O and apparent oxygen utilization (AOU). AOU was calculated as the difference between the saturation concentration and the *in situ* concentration of of dissolved O_2. ΔN_2O was calculated as the difference between the *in situ* concentration and the saturation concentration of N_2O at each sampling point. A positive correlation ($R^2 = 0.58$) supports the interpretation of a N_2O production source from nitrification.

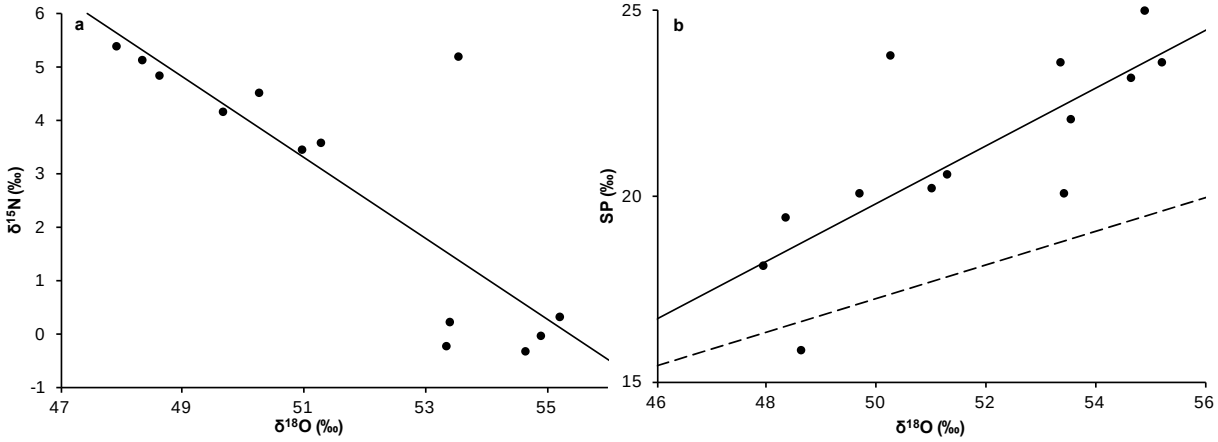

Figure A4. Trends in N_2O concentration and isotopic composition. (**a**) $\delta^{18}O$-N_2O and $\delta^{15}N$-N_2O are negatively correlated ($R^2 = 0.68$). (**b**) $\delta^{18}O$-N_2O and isotopic site preference (SP) are positively correlated ($R^2 = 0.60$) with a slope of 0.78 (solid line). N_2O reduction produces a characteristic $\delta^{18}O$-N_2O vs. SP slope of 0.45 (dotted line).

LITERATURE CITED

LITERATURE CITED

Andersson KK, Hooper AB (1983) O_2 and H_2O are each the source of one O in NO_2^- produced from NH_3 by *Nitrosomonas*: ^{15}NMR evidence. FEBS Lett 164(2):236-240. doi:10.1016/0014-5793(83)80292-0

APHA (2005) Standard methods for the examination of water and wastewater. American Public Health Association, Washington, D.C.

Audet J, Hoffmann CC, Andersen PM, Baattrup-Pedersen A, Johansen JR, Larsen SE, Kjaergaard, Elsgaard L (2014) Nitrous oxide fluxes in undisturbed riparian wetlands located in agricultural catchments: Emission, uptake, and controlling factors. Soil Biol Biochem 68:291-299. doi: 10.1016/j.soilbio.2013.10.011

Bange H, Freing A, Kock A, Löscher C (2010) Marine pathways to nitrous oxide. In: Smith K (ed) Nitrous Oxide and Climate Change. Earthscan, London, pp 36–62.

Bastviken D, Cole J, Pace M, Tranvik L (2004) Methane emissions from lakes: Dependence of lake characteristics, two regional assessments, and a global estimate. Global Biogeochem Cy 18:GB4009. doi:10.1029/2004GB002238

Beaulieu JJ, Smolenski RL, Nietch CT, Townsend-Small A, Elovitz MS, Schubauer-Berigan JP (2014) Denitrification alternates between a source and sink of nitrous oxide in the hypolimnion of a thermally stratified reservoir. Limnol Oceanogr 59(2):495-506. doi: 10.4319/lo.2014.59.2.0495

Beaulieu JJ, Nietch CT, Young JL (2015) Controls of nitrous oxide production and consumption in reservoirs of the Ohio River Basin. J Geophys Res Biogeosci 120:1995-2010. doi:10.1002/2015JG002941

Benson BB, Krause Jr. D (1984) The concentration and isotopic fractionation of oxygen dissolved in freshwater and seawater in equilibrium with the atmosphere. Limnol Oceanogr 29(3):620-632.

Biddanda BA (2012) Lake sentinel: Observatory for ecosystem changes in Muskegon Lake. InterChange, Newsletter of the Regional Math and Science Center, Grand Valley State University, http://www.gvsu.edu/rmsc/interchange/2012-may-connections-awri-651.htm

Bocaniov SA, Schiff SL, Smith REH (2012) Plankton metabolism and physical forcing in a productive embayment of a large oligotrophic lake: Insights from stable oxygen isotopes. Freshwater Biol 57:481-496. doi:10.1111/j.1365-2427.2011.02715.x

Brandes JA, Devol AH (1997) Isotopic fractionation of oxygen and nitrogen in coastal marine sediments. Geochim Cosmochim Ac 61(9):1793-1801. doi:10.1016/S0016-7037(97)00041-0

Carter GS, Nalepa TF, Rediske RR (2006), Status and trends of benthic populations in a coastal drowned river mouth lake of Lake Michigan. J Great Lakes Res 32:578-595

CENR (2000) Integrated assessment of hypoxia in the Northern Gulf of Mexico. National Science and Technology Council Committee on Environment and Natural Resources, Washington, D.C.

Conroy JD, Boegman L, Zhang H, Edwards WJ, Culver DA (2011) "Dead Zone" dynamics in Lake Erie: The importance of weather and sampling intensity for calculated hypolimnetic oxygen depleted rates. Aquat Sci 73(2):289-304. doi:10.1007/s00027-010-0176-1

del Giorgio PA, Peters RH (1994) Patterns in planktonic P:R ratios in lakes: Influence of lake trophy and dissolved organic carbon. Limnol Oceanogr 39(4):772-787. doi:10.4319/lo.1994.39.4.0772

Diaz RJ, Rosenberg R (2008) Spreading dead zones and consequences for marine ecosystems. Science 321:926-929. doi:10.1126/science.1156401

Dila DK, Biddanda BA (2015) From land to lake: Contrasting microbial processes across a Great Lakes gradient of carbon and nutrient inventories. J Great Lakes Res 41:75-85.

Dua RD, Bhandari B, Nicholas DJD (1979) Stable isotope studies on the oxidation of ammonia to hydroxylamine by *Nitrosomonas europaea*. FEBS Lett 106(2):401-404. doi:10.1016/0014-5793(79)80541-4

Emerson S, Quay P, Stump C, Wilbur D, Knox M (1991) O_2, Ar, N_2, and ^{222}Rn in surface waters of the subarctic ocean: Net biological O_2 production. Global Biogeochem Cy 5(1):49-69. doi:10.1029/90GB02656

Fallon RD, Harrits S, Hanson RS, Brock TD (1980) The role of methane in internal carbon cycling in Lake Mendota during summer stratification. Limnol Oceanogr 25(2):357-360. doi:10.4319/lo.1980.25.2.0357

Feldman DE, Yost Jr. HT, Benson BB (1959) Oxygen isotope fractionation in reactions catalyzed by enzymes. Science 129:146-147.

Frame CH, Casciotti KL (2010) Biogeochemical controls and isotopic signatures of nitrous oxide production by a marine ammonia-oxidizing bacterium. Biogeosciences 7:2695-2709. doi:10.5194/bg-7-2695-2010

Freedman P, Canale R, Auer M (1979) The impact of wastewater diversion spray irrigation on water quality in Muskegon County lakes, Rep. 905/9–79–006-A. U.S. Environmental Protection Agency, Washington, D.C.

Friedrich J, Janssen F, Aleynik D et al (2014) Investigating hypoxia in aquatic environments:

Diverse to addressing a complex phenomenon. Biogeosciences 11:1215-1259. doi:10.5194/bg-11-1215-2014

Fry B, Boyd B (2010) Oxygen concentration and isotope studies of productivity and respiration on the Louisiana continental shelf, July 2007. In: Ohkouchi N et al (ed) Earth, Life, and Isotopes. Kyoto University Press, Kyoto, pp 223-241.

Goreau TJ, Kaplan WA, Wofsy SC, McElroy MB, Valois FW, Watson SW (1980) Production of NO_2^- and N_2O by nitrifying bacteria at reduced concentrations of oxygen. Appl Environ Microb 40(3):526–532.

Hamilton SK, Ostrom NE (2007) Measurements of the stable isotope ratio of dissolved N_2 in ^{15}N tracer experiments. Limnol Oceanogr Methods 5:233-240.

Hanson, PC, Bade DL, Carpenter SR, Kratz TK (2003) Lake metabolism: Relationships with dissolved organic carbon and phosphorus. Limnol Oceanogr 48(3):1112-1119. doi:10.4319/lo.2003.48.3.1112

Hollocher TC, Tate ME, Nicholas DJ (1981) Oxidation of ammonia by *Nitrosomonas europaea*. Definite ^{18}O-tracer evidence that hydroxylamine formation involves a mono-oxygenase. J Biol Chem 256:10834-10836.

Huttunen JT, Juutinen S, Alm J, Larmola T, Hammar T, Silvola J, Martikainen PJ (2003) Nitrous oxide flux to the atmosphere from the littoral zone of a boreal lake. J Geophys Res 108(D14):4421. doi:10.1029/2002JD002989

Huttunen JT, Väisänen TS, Hellsten SK, Martikainen PJ (2006) Methane fluxes at the sediment-water interface in some boreal lakes and reservoirs. Boreal Environ Res 11:27-34.

IPCC (2007) Climate Change 2007: The Physical Science Basis. In: Solomon S et al (eds) Contribution of Working Group I to the Fourth Assessment Report of the Intergovernmental Panel on Climate Change. Cambridge University Press, New York.

IPCC (2013) Climate Change 2013: The Physical Science Basis. In: Stocker TF et al (eds) Contribution of Working Group I to the Fifth Assessment Report of the Intergovernmental Panel on Climate Change. Cambridge University Press, New York.

Jankowski T, Livingstone DM, Bührer H, Forster R, Niederhauser P (2006) Consequences of the 2003 European heat wave for lake temperature profiles, temperature stability, and hypolimnetic oxygen depletion: Implications for a warmer world. Limnol Oceanogr 51(2):815-819. doi:10.4319/lo.2006.51.2.0815

Kaushal SS, Mayer PM, Vidon PG, Smith RM, Pennino MJ, Newcomer TA, Duan S, Welty C, Belt KT (2014) Land use and climate variability amplify carbon, nutrient, and contaminant pulses: A review with management implications. U.S. Environmental Protection Agency Paper 234.

Knowles R (1982) Denitrification. Microbiological Rev 46(1):43-70.

Kumar S, Nicholas DJD, Williams EH (1983) Definitive ^{15}N NMR evidence that water serves as a source of 'O' during nitrite oxidation by *Nitrobacter agilis*. FEBS Lett 152(1):71-74. doi:10.1016/0014-5793(83)80484-0

Lemon E, Lemon D (1981) Nitrous oxide in freshwaters of the Great Lakes Basin. Limnol Oceanogr 26(5):867-879. doi:10.4319/lo.1981.26.5.0867

Lehman MF, Barnett B, Gélinas Y, Gilbert D, Maranger R, Mucci A, Sundby B, Thibodeau B (2009) Aerobic respiration and hypoxia in the Lower St. Lawrence Estuary: Stable isotope ratios of dissolved oxygen constrain oxygen sink partitioning. Limnol Oceanogr 54(6):2157-2169.

Lis G, Wassenaar LI, Hendry MJ (2008) High-precision laser spectroscopy D/H and $^{18}O/^{16}O$ measurements of microliter natural water samples. Anal Chem 80(1):287-293. doi:10.1021/ac701716q

Livingstone DM, Imboden DM (1996) The prediction of hypolimnetic oxygen profiles: A plea for a deductive approach. Can J Fish Aquat Sci 53:924-932. doi:10.1139/f95-230

Mariotti A, Germon JD, Hubert P, Kaiser P, Letolle R, Tardieux A, Tardieux P (1981) Experimental determination of nitrogen kinetic isotope fractionation: Some principles; Illustration for the denitrification and nitrification processes. Plant and Soil 62(3):413-430. doi:10.1007/BF02374138

McCarthy MJ, Carini SA, Liu Z, Ostrom NE, Gardner WS (2013) Oxygen consumption in the water column and sediments of the Gulf of Mexico hypoxic zone. Estuar Coast Shelf S 123:46-53. doi:10.1016/j.ecss.2013.02.019

McNair JN, Gereaux LC, Weinke AD, Sesselmann MR, Kendall ST, Biddanda BA (2013) New methods for estimating components of lake metabolism based on free-water dissolved-oxygen dynamics. Ecol Model 263:251-263. doi:10.1016/j.ecolmodel.2013.05.010

Michigan DEQ (2011) Stage 2 remedial action plan Muskegon Lake Area of Concern. Michigan Department of Environmental Quality, Lansing, Michigan

Michmerhuizen CM, Striegl RG, McDonald ME (1996) Potential methane emission from north-temperate lakes following ice melt. Limnol Oceanogr 41(5):985-991. doi:10.4319/lo.1996.41.5.0985

Miettinen H, Pumpanen J, Heiskanen JJ, Aaltonen H, Mammarella I, Ojala A, Levula J, Rantakari M (2015) Towards a more comprehensive understanding of lacustrine greenhouse gas dynamics – two-year measurements of concentrations and fluxes of CO_2, CH_4, and N_2O in a typical boreal lake surrounded by managed forests. Boreal Env Res 20:75-89.

Morse JL, Ardón M, Bernhardt ES (2012) Greenhouse gas fluxes in southeastern U.S. coastal plain wetlands under contrasting land uses. Ecol Appl 22(1):264-280.

Nevison C, Butler JH, Elkins JW (2003) Global distribution of N_2O and the ΔN_2O-AOU yield in the subsurface ocean. Global Biogeochem Cy 17(4):1119. doi:10.1029/2003GB002068

Opdyke MR, Ostrom NE, Ostrom PH (2009) Evidence for the predominance of denitrification as a source of N_2O in a temperate agricultural soils based on isotopologue measurements. Global Biogeochem Cy 23:GB4018. doi:10.1029/2009GB003523

Ortiz-Llorente MJ, Alvarez-Cobelas M (2012) Comparison of biogenic methane emissions from unmanaged estuaries, lakes, oceans, rivers and wetlands. Atmos Environ 59:328-337. doi:10.1016/j.atmosenv.2012.05.031

Ostrom NE, Carrick HJ, Twiss MR, Piwinski L (2005) Evaluation of primary production in Lake Erie by multiple proxies. Oecologia 144:115-124. doi:10.1007/s00442-005-0032-5

Ostrom NE, Gandhi H, Kamphuis B, DeCamp S, Liu Z, McCarthy MJ, Gardner WS (2014) Oxygen metabolism and water mass mixing in the northern Gulf of Mexico hypoxic zone in 2010. Geochim Cosmochim Ac 140:39-49. doi:10.1016/j.gca.2014.05.020

Ostrom NE, Ostrom PH (2011) The isotopomers of nitrous oxide: Analytical considerations and application to resolution of microbial production pathways. In: Baskaran M (ed) Handbook of Environmental Isotope Geochemistry. Springer-Verlag, New York, pp 453-476.

Ostrom NE, Pitt A, Sutka R, Ostrom PH, Grandy AS, Huizinga KM, Robertson GP (2007) Isotopologue effects during N_2O reduction in soils and in pure cultures of denitrifiers. J Geophys Res 112:G02005. doi:10.1029/2006JG000287

Ostrom NE, Russ ME, Popp B, Rust TM, Karl DM (2000) Mechanisms of nitrous oxide production in the subtropical North Pacific based on determinations of the isotopic abundances of nitrous oxide and di-oxygen. Chemosphere - Global Change Sci 2:281-290. doi:10.1016/S1465-9972(00)00031-3

Pataki DE, Ehleringer JR, Flanagan LB, Yakir D, Bowling DR, Still CJ, Buchmann N, Kaplan JO, Berry JA (2003) The application and interpretation of Keeling plots in terrestrial carbon cycle research. Global Biogeochem Cy 17(1):1022. doi:10.1029/2001GB001850

Popp BN, Westley MB, Toyoda S, Miwa T, Dore JE, Yoshida N, Rust TM, Sansone FJ, Russ ME, Ostrom NE, Ostrom PH (2002) Nitrogen and oxygen isotopomeric constraints on the origins and sea-to-air flux of N_2O in the oligotrophic subtropical North Pacific gyre. Global Biogeochem Cy 16(4):1064, doi:10.1029/2001GB001806

Poth M, Focht DD (1985) ^{15}N kinetic analysis of N_2O production by *Nitrosomonas europaea*: An examination of nitrifier denitrification. Appl Environ Microb 49(5):1134-1141.

Quiñones-Rivera ZJ, Wissel B, Justić D, Fry B (2007) Partitioning oxygen sources and sinks in a stratified, eutrophic coastal ecosystem using stable oxygen isotopes. Mar Ecol Prog Ser 342:69-83. doi:10.3354/meps342069

Rabalais NN, Diaz RJ, Levin LA, Turner RE, Gilbert D, Zhang J (2010) Dynamics and distribution of natural and human-caused hypoxia. Biogeosciences 7:585-619. doi:10.5194/bg-7-585-2010

Riera JL, Schindler JE, Kratz TK (1999) Seasonal dynamics of carbon dioxide and methane in two clear-water lakes and two bog lakes in northern Wisconsin, U.S.A. Can J Fish Aquat Sci 56:265-274. doi:10.1139/f98-182

Roberts BJ, Russ ME, Ostrom NE (2000) Rapid and precise determination of the $\delta^{18}O$ of dissolved gaseous dioxygen via gas chromatography-isotope ratio mass spectrometry. Environ Sci Technol 34(11):2337-2341. doi:10.1021/es991109d

Sansone FJ, Popp BN, Rust TM (1997) Stable carbon isotopic analysis of low-level methane in water and gas. Anal Chem 69(1):40-44. doi:10.1021/ac960241i

Sasaki Y, Koba K, Yamamoto M, Makabe A, Ueno Y, Nakagawa M, Toyoda S, Yoshida N, Yoh M (2011) Biogeochemistry of nitrous oxide in Lake Kizaki, Japan, elucidated by nitrous oxide isotopomers analysis. J Geophys Res 116:G04030. doi:10.1029/2010JG001589

Scavia D, Allan JD, Arend KK et al (2014) Assessing and addressing the re-eutrophication of Lake Erie: Central basin hypoxia. J Great Lakes Res 40:226-246. doi:10.1016/j.jglr.2014.02.004

Seitzinger S, Harrison JA, Böhlke JK, Bouwman AF, Lowrance R, Peterson B, Tobias C, Van Drecht G (2006) Denitrification across landscapes and waterscapes: A synthesis. Ecol Appl 16(6):2064-2090.

Seitzinger SP, Kroeze C (1998) Global distribution of nitrous oxide production and N inputs in freshwater and coastal marine ecosystems. Global Biogeochem Cy 12(1):93-113.

Stein LY (2011) Surveying N_2O-producing pathways in bacteria. In: Klotz MG (ed) Methods in Enzymology, vol 486. Elsevier Academic Press, San Diego, California, pp 131-152.

Steinman AD, Ogdahl M, Rediske R, Ruetz III CR, Biddanda BA, Nemeth L (2008) Current status and trends in Muskegon Lake, Michigan. J Great Lakes Res 34(1):169-188. doi:10.3394/0380-1330(2008)34[169:CSATIM]2.0.CO;2

Striegl RG, Michmerhuizen CM (1998) Hydrologic influence on methane and carbon dioxide dynamics at two north-central Minnesota lakes. Limnol Oceanogr 43(7):1519-1529.

Sutka RL, Adams GC, Ostrom NE, Ostrom PH (2008) Isotopologue fractionation during N_2O production by fungal denitrification. Rapid Commun Mass Spectrom 22(24):3989-3996. doi:10.1002/rcm.3820

Sutka RL, Ostrom NE, Ostrom PH, Breznak JA, Gandhi H, Pitt AJ, Li F (2006) Distinguishing nitrous oxide production from nitrification and denitrification on the basis of isotopomer abundances. Appl Environ Microb 72(1):638-644. doi:10.1128/AEM.72.1.638-644.2006

Sutka RL, Ostrom NE, Ostrom PH, Gandhi H, Breznak JA (2003) Nitrogen isotopomer site preference of N_2O produced by *Nitrosomonas europaea* and *Methylococcus capsulatus* Bath. Rapid Commun Mass Spectrom 17(7):738-745. doi:10.1002/rcm.968

Tang Z, Engel BA, Pijanowski BC, Lim KJ (2005) Forecasting land use change and its environmental impact at a watershed scale. J Environ Manage 76:35-45. doi:10.1016/j.jenvman.2005.01.006

Taylor PG, Townsend AR (2010) Stoichiometric control of organic carbon-nitrate relationships from the soil to the sea. Nature 464: 1178-1181. doi:10.1038/nature08985

Toyoda S, Mutobe H, Yamagishi H, Yoshida N, Tanji Y (2005) Fractionation of N_2O isotopomers during production by denitrifier. Soil Biol Biochem 37(8):1535-1545. doi:10.1016/j.soilbio.2005.01.009

Turner RE, Rabalais NN, Justic D (2008) Gulf of Mexico hypoxia: Alternate states and a legacy. Environ Sci Tech 42:2323-2327. doi:10.1021/es071617k

U.S. EPA (2013) Great Lakes Areas of Concern: Muskegon Lake. U.S. Environmental Protection Agency, Washington, D.C.

Vail J, Meyer A, Weinke A, Biddanda BA (2015) Water quality monitoring: Lesson plan for exploring time-series data. J Mich Sci Teach Assoc 60.1:37-48.

Walker JT, Stow CA, Geron C (2010) Nitrous oxide emissions from the Gulf of Mexico hypoxic zone. Environ Sci Technol 44(5):1617-1623. doi:10.1021/es902058t

Wang H, Wang W, Yin C, Wang Y, Lu J (2006) Littoral zones as the "hotspots" of nitrous oxide (N_2O) emission in a hyper-eutrophic lake in China. Atmos Environ 40:5522-5527. doi:10.1016/j.atmosenv.2006.05.032

Wanninkhof R (1992) Relationship between wind speed and gas exchange over the ocean. J Geophys Res 97(C5):7373-7382. doi:10.1029/92JC00188

Weinke AD, Kendall ST, Kroll DJ, Strickler EA, Weinert ME, Holcomb TM, Defore AA, Dila DK, Snider MJ, Gereaux LC, Biddanda BA (2014) Systematically variable planktonic carbon metabolism along a land-to-lake gradient in a Great Lakes coastal zone. J Plankton Res 0:1-15. doi:10.1093/plankt/fbu066

Westley MB, Yamagishi H, Popp BN, Yoshida N (2006) Nitrous oxide cycling in the Black Sea inferred from stable isotope and isotopomers distributions. Deep-Sea Res Pt II 53:1802-1816. doi:10.1016/j.dsr2.2006.03.012

Whitfield CJ, Aherne J, Baulch HM (2011) Controls on greenhouse gas concentrations in polymictic headwater lakes in Ireland. Sci Total Environ 410-411:217-225. doi:10.1016/j.scitotenv.2011.09.045

Williamson CE, Dodds W, Kratz TK, Palmer MA (2008) Lakes and streams as sentinels of environmental change in terrestrial and atmospheric processes. Front Ecol Environ 6(5):247-254. doi:10.1890/070140

World Meteorological Organization (2008) Guide to meteorological instruments and methods of observation, WMO-No. 8. World Meteorological Organization, Geneva, Switzerland

Wrage N, Velthof GL, van Beusichem ML, Oenema O (2001) Role of nitrifier denitrification in the production of nitrous oxide. Soil Biol Biochem 33(12-13):1723-1732. doi:10.1016/S0038-0717(01)00096-7

Yamagishi H, Westley MB, Popp BN, Toyoda S, Yoshida N, Watanabe S, Koba K, Yamanaka Y (2007) Role of nitrification and denitrification on the nitrous oxide cycle in the eastern tropical North Pacific and Gulf of California. J Geophys Res 112:G02015. doi:10.1029/2006JG000227

Yang H, Andersen T, Dörsch P, Tominaga K, Thrane J-E, Hessen DO (2015) Greenhouse gas metabolism in Nordic boreal lakes. Biogeochemistry 126:211-225. doi:10.1007/s10533-015-0154-8

Yang H, Gandhi H, Ostrom NE, Hegg EL (2014) Isotopic fractionation by a fungal P450 nitric oxide reductase during the production of N_2O. Environ Sci Technol 48:10707-10715. doi:10.1021/es501912d

Yoshida N, Toyoda S (2000) Constraining the atmospheric N_2O budget from intramolecular site preference in N_2O isotopomers. Nature 405:330-334. doi:10.1038/35012558

Yoshinari T (1976) Nitrous oxide in the sea. Mar Chem 4:189-202. doi:10.1016/0304-4203(76)90007-4

CHAPTER 2

WETLAND RESTORATION AND HYDROLOGIC RECONNECTION RESULT IN ENHANCED WATERSHED NITROGEN RETENTION AND REMOVAL

ABSTRACT

Restoration of wetlands presents a potential water quality benefit via removal of nutrients, including excess nitrogen (N) and phosphorus (P), but there is potential for complex and unresolved changes in nutrient cycling following restoration. In this study, we evaluated N removal and release in a former agricultural wetland under scenarios of hydrologic reconnection to the watershed and sediment dredging. We modeled potential downstream impacts of restoration activities in the context of N management. Denitrification, N_2O production, and anammox were measured via the isotope pairing technique in intact sediment cores, and probabilistic estimates of N cycling under restoration scenarios were modeled in a Bayesian framework. Anammox was not detected in this system, but denitrification and N_2O production were stimulated shortly following simulated dredging, indicating a temporary response to sediment disturbance. Owing to a decrease in NH_4^+ availability under hydrologic reconnection, coupled nitrification-denitrification was inhibited. Despite a decrease in denitrification activity, the wetland has the capacity to remove up to 10 % of stream $NO_3^=$ via denitrification following hydrologic reconnection. Restoration activities are predicted to mitigate NH_4^+ delivery to a downstream eutrophic lake, yet permanent N removal will be reduced due to the decoupling of nitrification and denitrification.

INTRODUCTION

Wetlands have the potential to provide significant ecosystem services, including wildlife habitat, nutrient retention, and groundwater recharge (Keddy 2000). Many natural wetlands in

the United States have been converted to agricultural production (Dahl 2000) but are now being targeted for restoration that in many cases is supported by financial incentives such as the Wetlands Reserve Program (USDA 2012). Agricultural wetland restoration presents benefits such as the creation of wildlife habitat (Bunn and Arthington 2002; Zelder and Kercher 2005). However, many restored wetland sediments in agricultural landscapes bear residual nutrients that impact the capacity for the wetland to retain phosphorus (P) and nitrogen (N). Restoration efforts must thus consider not only habitat benefits but also the implications for water quality in the face of eutrophication of many watersheds (Ardón et al. 2010a; Welti et al. 2012).

Wetlands are well known for their ability to remove substantial quantities of P and N (Fennessy and Cronk 1997; Reddy et al. 1999; Saunders and Kalff 2001). Although wetlands have a tremendous capacity to remove nutrients, restoration may induce a decrease in water quality, at least temporarily. Nutrient release can occur following reflooding and hydrologic reconnection (Aldous et al. 2005; Lindenberg and Wood 2009; Morse et al. 2012), particularly in systems with a history of nutrient loading such as agricultural soils (Newman and Pietro 2001; Pant and Reddy 2003; Steinman and Ogdahl 2011). Downstream release of P is common, whereas N has a greater capacity to be removed by sediments in restored wetlands (Ardón et al. 2010a; 2010b; Steinman and Ogdahl 2011). While mitigation of P loading has received greater attention owing to its role as a primary limiting nutrient for phytoplankton growth in freshwater environments (Schindler 1974; Carpenter et al. 1998), N is emerging as an important co-limiting nutrient that has recently been implicated in the growth and persistence of harmful algal blooms in lakes (Conley et al. 2009; Chaffin and Bridgeman 2014; Steffen et al. 2014; Paerl et al. 2016). The potential for wetlands to mitigate or exacerbate downstream N delivery is thus a key

determinant of downstream water quality, and N management should be incorporated alongside P management into restoration activities.

Denitrification is the predominant process that permanently removes N from wetlands (Seitzinger et al. 2006). Denitrification is the stepwise reduction of NO_3^- to N_2, with intermediates of NO_2^-, NO, and N_2O (Knowles 1982). Of particular concern is the proportion of N that is not completely reduced to N_2 and is lost as N_2O, a potent greenhouse gas (IPCC 2007). Thus, enhanced denitrification may have the unintended consequence of increasing greenhouse gas emissions. N_2O production rates and the N_2O:N_2 production ratio are likely to change following wetland restoration, owing to differences in NO_3^- supply, quality and quantity of organic carbon, and hydrologic pulses (Welti et al. 2012; Sun et al. 2014). Denitrification can be augmented by direct coupling with nitrification, which oxidizes NH_4^+ to NO_3^-. Coupled nitrification-denitrification can make up a significant proportion of total denitrification in wetlands (Scott et al. 2008).

Anammox, the transformation of NH_4^+ and NO_2^- to N_2 (van de Graaf et al. 1995), is an additional N removal process that is not well understood in wetland systems. This process is expected to be minor compared to denitrification in wetlands owing to the inferior ability of anammox bacteria to compete for substrates in organic-rich sediments (Thamdrup and Dalsgaard 2002; Humbert et al. 2012). However, anammox genes have been detected in wetlands (Zhu et al. 2011; Humbert et al. 2012; Waki et al. 2015) and hotspots of anammox activity have been observed at land-freshwater interfaces (Zhu et al. 2013). A complete understanding of the N removal regime of wetlands and their potential impact on water quality will therefore benefit from examination of both denitrification and anammox.

In this study, we aimed to quantify N removal and release by wetland sediments under restoration scenarios, using statistical modeling to produce probabilistic estimates of the rates of each N cycling process. Additionally, we evaluated potential downstream impacts of wetland restoration activities in the context of watershed N and P management. Together, this work provides an analysis of wetland N removal and release capacity before restoration activities occur, which can help guide management decisions and expectations.

METHODS

Study site

This research was conducted in the Bear Lake Wetland Restoration Area (BLWRA) in western Michigan, USA that is currently being subject to restoration activities (Figure 7). Historically, the BLWRA was a deltaic wetland that was hydrologically connected to Bear Creek on its north side. In the early 1900s, an earthen berm was constructed between Bear Creek and the wetland, and the wetland was drained and placed into celery production. Agricultural activities ceased and the pumps were turned off in 2002, allowing the wetland to be re-inundated as two separate ponds. The main purpose of the restoration was to create habitat for wildlife, although an additional benefit could be improved water quality. This study focused on the West Pond (0.09 km^2), which had not been subject to sediment dredging prior to 2016. Additional restoration activities, completed in the two years following this study, were completed to (1) dewater the pond, (2) dredge the sediment to a depth of approximately 0.5 m to remove the agriculturally-impacted layer, and (3) re-inundate the pond. Future restoration will remove the berm to reconnect the surface hydrology of the wetland and Bear Creek, assuming the nutrient

concentrations in the refilled ponds are lower than those in adjacent Bear Creek (Steinman and Ogdahl 2016).

Restoration has the potential to impact water quality in Bear Lake, a eutrophic drowned river mouth lake located approximately 250 m downstream of the West Pond that is connected via Bear Creek. Bear Lake is within the geographic boundary of the Muskegon Lake Area of Concern and is subject to evaluations of eutrophication and nutrient loading (USEPA 2013). Previous studies have examined the potential effects of hydrologic reconnection on P retention and release from the BLWRA (Smit and Steinman 2015; Steinman and Ogdahl 2016), and the examination of N cycling was compared with those results to evaluate potential downstream nutrient impacts on Bear Lake.

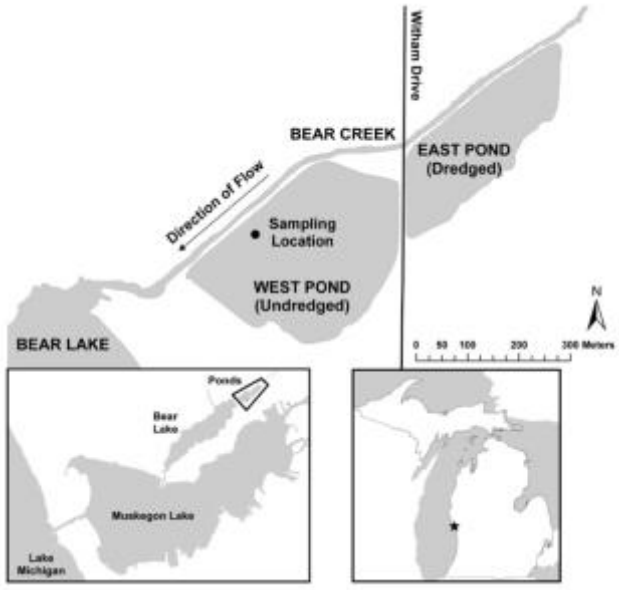

Figure 7. Map of the Bear Lake Wetland Restoration Area (BLWRA). Restoration activities in the West Pond include removal of the berm that separates Bear Creek from the wetland and sediment dredging of. Insets show the location of the ponds in the downstream portion of the watershed (left) and in Michigan, USA (right).

Intact sediment cores

Sediment was collected at a sampling location in the northwest side of the pond (Figure 7) using a modified piston corer described by Smit and Steinman (2015). Intact sediment cores were collected in polycarbonate tubes (7 cm i.d.) to a depth of 25 cm. Cores were then divided into three treatment groups: "Control," which simulates conditions without restoration, "HR," which simulates a hydrologic reconnection of the wetland to Bear Creek, and "HR+D," which simulates hydrologic reconnection and dredging of the top layer of sediment. Water from the West Pond was added to Control cores and water from Bear Creek was added to HR and HR+D cores to a depth of 20 cm inside the core tube (Table 3). The top 5 cm of sediment was removed from the cores in the HR+D treatment. Though 5 cm is shallower than the depth to which sediments are currently being dredged, it represents the removal of the most likely labile and microbially active sediment layer. Cores were pre-incubated 12 h in the dark at *in situ* temperature prior to the addition of $^{15}N\text{-}NO_3^-$ under gentle bubbling with air to maintain oxic conditions in the overlying water.

Table 3. DIN concentrations in the Bear Lake Wetland Restoration Area and adjacent Bear Creek.

Location	$NH_4^{\pm}$-N μM	NO_2^--N + NO_3^--N μM
Undredged Field	29.45	46.40
Bear Creek	1.35	22.34

Following pre-incubation, a water sample was taken for DIN concentration analysis (NO_3^-, NO_2^- and NH_4^+) by filtering through a 0.45 μm Millipore filter and freezing until analysis. $^{15}N\text{-}NO_3^-$ was then added to obtain a final concentration of 100 μM in the overlying water of

each sediment core. Cores were then capped with a rubber plug and equipped with a motorized stirring device inserted through a port in the plug. Stirring of the water overlying the core was maintained just below the sediment resuspension threshold. An equilibration period of 30 min was employed to allow for homogenization of NO_3^- between the overlying water and with the NO_3^- reduction zone in the sediment porewater (Dalsgaard et al. 2000). Cores from each treatment were sacrificed in triplicate at intervals of 0, 6, and 12 h. Upon sacrifice, dissolved O_2 was measured using a YSI 6600 sonde (Yellow Springs Instruments Inc., Yellow Springs, OH). A DIN sample was collected and processed as described above. Then, the top 2-4 cm of the sediment core were slurrified with a glass rod to mix the overlying water with porewater, and samples were collected for dissolved N_2 and N_2O analysis.

Samples for the determination of $\delta^{15}N_2$ were collected according to Hamilton and Ostrom (2007); briefly, dissolved gases were equilibrated with a He atmosphere, and the headspace was transferred into a pre-evacuated 12 mL Exetainer. Samples for analysis of dissolved N_2 concentration were siphoned into 12 mL Exetainers to overflowing and amended with 200 µL of saturated $ZnCl_2$ solution to halt biological activity. All Exetainers were stored underwater at room temperature to minimize diffusion of atmospheric N_2 during storage. Samples for analysis of the $\delta^{15}N_2O$ and N_2O concentration were siphoned into 250 and 60 mL serum bottles, respectively, to overflowing and sealed without a headspace. Biological activity was halted by addition of 1 and 0.25 mL of saturated $HgCl_2$ solution, respectively, to each serum bottle. Prior to analysis, a headspace of 20 mL He was injected into each 60 mL serum bottle, with atmospheric pressure maintained by allowing 20 mL of water to exit via a vent needle. Serum bottles were allowed to equilibrate under gentle shaking for at least 12 h prior to analysis.

Analyses

The concentration of NO_3^- was determined by ion chromatography on a Dionex DX500 (APHA 2005). NH_4^+ concentrations were analyzed by the automated phenate method (APHA 2005) on a on a Bran + Luebbe Autoanalyzer (SEAL Analytical, Mequon, WI). The isotopic composition of N_2 was analyzed by gas chromatograph (HP-5980, Hewlett Packard, Ramsey, MN) interfaced to an Isoprime isotope ratio mass spectrometer (Elementar Americas, Inc., Mount Laurel, NJ). Analytical reproducibility was 0.3 ‰. Concentrations of dissolved N_2 were analyzed by membrane inlet mass spectrometry according to Eyre et al. (2002). The headspace of the 60 mL serum bottles was analyzed for the concentration of N_2O by GC-ECD (Shimadzu Greenhouse Gas Analyzer GC-2014, Shimadzu Scientific Instruments, Columbia, MD). The original dissolved concentration of N_2O in each sample was calculated based on the headspace equilibrium concentration (Hamilton and Ostrom 2007). The isotopic composition of N_2O was analyzed by introducing the sample into a Trace Gas sample introduction system following He sparging and cryogenic trapping interfaced to an Isoprime isotope ratio mass spectrometer (Elementar Americas, Inc., Mount Laurel, NJ). Analytical reproducibility for replicate samples was 0.5 ‰ for bulk $\delta^{15}N$ and $\delta^{18}O$, 0.75 ‰ for $\delta^{15}N_\alpha$ $\delta^{15}N_\beta$, and 1.3 ‰ for SP.

Modeling

Rates of N removal were determined according to the isotope pairing technique (IPT). The original IPT calculates the denitrification rate (including coupled nitrification-denitrification) based on the production of $^{29}N_2$ and $^{30}N_2$ following addition of $^{15}NO_3^-$ (Nielsen 1992). Subsequent revisions of the IPT include calculation of rates of anammox and N_2O production by incorporating the analysis of $^{45}N_2O$ and $^{46}N_2O$ production (Risgaard-Petersen et al.

2003; Trimmer et al. 2006; Hsu and Kao 2013). Briefly, N_2 production by denitrification and anammox, respectively, were calculated as:

$$(r_{14\text{-}N2O} + 1) \cdot 2 \cdot r_{14\text{-}N2O} \cdot P_{30} \quad (7)$$

and

$$2 \cdot r_{14\text{-}N2O} \cdot (P_{29} - 2 \cdot r_{14\text{-}N2O} \cdot P_{30}) \quad (8)$$

where $r_{14\text{-}N2O}$ is the ratio of ^{14}N to ^{15}N in N_2O, P_{29} is the production of $^{29}N_2$, and P_{30} is the production of $^{30}N_2$. N_2O production in the absence of ^{15}N amendment was calculated as:

$$r_{14\text{-}N2O} \cdot (2 \cdot P_{46} + P_{45}) \quad (9)$$

where P_{45} and P_{46} are the production of $^{45}N_2O$ and $^{46}N_2O$, respectively. Coupled nitrification-denitrification, a subset of total denitrification, was calculated as:

$$P_{14} \cdot (1 - r_{14w}/r_{14\text{-}N2O}) \quad (10)$$

where P_{14} is the total production of ^{14}N-N_2 and ^{14}N-N_2O and r_{14w} is the ratio of ^{14}N to ^{15}N in the water overlying the core. NH_4^+ flux into or out of the sediment was calculated as the NH_4^+ concentration in the overlying water at the end of the incubation minus the NH_4^+ concentration in the overlying water at the start of the incubation.

Statistical analysis

A two-way interaction effects ANOVA was used to test for differences in denitrification, N_2O production, and NH_4^+ flux among the different restoration scenarios and incubation durations. Statistical models and posterior distributions were analyzed in a Bayesian framework using R (version 3.2.4) and JAGS (Su and Yajima 2015). For each test, 1,200 Markov-chain Monte Carlo iterations were run on three chains after a burn-in of 200 and thinned by two, yielding 1,500 samples in the posterior distribution. Credible intervals (95 %) were constructed

around the mean of each group. The probability of a significant difference between groups was determined by calculating the proportion of iterations in which the posterior estimate of one group was smaller than another (Turner et al. 2010). The difference between groups was considered significant when less than 5 % of the posterior estimates were smaller than those of another group. Posterior estimates of 95 % credible intervals for denitrification and N_2O production generally encompassed measured rates, whereas posterior estimates for NH_4^+ flux tended to occupy a narrower range than the observed fluxes.

RESULTS

Anammox was not detected in wetland sediments. The absence of anammox activity was confirmed by comparing the proportion of ^{15}N in N_2 with that of N_2O ($q$$N_2$ and $q$$N_2O$, respectively; Trimmer et al. 2006). Anammox activity is suggested if $q$$N_2$ is lower than $q$$N_2O$, illustrating disproportionate production of $^{29}N_2$ relative to $^{45}N_2O$ (Erler et al. 2008). In our study, $q$$N_2$ values were consistently higher than $q$$N_2O$ values, indicating production of $^{45}N_2O$ that outweighed production of $^{29}N_2$.

Denitrification was the only appreciable mechanism of N removal in Bear Creek wetland sediments. Posterior estimates generated by statistical modeling indicated that denitrification rates were lower in the HR and HR+D scenarios than in the Control scenario across both incubation durations (Figure 8; Table 4). Incubation duration had a significant effect on the denitrification rate in the HR+D scenario, where denitrification rates in the 6 h incubation were significantly higher than in the 12 h incubation (Figure 8a, Table 4). Coupled nitrification-denitrification (mean ± SD), a subset of total denitrification, was significantly higher in the

Control scenario (60.4 ± 10.9 µmol N m^{-2} h^{-1}) than in the HR and HR+D scenarios (18.6 ± 10.3 and 16.6 ± 11.3 µmol N m^{-2} h^{-1}, respectively; Figure 8b).

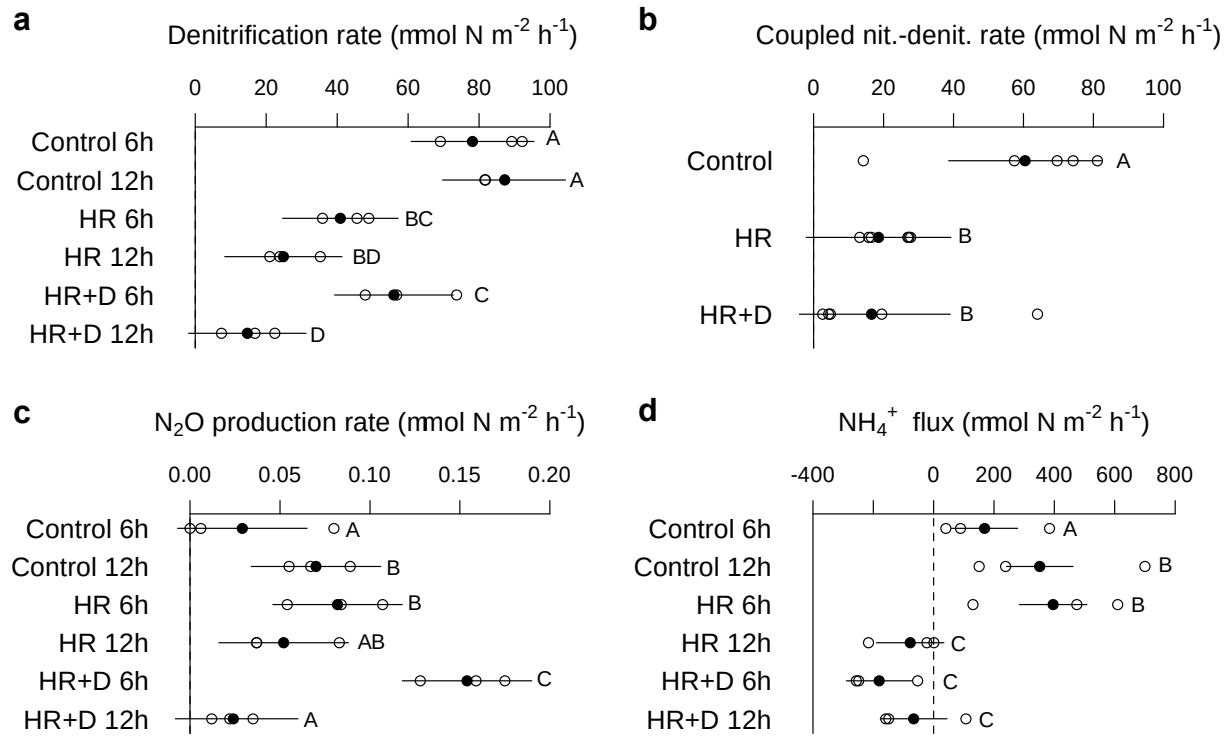

Figure 8. Posterior estimates of (a) denitrification, (b) coupled nitrification-denitrification, (c) N_2O production rates, and (d) NH_4^+ flux. Rates were measured from incubations of 6 and 12 h duration under three restoration scenarios: (1) no restoration (control), (2) simulated hydrologic reconnection (HR), and (3) simulated hydrologic reconnection and dredging (HR+D). Open circles represent measured rates and closed circles represent the mean of the posterior estimate for each treatment-duration combination. Lines represent the 95 % credible interval around each posterior mean estimate. In (d), positive values indicate a net release of NH_4^+ to the water column from the sediment, and negative values indicate a net uptake of NH_4^+ by the sediment from the water column. Note the different scales for the axes among panels. Statistical groupings of posterior estimates at the $p < 0.05$ level are indicated by letters.

The N_2O production rate was below 0.10 µmol N m^{-2} h^{-1} for all treatments and incubation durations except the HR+D scenario in the 6 h incubation, which was significantly greater than any other treatment and duration (Figure 8c, Table 4). As a percentage of total denitrification, N_2O production was similar between incubation durations within a single restoration scenario. In

the control, HR, and HR+D scenarios, N_2O made up (mean ± SD) 0.06 ± 0.05 %, 0.19 ± 0.04 %, and 0.21 ± 0.08 % of total denitrification, respectively.

NH_4^+ flux data indicated a net release (positive flux) or net uptake (negative flux) of NH_4^+ from the sediment depending on the restoration scenario. The NH_4^+ fluxes for the Control scenario for both incubation durations and for the HR scenario for the 6 h duration were positive. The NH_4^+ fluxes for the HR scenario for the 12 h incubation durations and for the HR+D scenario for both incubation scenarios were negative and were significantly different from the positive fluxes but not from one another. In terms of magnitude, NH_4^+ flux was the dominant N cycling process of those studied (Figure 8d, Table 4).

Table 4. Posterior estimates of denitrification, N_2O production, and NH_4^+ flux under restoration scenarios. HR = hydrologic reconnection, HR+D = hydrologic reconnection and dredging, CI = credible interval.

	Denitrification (μmol N m^{-2} h^{-1})			**N_2O production (μmol N m^{-2} h^{-1})**			**NH_4^+ flux (μmol N m^{-2} h^{-1})**		
	5% CI	**Mean**	**95% CI**	**5% CI**	**Mean**	**95% CI**	**5% CI**	**Mean**	**95% CI**
Control									
6 h	59.1	78.2	93.1	-0.008	0.029	0.065	59.8	168.7	275.0
12 h	67.0	87.2	102.0	0.034	0.070	0.105	239.4	351.2	456.1
HR									
6 h	24.7	40.9	56.0	0.045	0.082	0.118	289.6	396.0	505.6
12 h	7.0	24.8	41.1	0.017	0.052	0.090	-185.93	-77.4	31.7
HR+D									
6 h	37.9	56.0	71.5	0.119	0.154	0.190	-286.9	-180.3	-76.4
12 h	-2.4	14.7	30.1	-0.010	0.024	0.060	-173.9	-66.0	44.1

DISCUSSION

This study evaluated N cycling pathways in intact sediment cores from a restored wetland and the potential response of restoration activities on these processes. By analyzing N cycling in

experiments that represented different restoration scenarios, we modeled the potential effects of restoration on N cycling in the context of watershed nutrient management. N cycling was evaluated with a Bayesian analysis, which offers the advantage of providing probabilistic estimates of environmental processes by quantifying the uncertainty associated with modeled parameters (Kéry 2010).

We demonstrate that the west pond of the BLWRA, like other wetland systems, has a substantial capacity to remove N from the watershed via N_2 production (Saunders and Kalff 2001; Seitzinger et al. 2006). While the IPT model has the capacity to quantify both denitrification and anammox, denitrification was the only N_2 production process detected in this system. The absence of anammox activity is not surprising, as denitrification tends to outcompete anammox in organic-rich sediments (Ahn 2006; Algar and Vallino 2014). Indeed, sediment in this location in the BLWRA contains a high amount of organic matter (~20 % by mass), and this organic content is consistent from 0 to 43 cm depth (Steinman and Ogdahl 2016). Further, while anammox is a prominent N removal process in marine environments, it has been observed at a much lower frequency in freshwaters (Burgin and Hamilton 2007; Hu et al. 2011).

Denitrification rates differed significantly among experimental treatments, which included introduction of water from Bear Creek and removal of sediments from intact cores. Across treatments, posterior estimates of denitrification rates varied over three orders of magnitude, indicating strong responsiveness of denitrification activity to hydrologic changes that is common to other wetland systems (Ardón et al. 2010a). When sediment cores were exposed to water from Bear Creek under simulated hydrologic reconnection (HR and HR+D treatments), there was a two-fold decrease in the mean denitrification rate relative to the control (Figure 8a, Table 4). This decreased rate could be due to a difference in NO_3^- supply via two mechanisms.

First, the concentration of NO_3^- in Bear Creek water was ~½ of that present in the wetland water column (Table 3). If these results are indicative of the BLWRA, they suggest that hydrologic reconnection would decrease the NO_3^- supply to denitrifiers in the sediment, resulting in lower rates of denitrification (Tiedje et al. 1982). Second, the NH_4^+ concentration in the stream was ~20 times lower than that of the wetland, and the rate of coupled nitrification-denitrification was significantly reduced under hydrologic reconnection scenarios (Figure 8b). This suggests that a dramatic decrease in NH_4^+ supply following hydrologic reconnection could limit nitrification activity, which in turn could limit the supply of NO_3^- to denitrification. Reconnection therefore may result in a decoupling of nitrification and denitrification, reducing the capacity for denitrification to remove N from the wetland.

Incubation length had a significant effect on denitrification and N_2O production under simulated hydrologic reconnection with dredging. Denitrification and N_2O production rates were greater for the 6 h duration than for the 12 h duration in the HR+D scenario. While the removal of wetland sediments throughout the range of depths encompassed by dredging activities (5 cm this study, ~0.5 m expected) is not expected to alter the quantity of organic matter in the surface sediment (Steinman and Ogdahl 2016), physical disturbance and reoxygenation of the sediment has been shown liberate labile pools of particulate and dissolved carbon and N (Aller 1994). The stimulation of denitrification and N_2O production shortly following dredging could represent rapid utilization of newly exposed substrates followed by a return to more modest rates as rate-limiting substrates are consumed. In the context of restoration, we may expect dredging to result in a temporary spike in N_2 and N_2O production prior to a return to a *quasi*-equilibrium characterized by more moderate rates (Morse et al. 2012).

In general, the BLWRA displayed N_2O production typical of wetland environments (Huttunen et al. 2003; Morse et al. 2012; Audet et al. 2014), and changes in N_2O production were suggestive of changes in substrate availability in the context of restoration activities. For a wetland that has historically been subject to high levels of nutrient loading, denitrification was remarkably efficient; the proportion of N lost as N_2O (0.06 to 0.21 %) is typical of benthic sediments that are not heavily nutrient-impacted (Seitzinger and Kroeze 1998). While the N_2O:N_2 ratio remained comparatively low across all restoration scenarios, a threefold increase in the proportion of N lost as N_2O and a spike in N_2O production in the HR+D scenario is indicative of a decrease in the degree to which denitrification proceeds to completion. This observation could relate to a change in the energetic yield of N_2O reduction compared to other steps in denitrification following sediment disturbance (Tiedje et al. 1982), which could result in a brief yet substantial increase in greenhouse gas production by the wetland following restoration.

Restoration scenarios resulted in a shift from net NH_4^+ release to net NH_4^+ uptake from BLWRA sediments, providing insight into the behavior of nitrification in this system. In the absence of hydrologic reconnection, NH_4^+ was released from the sediment and high NH_4^+ concentrations were present in the water, indicating there was ample NH_4^+ supply provided by mineralization to fuel nitrification. With a non-limiting supply of NH_4^+, nitrification supplied a steady source of NO_3^- for denitrification as indicated by high coupled nitrification-denitrification rates in the Control scenario. Under conditions of hydrologic reconnection, however, the supply of NH_4^+ from the overlying water decreased by 20-fold, and the sediments shifted from net NH_4^+ release to net NH_4^+ uptake from the 6 h to the 12 h incubation duration in the HR scenario and displayed net uptake of NH_4^+ throughout both incubation durations in the HR+D scenario. This shift suggests that demand for NH_4^+ by nitrification exceeded its supply, resulting in less NO_3^-

generated by nitrification. Coupled nitrification-denitrification was thus hindered and total denitrification rates decreased.

To estimate the possible changes in the NO_3^- and NH_4^+ load to Bear Lake that would result from reconnecting the wetland to Bear Creek, we modeled several scenarios relating the N cycling capacity of the wetland sediment to the N load from Bear Creek. These scenarios are hypothetical, as our experiments were conducted prior to current restoration efforts. However, the modeling does offer opportunities to evaluate the impacts of management decisions, develop a baseline for expectations about downstream nutrient delivery, and monitor progress in the context of expected impacts (Maack 2001). We evaluated NO_3^- mitigation capacity as the proportion of stream nitrate removed by the wetland ($NO_{3\text{-}rem}^-$):

$$NO_{3-\mathrm{rem}}^- = \frac{\text{denitrification rate} \cdot \text{wetland sediment surface area}}{\text{stream } NO_3^- \cdot \text{stream discharge} \cdot \text{fraction}} \tag{11}$$

where the denitrification rate under restoration scenarios (μmol m^{-2} h^{-1}) was incorporated as the posterior estimate of the mean and 95 % credible interval, wetland sediment surface area (m^2) and measured stream NO_3^- concentration (μmol L^{-1}) were incorporated as constant parameters, and stream discharge (L h^{-1}) was incorporated as the mean discharge rate of Bear Creek (Cadmus Group and AWRI 2007). A "fraction" term was added to represent the portion of Bear Creek water that will enter the wetland following hydrologic reconnection, which is currently unknown but will be engineered to maximize hydrologic exchange. A range of fractions between 0.1 and 1 were thus incorporated to represent the maximum probable range of hydrologic exchange between Bear Creek and the wetland. NH_4^+ retention capacity was modeled similarly by replacing the denitrification rate and stream NO_3^- concentration with NH_4^+ flux rate and stream NH_4^+ concentration.

The BLWRA has the potential to intercept a substantial amount of NO_3^- and NH_4^+ from Bear Creek. Wetland denitrification can remove up to 10 % of stream NO_3^- (Figure 9a), providing a potential water quality benefit to downstream Bear and Muskegon Lakes given sufficient diversion of Bear Creek water through the wetland. Although several studies have reported the capacity of riparian wetlands to remove up to 100 % of NO_3^- inputs (Fennessy and Cronk 1997; Ardón et al. 2010a), clearly this assumption cannot be made across all wetland restoration settings. Although BLWRA denitrification rates are typical of many wetland environments, the NO_3^- load and discharge from Bear Creek are sufficiently high to limit the capacity for denitrifying bacteria to fully consume stream NO_3^-. An *a priori* assessment of the wetland N removal capacity, as was conducted here, can therefore be helpful in establishing expectations for the potential impact of restoration activities on water quality. Three out of four restoration scenarios project a net uptake of NH_4^+, translating to a capacity of the wetland to retain all incoming NH_4^+ from Bear Creek, potentially with an initial pulse of NH_4^+ released from the wetland following hydrologic reconnection (Figure 9b). These results are consistent with previous studies, which suggest is not uncommon for wetlands to shift back and forth between the retention and release of NH_4^+ following restoration (Ardón et al. 2010a).

Restoration activities in the BLWRA are predicted to result in major changes in N cycling, illustrating a probable shift in the biogeochemistry of this watershed. However, restoration activities must be evaluated in the context of P cycling in addition to N cycling. Analysis by Smit and Steinman (2015) indicates that hydrologic reconnection could result in enhanced release of P to downstream Bear Lake (20 to 81 µmol P m^{-2} h^{-1} across treatments), while dredging activities could substantially limit this release owing to the exposure of sediments with higher P sorption capacity. While it appears that P loading will likely remain an ongoing

issue for the eutrophication of Bear Lake, restoration activities are predicted to decrease downstream N loading from the BLWRA. Our analyses indicate that N retention and removal in this wetland depend on nitrification; hydrologic reconnection could reduce the supply of NH_4^+ available for nitrification, resulting in a shift from net NH_4^+ release to uptake and a decoupling of nitrification and denitrification. Despite the decreased rate of permanent N removal from the wetland under restoration scenarios, the total projected amount of N removed from the wetland via denitrification is roughly equivalent to the total projected amount of P released. Furthermore, the magnitude of NH_4^+ uptake under restoration scenarios is tenfold that of denitrification and P release, demonstrating a high capacity for the wetland to reduce downstream N loading. The marked shift in N cycling displayed here indicates that nitrification is a strong regulator of permanent N removal that can be heavily influenced by NH_4^+ availability.

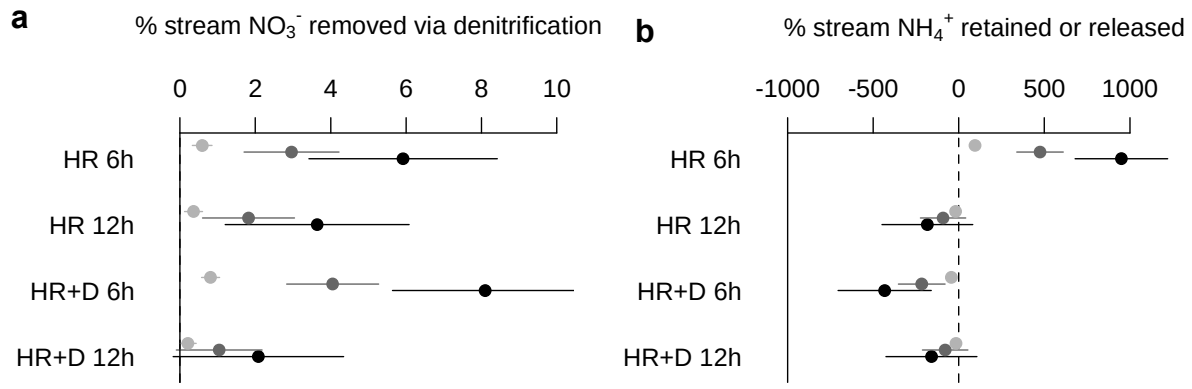

Figure 9. (a) NO_3^- and (b) NH_4^+ mitigation capacity of the wetland with respect to the potential load delivered by Bear Creek. Denitrification and NH_4^+ flux were measured from incubations of 6 and 12 h duration under restoration scenarios of simulated hydrologic reconnection (HR) and simulated hydrologic reconnection with dredging (HR+D). Closed circles represent the mean of the posterior estimate for each treatment-duration combination. Lines represent the 95 % credible interval around each posterior mean estimate. Fractions of Bear Creek water reaching the wetland sediment (0.1, 0.5, and 1.0) are represented by light gray, dark gray, and black lines, respectively.

Changes in wetland N cycling carry implications for downstream receiving water bodies. In the case of Bear Lake, as well as other lakes that are either limited by N or co-limited by P and N (Paerl et al. 2016), reducing N loads through reconnection may drive the lake to stronger N limitation, which may contribute to larger blooms of toxic cyanobacteria (Chaffin and Bridgeman 2014). However, because reduced forms of N are needed for toxin production genes to be expressed (Kuniyoshi et al. 2011), N cycling in the BLWRA may actually inhibit bloom toxicity, even as the reduction in N concentrations stimulates bloom formation. These results, in combination with those of Smit and Steinman (2015) and Steinman and Ogdahl (2016) suggest that nutrient management must consider both N and P, not just a single nutrient (Conley et al. 2009; Paerl et al. 2016). The current study provides a mechanistic understanding of N mitigation in a wetland undergoing restoration, and reveals that future studies need to investigate not only denitrification but also the processing of NH_4^+ and its effects on nitrification.

LITERATURE CITED

LITERATURE CITED

Ahn Y-H (2006) Sustainable nitrogen elimination biotechnologies: A review. Process Biochem 41:1709-1721. doi:10.1016/j.procbio.2006.03.033

Aldous A, McCormick C, Ferguson C, Graham S, Craft C (2005) Hydrologic regime controls soil phosphorus fluxes in restoration and undisturbed wetlands. Restor Ecol 13:341-347.

Algar CK, Vallino JJ (2014) Predicting microbial nitrate reduction pathways in coastal sediments. Aquat Microb Ecol 71:223-238. doi:10.3354/ame01678

Aller RC (1994) Bioturbation and remineralization of sedimentary organic matter: Effects of redox oscillation. Chem Geol 114:331-345.

APHA (2005) Standard methods for the examination of water and wastewater. American Public Health Association, Washington, D.C.

Ardón M, Morse JL, Doyle MW, Bernhardt ES (2010a) The water quality consequences of restoring wetland hydrology to a large agricultural watershed in the southeastern coastal plain. Ecosystems 13:1060-1078. doi:10.1007/s10021-010-9374-x

Ardón M, Montanari S, Morse JL, Doyle MW, Bernhardt ES (2010b) Phosphorus export from a restored wetland ecosystem in response to natural and experimental hydrologic fluctuations. J Geophys Res 115:G04031. doi:10.1029/2009JG001169

Audet J, Hoffman CC, Andersen PM, Baattrup-Pedersen A, Johansen JR, Larsen SE, Kjaergaard C, Elsgaard L (2014) Nitrous oxide fluxes in undisturbed riparian wetlands located in agricultural catchments: Emission, uptake and controlling factors. Soil Biol Biochem 68:291-299. doi:10.1016/j.soilbio.2013.10.011

Bunn SE, Arthington AH (2002) Basic principles and ecological consequences of altered flow regimes for aquatic biodiversity. Environ Manage 30(4):492-507. doi:10.1007/s00267-002-2737-0

Burgin AJ, Hamilton SK (2007) Have we overemphasized the role of denitrification in aquatic ecosystems? A review of nitrate removal pathways. Front Ecol Environ 5(2):89-96.

Cadmus Group, AWRI (2007) Bear Lake Nutrient Study; U.S. Environmental Protection Agency, Contract No. 68-C-02-109.

Carpenter SR, Caraco NF, Correll DL, Howarth RW, Sharpley AN, Smith VH (1998) Nonpoint pollution of surface waters with phosphorus and nitrogen. Ecol Appl 8(3):559-568.

Chaffin JD, Bridgeman TB (2014) Organic and inorganic nitrogen utilization by nitrogen-stressed cyanobacteria during bloom conditions. J Appl Phycol 26:299-309. doi:10.1007/s10811-013-0118-0

Conley DJ, Paerl HW, Howarth RW, Boesch DF, Seitzinger SP, Havens KE, Lancelot C, Likens GE (2009) Controlling eutrophication. Science 323:1014−1015.

Dahl TE (2000) Status and trends of wetlands in the conterminous United States 1986-1997. U.S. Department of the Interior, Fish and Wildlife Service; Washington, D.C.

Dalsgaard T, Nielsen LP, Brotas V, Viaroli P, Underwood G, Nedwell D, Sundbäck K, Rysgaard S, Miles A, Bartoli M, Dong L, Thornton DCO, Ossosen LDM, Castaldelli G, Risgaard-Petersen N (2000) Protocol handbook for NICE- Nitrogen cycling in estuaries. National Environmental Research Institute, Silkeborg, Denmark.

Erler DV, Eyre BD, Davidson L (2008) The contribution of anammox and denitrification to sediment N_2 production in a surface flow constructed wetland. Environ. Sci. Technol. 42:9144-9150. doi:10.1021/es801175t

Eyre BD, Rysgaard S, Dalsgaard T, Christensen PB (2002) Comparison of isotope pairing and N_2:Ar methods for measuring sediment denitrification: Assumptions, modifications and implications. Estuaries 25(6A):1077-1087.

Fennessy MS, Cronk JK (1997) The effectiveness and restoration potential of riparian ecotones for the management of nonpoint source pollution, particularly nitrate. Crit Rev Env Sci Tec 27(4):285-317. doi:10.1080/10643389709388502

Hamilton SK, Ostrom NE (2007) Measurements of the stable isotope ratio of dissolved N_2 in ^{15}N tracer experiments. Limnol Oceanogr Methods 5:233-240.

Hsu T-C, Kao S-J (2013) Technical note: Simultaneous measurement of sedimentary N_2 and N_2O production and new ^{15}N isotope pairing technique. Biogeosciences 10:7847-7862. doi:10.5194/bg-10-7847-2013

Hu B-I, Shen L, Xu X, Zheng P (2011) Anaerobic ammonium oxidation (anammox) in different natural ecosystems. Biochem Soc Trans 39:1811-1816. doi:10.1042/BST20110711

Humbert S, Zopfi J, Tarnawski S-E (2012) Abundance of anammox bacteria in different wetland soils. Environ. Microbiol. Rep. 4(5):484-490. doi:10.1111/j.1758-2229.2012.00347.x

Huttunen JT, Juutinen S, Alm J, Larmola T, Hammar T, Silvola J, Martikainen PJ (2003) Nitrous oxide flux to the atmosphere from the littoral zone of a boreal lake. J Geophys Res 108(D14):4421. doi:10.1029/2002JD002989

IPCC (2007) Climate Change 2007: The Physical Science Basis. In: Solomon S et al (eds) Contribution of Working Group I to the Fourth Assessment Report of the Intergovernmental Panel on Climate Change. Cambridge University Press, New York.

Keddy PA (2000) Wetland Ecology: Principles and Conservation, 1st ed.. Cambridge University Press, Cambridge, U.K.

Kéry M (2010) Introduction to WinBUGS for Ecologists: Bayesian Approach to Regression, ANOVA, Mixed Models and Related Analyses. Academic Press, Cambridge, MA, U.S.

Knowles R (1982) Denitrification. Microbiological Rev 46(1):43-70

Kuniyoshi TM, Gonzalez A, Lopez-Gomollon S, Valladares A, Bes MT, Fillat MF, Peleato ML (2011) 2-oxoglutarate enhances NtcA binding activity to promoter regions of the microcystin synthesis gene cluster. FEBS Lett 585(24):3921−3926.

Lindenberg MK, Wood TM (2006) Water quality of a drained wetland, Caledonia Marsh on upper Klamath Lake, Oregon, after flooding in 2006. U. S. Geological Survey, Oregon.

Maack JN (2001) Scenario analysis: a tool for task managers. In: Krueger RA, Casey MA, Donner J, Kirsch S, Maack JN (eds) Social Analysis Selected Tools and Techniques. The World Bank, Washington, D.C. pp 62-86.

Morse JL, Ardón M, Bernhardt ES (2012) Greenhouse gas fluxes in southeastern U.S. coastal plain wetlands under contrasting land uses. Ecol Appl 22(1):264-280.

Newman S, Pietro K (2001) Phosphorus storage and release in response to flooding: implications for Everglades stormwater treatment areas. Ecol Engineer 18:23-38.

Nielsen LP (1992) Denitrification in sediment determined from nitrogen isotope pairing. FEMS Microbiol Ecol 86:357-362.

Paerl HW, Scott JT, McCarthy MJ, Newell SE, Gardner WS, Havens KE, Hoffman DK, Wilhelm SW, Wurtsbaugh WA (2016) It takes two to tango: When and where dual nutrient (N & P) reductions are needed to protect lakes and downstream ecosystems. Environ Sci Technol 50(20):10805-10813. doi:10.1021/acs.est.6b02575

Pant HK, Reddy KR (2003) Potential internal loading of phosphorus in a wetland constructed in agricultural land. Water Res 37:965–72.

Reddy KR, Kadlec RH, Flaig E, Gale PM (1999) Phosphorus retention in streams and wetlands: A review. Crit Rev Env Sci Tec 29(1):83-146.

Risgaard-Petersen N, Nielsen LP, Rysgaard S, Dalsgaard T, Meyer RL (2003) Application of the isotope pairing technique in sediments where anammox and denitrification coexist. Limnol Oceanogr Methods 1:63-73.

Saunders DL, Kalff J (2001) Nitrogen retention in wetlands, lakes, and rivers. Hydrobiologia 443:205-212. doi:10.1023/A:1017506914063

Schindler DW (1974) Eutrophication and recovery in experimental lakes: implications for lake management. Science 184:897-899.

Scott JT, McCarthy MJ, Gardner WS, Doyle RD (2008) Denitrification, dissimilatory nitrate reduction to ammonium, and nitrogen fixation along a nitrate concentration gradient in a created freshwater wetland. Biogeochemistry 87:99-111. doi:10.1007/s10533-007-9171-6

Seitzinger SP, Kroeze C (1998) Global distribution of nitrous oxide production and N inputs in freshwater and coastal marine ecosystems. Global Biogeochem Cy 12(1):93-113.

Seitzinger S, Harrison JA, Böhlke JK, Bouwman AF, Lowrance R, Peterson B, Tobias C, Van Drecht G (2006) Denitrification across landscapes and waterscapes: A synthesis. Ecol Appl 16(6):2064-2090.

Smit JT, Steinman AD (2015) Wetland sediment phosphorus flux in response to proposed hydrologic reconnection and warming. Wetlands 35:655-665. doi:10.1007/s13157-015-0655-1

Steffen MM, Belisle BS, Watson SB, Boyer GL, Wilhelm SW (2014) Status, causes and controls of cyanobacterial blooms in Lake Erie. J Great Lakes Res 40:215-225. doi:10.1016/j.jglr.2013.12.012

Steinman AD, Ogdahl ME (2011) Does converting agricultural fields to wetlands retain or release phosphorus? J N Am Benthol Soc 30:820-830.

Steinman AD, Ogdahl ME (2016) From wetland to farm and back again: phosphorus dynamics of a proposed restoration project. Environ Sci Pollut Res 23(22):22596-22605. doi:10.1007/s11356-016-7485-4

Su Y-S, Yajima M (2015) R2jags: A Package for Running jags from R. R package version 0.05-01. http://CRAN.R-project.org/package=R2jags

Sun WG, Sun ZG, Gan ZT, Sun WL, Wang W (2014) Contribution of different processes in wetland soil N_2O production in different restoration phases of the Yellow River estuary, China. Huanjing Kexue 35(8):3110-3119.

Thamdrup B, Dalsgaard T (2002) Production of N_2 through anaerobic ammonium oxidation coupled to nitrate reduction in marine sediments. Appl Environ Microbiol 68:1312-1318. doi:10.1128/AEM.68.3.1312-1318.2002

Tiedje JM, Sexstone AJ, Myrold DD, Robinson JA (1982) Denitrification: Ecological niches, competition and survival. Antonie van Leeuwenhoek 48:569-583.

Trimmer M, Risgaard-Petersen N, Nicholls JC, Engström P (2006) Direct measurement of anaerobic ammonium oxidation (anammox) and denitrification in intact sediment cores. Mar Ecol Prog Ser 326:37-47.

Turner TF, Collyer ML, Krabbenhoft TJ (2010) A general hypothesis-testing framework for stable isotope ratios in ecological studies. Ecology 91(8):2227-2233.

[USDA] U. S. Department of Agriculture (2012) Restoring America's Wetlands : A Private Lands Conservation Success Story. U.S. Department of Agriculture, Washington, D.C.

[USEPA] U.S. Environmental Protection Agency (2013) Great Lakes Areas of Concern: Muskegon Lake. U.S. Environmental Protection Agency, Washington, D.C.

van de Graaf AA, Mulder A, de Bruijn P, Jetten MSM, Robertson LA, Kuenen JG (1995) Anaerobic oxidation of ammonium is a biologically mediated process. Appl Environ Microbiol 61:1246-1251.

Waki M, Yasuda T, Suzuki K, Komada M, Abe K (2015) Distribution of anammox bacteria in a free-water-surface constructed wetland with wild rice (Zizania latifolia). Ecol Eng 81:165-172. doi:10.1016/j.ecoleng.2015.04.005

Welti N, Bondar-Kunze E, Mair M, Bonin P, Wanek W, Pinay G, Hein T (2012)Mimicking floodplain reconnection and disconnection using ^{15}N mesocosm incubations. Biogeosciences 9:4263-4278. doi:10.5194/bg-9-4263-2012

Zelder JB, Kercher S (2005) Wetland resources: Status, trends, ecosystem services, and restorability. Annu Rev Environ Resour 30:39-74. doi:10.1146/annurev.energy.30.050504.144248

Zhu G, Wang S, Feng X, Fan G, Jetten MSM, Yin C (2011) Anammox bacterial abundance, biodiversity and activity in a constructed wetland. Environ Sci Tech 45:9951-9958. doi:10.1021/es202183w

Zhu G, Wang S, Wang W, Wang Y, Zhou L, Jian B, Op den Camp HJM, Risgaard-Petersen N, Schwark L, Peng Y, Hefting MM, Jetten MSM, Yin C (2013) Hotspots of anaerobic ammonium oxidation at land-freshwater interfaces. Nature Geoscience 6:103-107. doi:10.1038/NGEO1683

CHAPTER 3

UNEXPECTEDLY HIGH DEGREE OF ANAMMOX AND DNRA IN SEAGRASS SEDIMENTS: DESCRIPTION AND APPLICATION OF A REVISED ISOTOPE PAIRING TECHNIQUE

ABSTRACT

Understanding the magnitude of nitrogen (N) loss and recycling pathways is crucial for coastal N management efforts. However, quantification of denitrification and anammox by a widely-used method, the isotope pairing technique, is challenged when dissimilatory NO_3^- reduction to NH_4^+ (DNRA) occurs. In this study, we describe a revised isotope pairing technique that accounts for the influence of DNRA on NO_3^- reduction (R-IPT-DNRA). The new calculation procedure improves on previous techniques by (1) accounting for N_2O production, (2) distinguishing canonical anammox from coupled DNRA-anammox, and (3) including the production of $^{30}N_2$ by anammox in the quantification of DNRA. We apply this technique to simultaneously quantify rates of anammox, denitrification, and DNRA in intact sediments adjacent to a seagrass bed in subtropical Australia. The effect of organic carbon lability on NO_3^- reduction was also addressed by adding detrital sources with differing C:N (phytoplankton- or seagrass-derived). DNRA was the predominant pathway, contributing 49-74% of total NO_3^- reduction (mean 0.42 μmol N m^{-2} h^{-1}). In this high C:N system, DNRA outcompetes denitrification for NO_3^-, functioning to recycle rather than remove N. Anammox exceeded denitrification (mean 0.18 and 0.04 μmol N m^{-2} h^{-1}, respectively) and accounted for 64-86% of N loss, a rare high percentage in shallow coastal environments. Owing to low denitrification activity, N_2O production was ~100-fold lower than in other coastal sediments (mean 7.7 nmol N m^{-2} h^{-1}). All NO_3^- reduction pathways were stimulated by seagrass detritus but not by phytoplankton detritus, suggesting this microbial community is adapted to process organic matter

that is typically encountered. Our new model, the R-IPT-DNRA, is widely applicable in other environments where the characterization of co-existing NO_3^- reduction pathways is desirable.

INTRODUCTION

Coastal ecosystems are important regions of nitrogen (N) loss, the conversion of bioavailable N to gaseous N, particularly as N loading to marine environments has intensified in response to agricultural activities (Schlesinger 2009). While it is known that coastal systems remove significant quantities of inorganic N from watershed loading (e.g., Seitzinger et al. 2006; Murray et al. 2015; Eyre et al. 2016), the magnitudes, pathways, and environmental controls on N loss are not completely resolved. The potential for natural microbial processes to mitigate the detrimental effects of N loading such as eutrophication and harmful algal blooms will depend on a more complete understanding of N loss mechanisms in coastal environments (Howarth 2008).

Denitrification via the respiratory reduction of NO_3^- to N_2 is generally recognized as the predominant mechanism for N loss in coastal marine systems (Seitzinger et al. 2006). This heterotrophic process occurs in hypoxic to anoxic environments and requires a supply of NO_3^- and organic carbon (Knowles 1982). A variable but usually small fraction of reduced NO_3^- is not fully reduced to N_2 and is released as N_2O, a potent greenhouse gas with nearly 300 times the global warming potential of CO_2 over a 100-year timespan (IPCC 2007). The factors regulating the N_2O:N_2 production ratio include O_2 concentration, carbon availability, and substrate concentration (Betlach and Tiedje 1981; Knowles 1982; Davidson and Verchot 2000; Hwang et al. 2006), although the relative importance of these factors in concert is not well understood (Murray et al. 2015).

An alternate N loss pathway, anaerobic ammonium oxidation (anammox), was discovered only two decades ago (van de Graaf et al. 1995) and has since been recognized as a globally important process that rivals denitrification in its removal of N from offshore marine systems. A chemoautotrophic process, anammox produces N_2 via the reaction of NO_2^- and NH_4^+ with no direct organic carbon demand. Anammox does not produce an appreciable amount of N_2O (Kartal et al. 2012). Anammox is now estimated to contribute 1/3 to 1/2 of global marine N loss from sediments and anoxic water columns (Dalsgaard et al. 2005). However, owing to its recent discovery, the environmental controls of anammox in a variety of natural environments are not well constrained, particularly as they relate to the interplay between anammox and denitrification.

The isotope pairing technique (IPT) is a widely used technique for measuring N loss rates (i.e., those that would naturally occur in the absence of ^{15}N addition) from aquatic sediments. The original isotope pairing technique quantifies N_2 production via denitrification (Fig. 10a; Nielsen 1992). Following the discovery of anammox as an additional N_2 production pathway, a revision to the isotope pairing technique (R-IPT) that distinguished N_2 production by denitrification and anammox was developed (Fig. 10a; Risgaard-Petersen et al. 2003). Contemporary applications of the isotope pairing technique utilize the R-IPT rather than the IPT. An addition to the isotope pairing technique has enabled the quantification of N_2O production (IPT_{anaN2O}; Fig. 10b; Hsu and Kao 2013). In practice, the isotope pairing technique is carried out by adding $^{15}NO_3^-$ to the ambient NO_3^- pool of a sediment slurry, water sample, or intact sediment core. Supposing random isotope pairing, rates of denitrification and anammox are then calculated based on the $^{14}N/^{15}N$ ratio in the NO_3^- pool undergoing reduction (r_{14}) and the isotopic composition of nitrogenous end products (N_2 and N_2O).

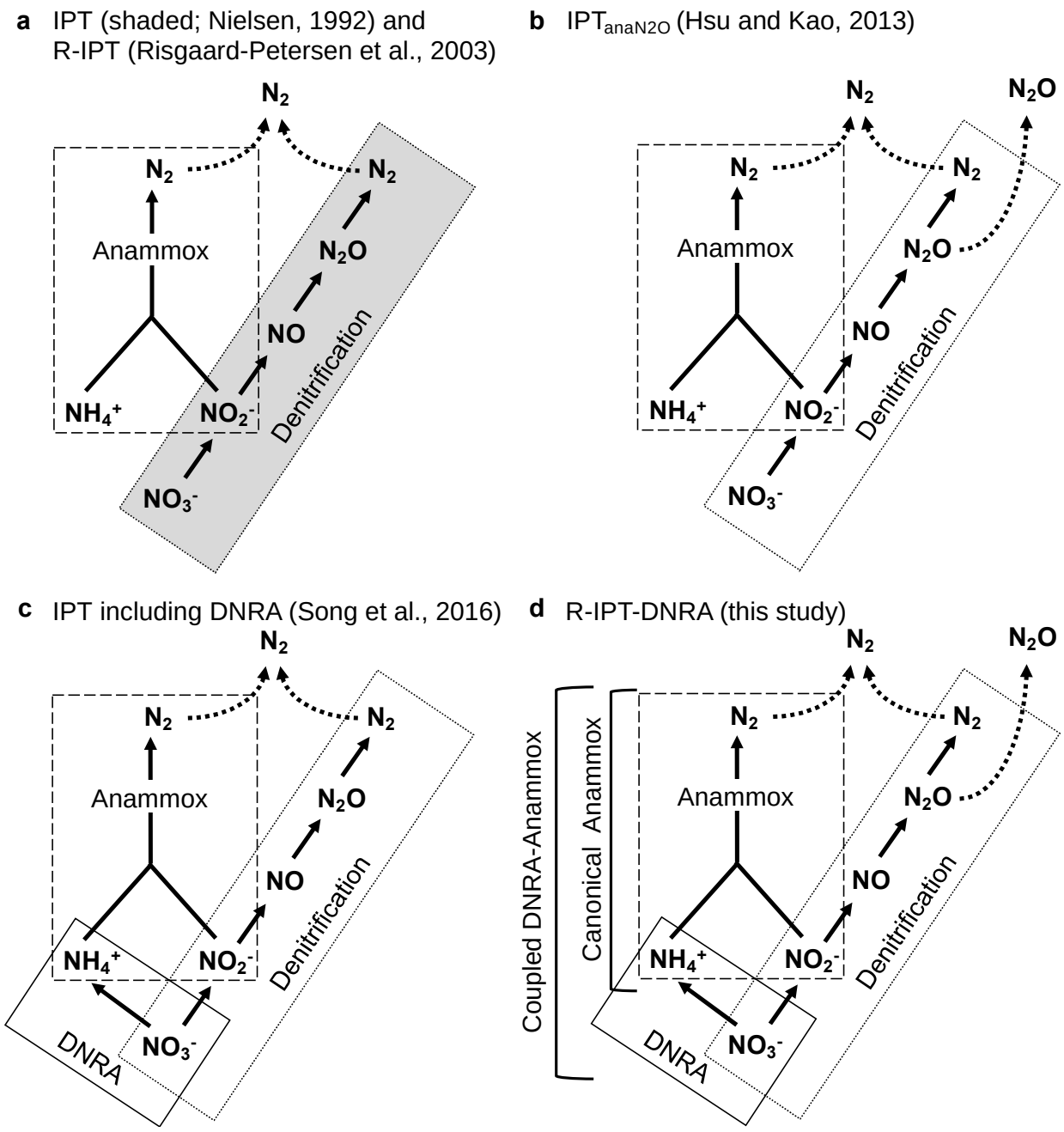

Figure 10. (a) The original IPT model (shaded; Nielsen 1992) that quantifies N_2 production via denitrification and a subsequent revision to the IPT (R-IPT; Risgaard-Petersen et al., 2003) that includes the production of N_2 via anammox as well as denitrification. (b) The IPT_{anaN2O} model (Hsu and Kao 2013), which adds the capacity to quantify N_2O production via denitrification to the R-IPT. (c) A revision to the IPT model (Song et al. 2016) which enables quantification of the production of NH4+ via DNRA to the R-IPT. (d) The R-IPT-DNRA model (this study), which adds the ability to quantify N_2O production via denitrification and NH_4^+ production via DNRA to the R-IPT while simultaneously distinguishing canonical anammox and coupled DNRA-anammox.

In addition to N loss via denitrification and anammox in coastal sediments, N recycling processes can compete with N loss pathways for inorganic N substrates. The dissimilatory reduction of NO_3^- to NH_4^+ (DNRA) has a similar energetic yield as denitrification and also occurs under low O_2 conditions (Tiedje et al. 1982). DNRA makes up a significant proportion of total NO_3^- reduction in coastal sediments (Burgin and Hamilton 2007; Dong et al. 2011; Giblin et al. 2013) and tends to outcompete denitrification in high carbon, low NO_3^- systems (Algar and Vallino 2014; Kraft et al. 2014; Brin et al. 2015; Hardison et al. 2015; van den Berg et al. 2015). In coastal marine systems where DNRA dominates, N is retained rather than lost, which could result in sustained or enhanced eutrophication (Hardison et al. 2015).

A key assumption of the isotope pairing technique is that NO_3^- is the only appreciable source of ^{15}N, but this assumption is violated when $^{15}NH_4^+$ is produced by DNRA. The coupling of DNRA-anammox, in this case, results in production of $^{30}N_2$ that is incorrectly attributed to denitrification, resulting in an underestimate of anammox and an overestimate of denitrification. Song et al. (2016) have recently proposed a revision to the isotope pairing technique that simultaneously quantifies the NO_3^- reduction processes of denitrification, anammox, and DNRA, thus resolving the issues from the isotope pairing technique that occur when DNRA is active (Fig. 10c). This approach hinges on the evaluation of the ratio of $^{14}N/^{15}N$ in the NH_4^+ pool (r_{14a}). Further improvements to these models can be made by (1) quantifying N_2O production, (2) distinguishing coupled DNRA-anammox from uncoupled (canonical) anammox, and (3) including the production of $^{30}N_2$ by anammox in the quantification of DNRA (Fig. 10d).

Simultaneous quantification of denitrification, anammox, N_2O production, and DNRA will enable an examination of the competitive interactions among these processes under varying environmental conditions. For instance, organic carbon has been identified as a predominant

control on the relative importance of NO_3^- reduction pathways in marine systems (Algar and Vallino 2014). It is expected that anammox should dominate NO_3^- reduction at low C:N ratios, denitrification at intermediate C:N ratios, and DNRA at high C:N ratios (Thamdrup and Dalsgaard 2002; Dalsgaard et al. 2005; Algar and Vallino 2014; Hardison et al. 2015). However, this relationship is not definitive (Trimmer et al. 2003; Trimmer and Nicholls 2009), and few studies have simultaneously measured these processes (e.g., Erler et al. 2013), particularly with regard to carbon quality (i.e., C:N ratio and organic carbon lability).

There have been a number of N cycling studies in subtropical seagrass environments (e.g., Eyre et al. 2011a; 2011b; 2013; 2016), but to our knowledge, there have been no published studies on anammox rates or N_2O production in intact sediments from seagrass ecosystems. Further, seagrass ecosystems are exemplified by a largely refractory pool of organic carbon (Khan et al. 2015) that could serve as the basis of an investigation of the effect of carbon quality on N loss and recycling processes. While microbial activity is expected to be dampened in bare sediments compared to vegetated sediments, microbial communities tend to have similar taxonomic composition and metabolism in both settings (Boschker et al. 2000; Jones et al. 2003; Holmer et al. 2004). In addition, sediments adjacent to seagrass stands tend to have stable redox conditions (Enríquez et al. 2001), making them an ideal environment in which to apply a new revision to the IPT that includes denitrification, anammox, N_2O production, and DNRA.

This study has three objectives: (1) revise the isotope pairing technique to simultaneously quantify rates of anammox, denitrification, N_2O production, and DNRA; (2) generate the first estimates of anammox and N_2O production in intact sediments in a seagrass ecosystem; and (3) assess the competitive interactions among DNRA, denitrification, and anammox under differing organic carbon quality.

METHODS

Study site

This study was conducted in Shaws Bay, New South Wales, Australia (28.8675 S, 153.5871 E), a subtropical estuarine system. Throughout the course of the study, non-vegetated (i.e., no plant or root biomass) sediments were collected from in and around the edge of a seagrass bed (consisting primarily of *Zostera muelleri*) that covers approximately 0.02 km^2 of the eastern part of the bay (Ballina Shire Council 2000). Sediment and water collections took place in June and July 2014.

Sediment slurry incubations

The presence of anammox and denitrification activity in Shaws Bay sediments was evaluated by sediment slurry assays following the approach outlined in Thamdrup and Dalsgaard (2002) and Trimmer et al. (2003). Briefly, sediments from 0 – 10 cm depth were collected from the edge of the seagrass bed and homogenized. Sediments were then transferred to an anoxic glove box, combined in a 1:1 volumetric ratio with He-sparged site water, and pre-incubated overnight. Following pre-incubation, sediment slurries were incubated in 12 mL Exetainers™ without a headspace either unamended or after addition of $^{15}NH_4^+$, $^{15}NH_4^+ + {}^{14}NO_3^-$, or $^{15}NO_3^-$ at a concentration of 100 μM. Biological activity was halted with addition of 100 μL of saturated solution of $HgCl_2$ at 6 h intervals for a total of 18 h. The isotope ratio of N_2 was then analyzed using a Thermo Trace GC Ultra with a 30 m x 0.32 mm CarboPLOT column interfaced to a Thermo Delta V Plus isotope ratio mass spectrometer (IRMS). Anammox activity was confirmed by an increase in the isotope fraction of $^{29}N_2$ in the $^{15}NH_4^+ + {}^{14}NO_3^-$ and $^{15}NO_3^-$ incubations, and

denitrification activity was confirmed by an increase in the isotope fraction of $^{30}N_2$ in the $^{15}NO_3^-$ incubation (Appendix Fig. A5).

Intact sediment incubations

Intact sediment cores (21-30 cm depth) were collected in 9 cm i.d. transparent PVC tubes, leaving approximately 1 cm of water overlying each core. Upon return to the lab, sediment core tubes were placed into an enclosure containing site water held at *in situ* temperature (16.5 °C). Oxic conditions throughout the enclosure were maintained by bubbling, and water was circulated throughout the enclosure with an aquarium pump. The water inside the sediment core tubes was circulated throughout the experiment by magnetic stir bars placed 5 cm above the sediment surface and rotated just below the resuspension threshold by an external magnet. Sediment core tubes were left uncapped and pre-incubated overnight (Ferguson et al. 2004).

Immediately prior to initiation of the incubation, a sample for dissolved inorganic N (NH_4^+ and $NO_3^- + NO_2^-$, hereafter NO_x) analysis were taken from each core, filtered through a 0.45 μm cellulose acetate syringe filter into a 10 mL polyethylene vial, and frozen until analysis. Cores were then sealed with a cap equipped with a syringe port and a vent port with on-off valves. $^{15}N\text{-}NO_3^-$ was added to obtain a final concentration of 100 μM in the overlying water of each core via the syringe port. Cores were left either unamended (control) or amended with 1.5 g m^{-2} of dried seagrass or phytoplankton detritus, which was added through the syringe port. Seagrass detritus consisted of dead seagrass and epiphytes was collected from the benthos of Shaws Bay, rinsed with deionized water, dried at 60 °C, and ground finely with a mortar and pestle. This represented the type of detritus regularly encountered in the system. Phytoplankton

detritus consisted of laboratory-cultured phytoplankton that was rinsed and dried at 60 °C. The C and N contents of Shaws Bay sediment, seagrass detritus, and phytoplankton detritus were measured using a Thermo Finnigan Flash EA 1112 interfaced with a Thermo Conflo III and a Thermo Delta V Plus IRMS. Sediment from Shaws Bay had a C:N molar ratio of 20.1 (0.15% C; 0.008% N). Seagrass detritus had a C:N molar ratio of 40.7 (34.9% C; 1.0% N), and phytoplankton detritus had a C:N molar ratio of 7.7 (40.3% C; 6.1% N).

Cores were allowed to equilibrate for 30 min to ensure homogenization of the NO_3^- pool in the overlying water and NO_3^- reduction zone at the sediment-water interface (Dalsgaard et al. 2000). At intervals of 0, 6, 12, and 19.5 h, cores from each organic carbon treatment were sacrificed in triplicate. Dissolved oxygen concentration and pH of the overlying water were measured with a Hach HQ40D dissolved O_2/pH probe that was calibrated to manufacturer specifications prior to use. A final dissolved nutrient sample was collected, as above, and an additional 30 mL sample was filtered and frozen for $^{15}N\text{-}NH_4^+$ analysis. The top 2-4 cm of the core were then slurrified with a glass rod, and samples were collected for dissolved gas analysis. Samples for isotopic and concentration analysis of dissolved N_2 were collected in 12 mL Exetainers and 7 mL glass vials, respectively, to overflowing. 20 µL of a saturated solution of $HgCl_2$ was then added to halt biological activity, and the container was capped with a screw top septum (Exetainer) or a ground-glass stopper (glass vial) without a headspace. NO_2^- was not detected in samples, and thus inorganic N_2O production in response to $HgCl_2$ addition was not considered a concern. A 2 mL He headspace was added to the Exetainers at atmospheric pressure and allowed to equilibrate for at least 12 h prior to analysis. N_2 samples were stored underwater at *in situ* temperature until analysis to minimize diffusion of atmospheric N_2 during storage. Samples for the isotopic and concentration analysis of N_2O were introduced by siphon into 300

mL glass serum bottles to overflowing and capped without a headspace with screw cap septa. One mL of a saturated solution of $HgCl_2$ was added to halt biological activity. A 25 mL headspace of He was added at atmospheric pressure using a vent needle, and N_2O samples were allowed to equilibrate for least 12 h prior to analysis.

Analyses

Concentrations of NH_4^+ and NO_x were measured colorimetrically on a Lachat QuickChem 8000 four channel Flow Injection Analyzer according to Eyre (2000). Headspace gas samples from the Exetainers were analyzed for the isotopic composition of N_2 on a Thermo Trace GC Ultra with a 25 m x 0.32 mm PoraPLOT Q column interfaced to a Thermo Delta V Plus IRMS. Concentrations of dissolved N_2 were analyzed by membrane inlet mass spectrometry (Eyre et al. 2002). The concentration and isotopic composition of N_2O were analyzed by a Thermo Fisher GasBench II interfaced to a Thermo Delta V Plus IRMS following He sparging and cryogenic trapping. The isotopic composition of NH_4^+ was analyzed following oxidation to NO_2^- by hypobromite and subsequent reduction to N_2O by sodium azide and acetic acid according to Zhang et al. (2007). The isotope ratio of the N_2O was analyzed by IRMS as above. NO_2^- was not detected in the samples and did not require removal prior to $^{15}NH_4^+$ analysis.

IPT modeling

N_2 production via denitrification and anammox (P_{14}) was calculated according to the R-IPT (Figure 10a, Table 5; Risgaard-Petersen et al. 2003). N_2O production via denitrification was

calculated according to the IPT_{anaN2O} and was also included in P_{14} (Figure 10b, Table 5; Hsu and Kao 2013). The ratio of $^{14}NO_3^-$:$^{15}NO_3^-$ in the NO_3^- reduction zone (r_{14}) was estimated by determining the ratio of ^{14}N:^{15}N in N_2O. Unlike r_{14} derived from the NO_3^- pool, r_{14} derived from the N_2O pool produces values for N_2 and N_2O production that are independent from the amount of $^{15}NO_3^-$ added and allows for variation among individual cores (Trimmer et al. 2006). The r_{14} derived from N_2O thus represents a more direct representation of N undergoing reduction than r_{14} derived from NO_3^-.

If DNRA occurs, $^{15}NO_3^-$ is reduced to $^{15}NH_4^+$, introducing ^{15}N into the NH_4^+ pool. If ^{15}N labeling of the NH_4^+ pool is high enough, this violates a central assumption of the isotope pairing technique, as both denitrification and anammox are capable of producing $^{30}N_2$ if DNRA is active. The isotope pairing technique equations were therefore revised to account for the influence of DNRA, which we call the R-IPT-DNRA (Fig. 10d; Table 5). A key addition of this approach is the quantification of the degree of ^{15}N labeling of the NH_4^+ pool, namely the ratio of $^{14}NH_4^+$:$^{15}NH_4^+$ (r_{14a}). The R-IPT-DNRA utilizes r_{14a} to quantify production of $^{28}N_2$, $^{29}N_2$ (via coupled DNRA-anammox and canonical anammox), and $^{30}N_2$ by anammox, respectively:

$$A_{28} = (r_{14} * A_{29})/(r_{14}/r_{14a} + 1) \quad (12)$$

$$A_{29\text{-}DNRA} = A_{29}/(1 + r_{14a}/r_{14}) \quad (13)$$

$$A_{29\text{-}ana} = A_{29} - A_{29\text{-}DNRA} \quad (14)$$

$$A_{30} = (P_{29} - 2P_{30} * r_{14})/(r_{14a} - r_{14}) \quad (15)$$

Quantification of $A_{29\text{-}DNRA}$ and $A_{29\text{-}ana}$ enables the distinction of production of N_2 via coupled DNRA-anammox from canonical anammox, respectively:

$$A_{14\text{-}DNRA} = A_{29\text{-}DNRA} + 2A_{28} * (A_{29\text{-}DNRA}/A_{29}) \quad (16)$$

$$A_{14\text{-}ana} = 2A_{28} * (A_{29\text{-}ana}/A_{29}) \quad (17)$$

Detailed derivations of equations are listed in the Appendix.

Genuine DNRA rates were calculated as:

$$\text{DNRA} = r_{14}\,(P_{15NH4+} + A_{30}) \quad (18)$$

where P_{15NH4+} indicates the production in $^{15}NH_4^+$ over time and A_{30} indicates the production of $^{30}N_2$ by anammox (Table 5). Given the short length of the incubations and the fact that incubations were run in the dark, it is unlikely that significant assimilation of NO_3^- and subsequent remineralization of organic matter to NH_4^+ occurred. However, it is not possible to distinguish NO_3^- assimilation and subsequent remineralization to NH_4^+ from DNRA using the R-IPT-DNRA, so the rate of DNRA could include this coupled process.

Rates of N_2 production by anammox and denitrification and N_2O production by denitrification are together termed "total N loss." Adding the rate of DNRA to these processes is termed "total NO_3^- reduction."

Table 5. Parameters and equations used in the R-IPT (Risgaard-Petersen et al. 2003) and the R-IPT-DNRA.

Parameter	Designation	R-IPT	R-IPT-DNRA
P_{29}	Production of $^{29}N_2$ (measured directly)		
P_{30}	Production of $^{30}N_2$ (measured directly)		
P_{45}	Production of $^{45}N_2O$ (measured directly)		
P_{46}	Production of $^{46}N_2O$ (measured directly)		
r_{14}*	Ratio of $^{14}N/^{15}N$ in NO_3^- (measured directly in N_2O)		
r_{14a}	Ratio of $^{14}N/^{15}N$ in NH_4^+ (measured directly)		
D_{28}	Production of $^{28}N_2$ via denitrification	$r_{14}^2 \cdot P_{30}$	$r_{14}^2 \cdot (P_{30} - A_{30})$
D_{29}	Production of $^{29}N_2$ via denitrification	$2r_{14} \cdot P_{30}$	$2r_{14} \cdot (P_{30} - A_{30})$
D_{30}	Production of $^{30}N_2$ via denitrification	P_{30}	$P_{30} - A_{30}$
A_{28}	Production of $^{28}N_2$ via anammox	$r_{14} \cdot A_{29}$	$\frac{r_{14} \cdot A_{29}}{r_{14}/r_{14a}+1}$
A_{29}	Production of $^{29}N_2$ via anammox	$P_{29} - D_{29}$	$P_{29} - D_{29}$
$A_{29\text{-DNRA}}$	Production of $^{29}N_2$ via coupled DNRA-anammox	-	$\frac{A_{29}}{1 + r_{14a}/r_{14}}$
$A_{29\text{-ana}}$	Production of $^{29}N_2$ via canonical anammox	-	$A_{29} - A_{29\text{-DNRA}}$
A_{30}·**	Production of $^{30}N_2$ via anammox	-	$\frac{P_{29} - 2P_{30} \cdot r_{14}}{r_{14a} - r_{14}}$
D_{14}	Genuine N_2 production via denitrification	$2D_{28} + D_{29}$	$2D_{28} + D_{29}$
A_{14}	Genuine N_2 production via anammox	$2A_{28}$	$2A_{28} + A_{29\text{-DNRA}}$
$A_{14\text{-DNRA}}$	Genuine production of N_2 via coupled DNRA-anammox	-	$A_{29\text{-DNRA}} + 2A_{28} \cdot (A_{29\text{-DNRA}}/A_{29})$
$A_{14=ana}$	Genuine production of N_2 via canonical anammox	-	$2A_{28} \cdot (A_{29\text{-ana}}/A_{29})$
$D_{14\text{-N2O}}$***	Genuine N_2O production via denitrification	$r_{14} \cdot (2P_{46} + P_{45})$	$r_{14} \cdot (2P_{46} + P_{45})$
P_{14}	Total genuine $N_2 + N_2O$ production	$D_{14} + A_{14} + D_{14\text{-N2O}}$	$D_{14} + A_{14} + D_{14\text{-N2O}}$

*Estimated from the direct measurement of $^{14}N/^{15}N$ in N_2O (Trimmer et al. 2006)
**Modified from Song et al. (2013)
***From Hsu and Kao (2013)

Statistical modeling

A simple linear regression was used to evaluate a potential linear increase in the fraction of ^{15}N in NH_4^+ over time. The effect of carbon treatment and incubation duration on each N cycling rate was tested by main effects two-way ANOVA and analyzed in a Bayesian framework using the programs R (version 3.1.2) and JAGS (Su and Yajima, 2015). For each test, 1,200 Markov-chain Monte Carlo iterations were run on three chains after a burn-in of 200 and thinned by two, yielding 1,500 samples in the posterior distribution. Credible intervals (95%) were constructed around the mean of each treatment-time group. The probability of a significant difference between treatment-time groups was determined by calculating the proportion of iterations in which the posterior estimate of one group was smaller than another (Turner et al., 2010). The difference between groups was considered significant when less than 5% of the posterior estimates were smaller than those of another group.

RESULTS

Application of R-IPT-DNRA

An increase in ^{15}N was detected in the NH_4^+ pool in intact sediment cores, indicating DNRA was occurring in Shaws Bay sediments. The fraction of ^{15}N in the NH_4^+ pool increased linearly over time for control ($df = 8$, $p < 0.01$, $R^2 = 0.58$) and seagrass ($df = 8$, $p < 0.05$, $R^2 = 0.41$) treatments. Although there was a trend, there was insufficient replication to confirm a linear relationship for the phytoplankton treatment ($df = 1$, $p = 0.14$, $R^2 = 0.90$) (Fig. 11). The degree of $^{15}NH_4^+$ labeling was sufficient to generate the production of $^{30}N_2$ from anammox (A_{30}), which made up 6 – 87% of the total production of $^{30}N_2$ (P_{30}). When rates modeled by the R-IPT

were compared to those modeled by the R-IPT-DNRA, anammox rates across treatments were underestimated by 1.7 – 15.0% and denitrification rates across treatments were overestimated by 6.8 – 690.4% by the R-IPT (Fig. 12). The degree of overestimation of denitrification was tightly controlled by the proportion of $^{30}N_2$ (P_{30}) attributed to anammox (A_{30}) (Fig. 13). As a percentage of total anammox rates, DNRA-dependent anammox rates were 4.85 ± 1.85% for the control, 13.51 ± 1.96% for the phytoplankton treatment, and 3.17 ± 0.91% for the seagrass treatment.

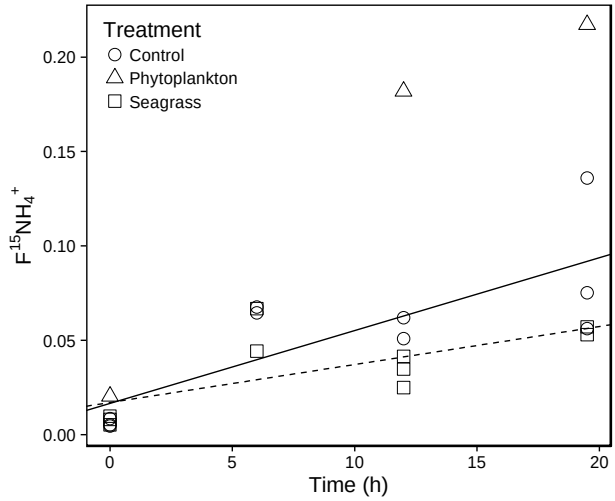

Figure 11. Increase in the fraction of ^{15}N in the NH_4^+ pool by treatment. $F^{15}NH_4^+$ increased linearly over time for control (df = 8, $p < 0.01$, $R^2 = 0.58$) and seagrass (df = 8, $p < 0.05$, $R^2 = 0.41$) treatments. Although there was a trend, there was insufficient replication to confirm a linear relationship for the phytoplankton treatment (df = 1, $p = 0.14$, $R^2 = 0.90$).

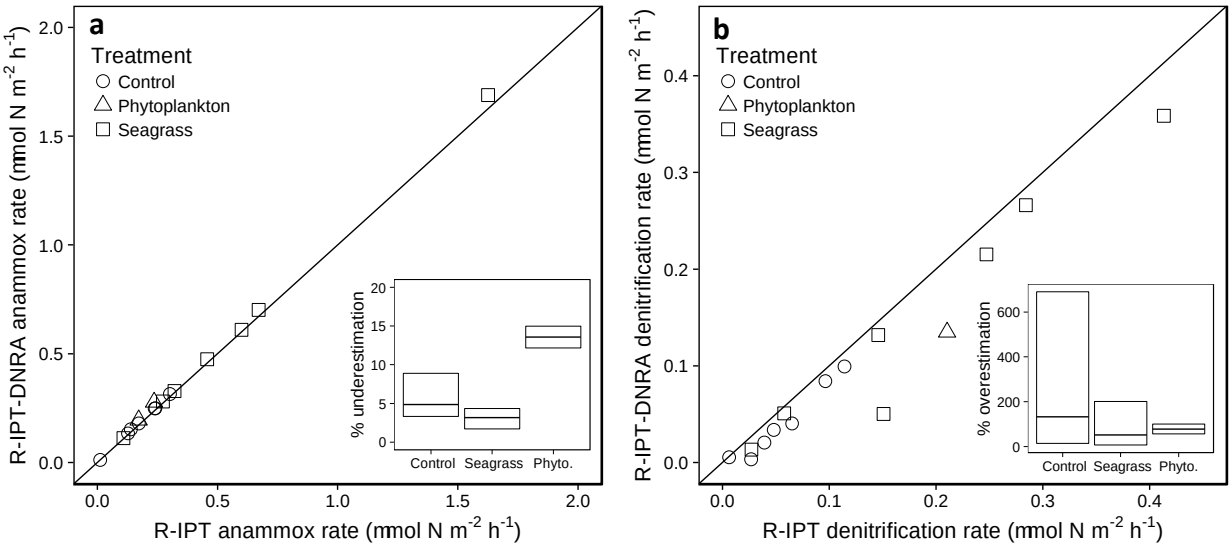

Figure 12. Comparison of (a) anammox and (b) denitrification rates from the R-IPT (Risgaard-Petersen et al. 2003) to rates from the R-IPT-DNRA method presented here for control, phytoplankton, and seagrass treatments. The solid line represents a 1:1 relationship. Insets represent the total range of under/overestimation by anammox and denitrification across treatments, with the mean represented by the thick line.

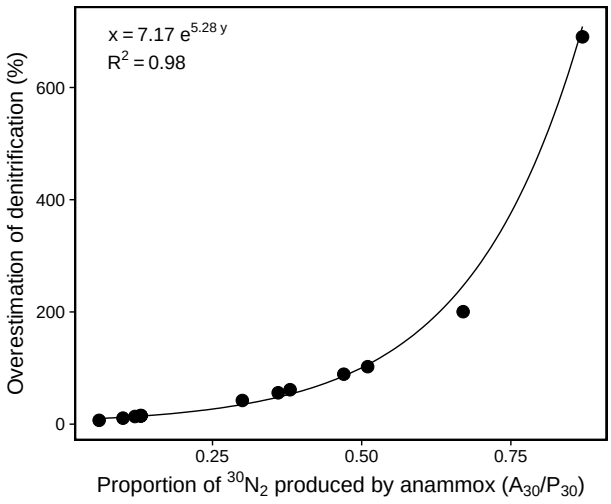

Figure 13. Overestimation of denitrification rate (D_{14}) by the R-IPT model compared to the R-IPT-DNRA model as a function of the production of $^{30}N_2$ by anammox relative to total $^{30}N_2$ production (A_{30}/P_{30}).

Rates of NO_3^- reduction processes

DNRA rates (mean ± SD) were 0.42 ± 0.22, 0.88 ± 0.60, and 1.03 ± 0.90 μmol N m^{-2} h^{-1} for control, phytoplankton, and seagrass treatments, respectively (Fig. 14a). Anammox rates were 0.18 ± 0.10, 0.26 ± 0.10, and 0.60 ± 0.52 μmol N m^{-2} h^{-1} for control, phytoplankton, and seagrass treatments, respectively (Fig. 14b). Denitrification rates were 0.04 ± 0.04, 0.08 ± 0.08, and 0.16 ± 0.13 μmol N m^{-2} h^{-1} for control, phytoplankton, and seagrass treatments, respectively (Fig. 14c). N_2O production was 0.008 ± 0.004, 0.012 ± 0.014, and 0.018 ± 0.018 μmol N m^{-2} h^{-1} for control, phytoplankton, and seagrass treatments, respectively (Fig. 14d). However, rates of NO_3^- reduction were not uniform across incubation duration, and figures are divided by incubation duration to illustrate these differences. The addition of seagrass detritus resulted in significantly greater rates of anammox, denitrification, and DNRA in the first 6 h of the incubation relative to the control ($p < 0.05$), whereas the addition of phytoplankton detritus did not result in greater rates of N cycling compared to the control. DNRA was the most important NO_3^- reduction process, comprising 49-74% of total NO_3^- reduction across carbon treatments and incubation durations (Fig. 15a). Proportions of N loss processes were also similar across treatment and incubation duration (Fig. 15b). N_2 production by anammox comprised 13-38% of NO_3^- reduction and 64-86% of total N loss, whereas N_2 production by denitrification comprised 6-13% of NO_3^- reduction and 11-31% of total N loss. N_2O production comprised < 3% of NO_3^- reduction < 9% of total N loss.

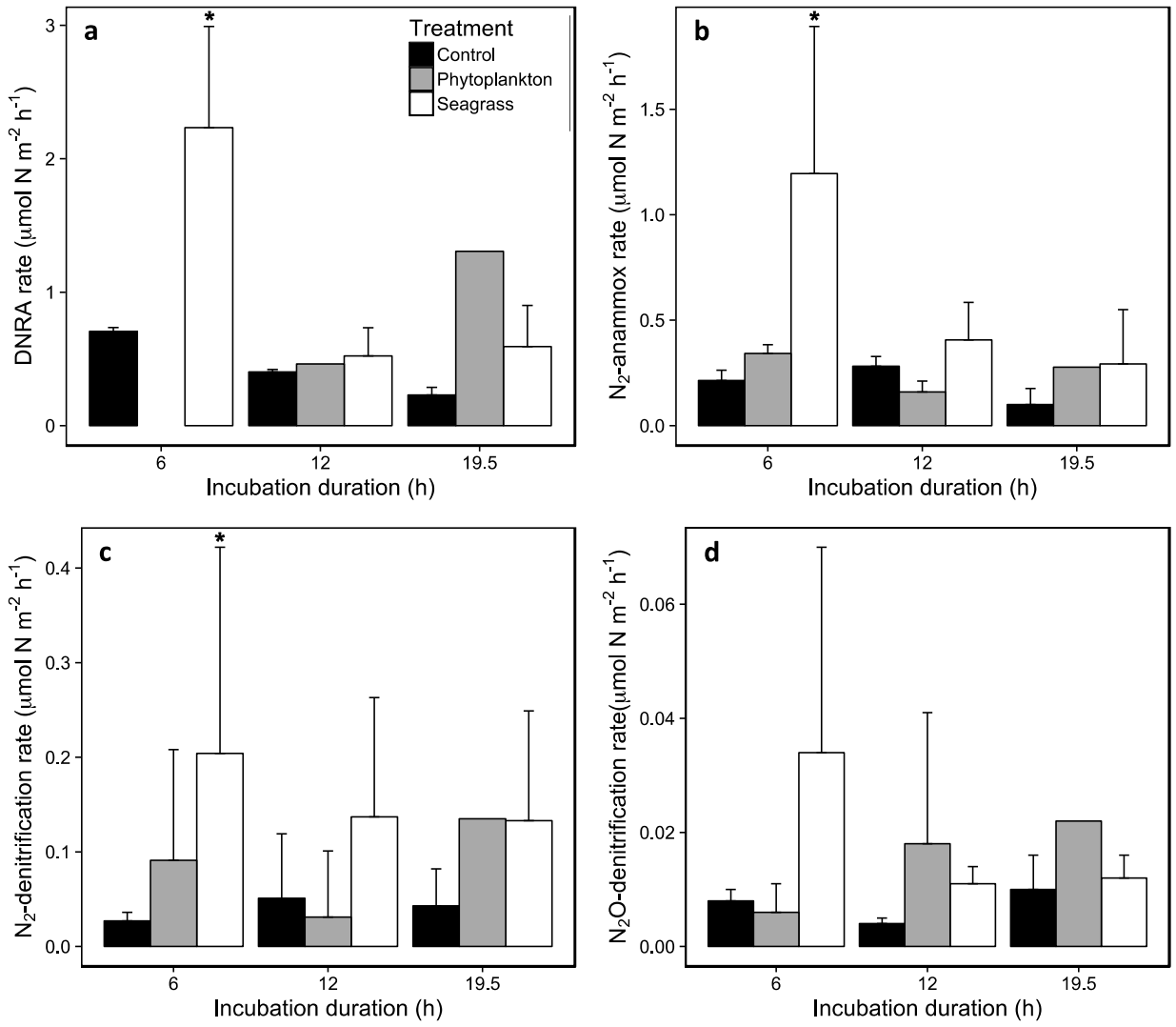

Figure 14. Rates of (a) DNRA, (b) N_2 production by anammox, (c) N_2 production by denitrification, and (d) N_2O production by denitrification. Rates were determined from incubations of three different durations and under three organic carbon treatments (control – no addition, addition of phytoplankton detritus, and addition of seagrass detritus). Error bars represent +1 standard deviation. DNRA rate data were not available at the 6 h time point with phytoplankton addition. Note the difference in y-axis scales among panels.

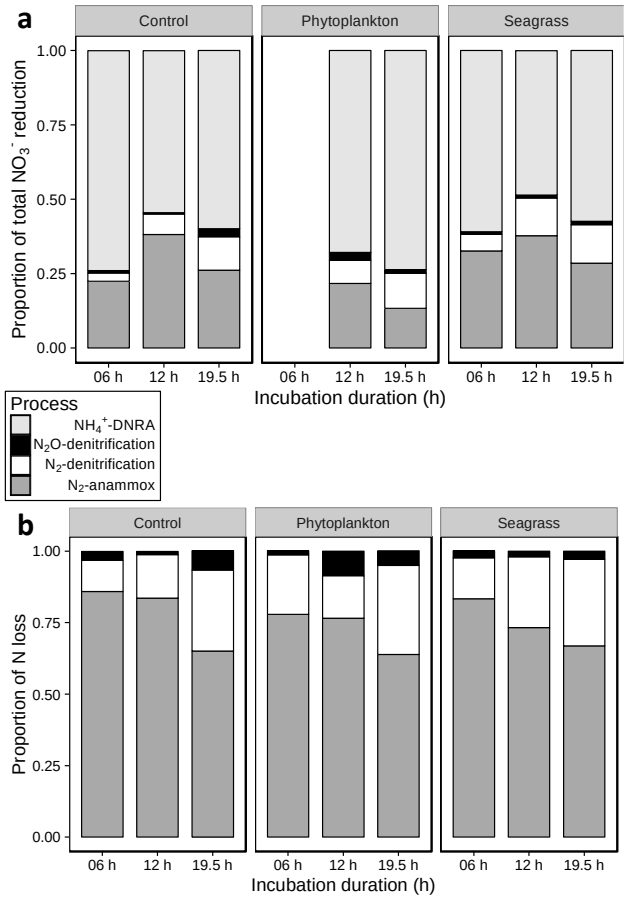

Figure 15. N_2 production by anammox and denitrification, N_2O production by denitrification, and DNRA as a proportion of (a) total NO_3^- reduction and (b) total N loss to N_2 and N_2O. Proportions of each process were measured at three different incubation durations under three carbon treatments (control – no addition, addition of phytoplankton detritus, and addition of seagrass detritus).

DISCUSSION

Evaluation of R-IPT-DNRA when DNRA is active

In Shaws Bay sediments where DNRA was a substantial N cycling pathway, quantifying DNRA simultaneously with anammox and denitrification yielded more accurate rate estimates than quantifying anammox and denitrification alone. High proportional rates of DNRA resulted in overestimation of denitrification and underestimation of anammox rates by the R-IPT model relative to the R-IPT-DNRA model. The degree of over/underestimation was an order of

magnitude greater, on average, for denitrification than for anammox. Further, the overestimation of denitrification increased exponentially as the proportion of $^{30}N_2$ produced by anammox (A_{30}/P_{30}) increased. This result is in agreement with Song et al. (2016), who propose that rates of denitrification are more greatly overestimated when anammox makes up the majority of N loss. Although previous studies have suggested that the majority of N loss in marine sediments is dominated by denitrification (Trimmer and Engström 2011) and the overestimation of denitrification is unlikely to be appreciable in shallow marine systems (Song et al., 2016), our results indicate this assumption is not always valid. Thus, denitrification rates determined by the R-IPT model in marine sediments where DNRA is active could be significantly overestimated. The variability in this overestimation cannot be identified without quantifying DNRA via analysis of the isotopic composition of NH_4^+ (r_{14a}). Published studies of R-IPT-derived denitrification rates, in sediments where appreciable DNRA is suspected, should thus be interpreted with caution, and future studies should utilize the R-IPT-DNRA to obtain accurate anammox and denitrification measurements.

The R-IPT-DNRA model calculated anammox rates in Shaws Bay sediments, but future applications of the R-IPT-DNRA model could be impeded if substantial ^{15}N labeling of the NH_4^+ pool occurs. If the *in situ* NH_4^+ concentration is low and the DNRA rate is large, the abundance of NH_4^+ could increase to the point of stimulating anammox beyond the rate accounted for in the model. While DNRA rates were considerable in this study, $^{15}NH_4^+$ made up 7.7 ± 5.4% of the total NH_4^+ pool at the end of the incubation and was therefore unlikely to have stimulated anammox activity beyond the rates accounted for in the R-IPT. The concentration and isotopic composition of NH_4^+ should be carefully monitored to evaluate if anammox rates derived from the R-IPT-DNRA model may have been enhanced.

The application of the R-IPT-DNRA model allows coupled DNRA-anammox and canonical anammox to be distinguished, a unique attribute of this modeling approach in comparison to that presented by Song et al. (2016). Despite high relative rates of both DNRA and anammox, coupled DNRA-anammox ($A_{14\text{-}DNRA}$) made up a small proportion (< 15%) of total anammox in Shaws Bay. While DNRA generated 22 ± 14% of ambient NH_4^+ on an hourly basis, the lack of strong coupling between DNRA and anammox suggests that remineralization supplies the majority of NH_4^+ to anammox in Shaws Bay.

Anammox, denitrification, and DNRA in seagrass ecosystem sediments

In this study we have quantified, for the first time, the co-occurrence of DNRA, anammox and denitrification in intact sediments from a seagrass-dominated environment. Typical of seagrass ecosystems, sediment in Shaws Bay has a moderately high C:N ratio compared to other coastal ecosystems (Eyre et al. 2013; Khan et al. 2015) and receives detrital organic matter with a higher C:N ratio than that of the sediment. DNRA was the predominant NO_3^- reduction pathway in Shaws Bay sediments, illustrating that this high C:N environment functions to retain N that might otherwise be denitrified. Similar N retention has been reported previously in seagrass communities (Eyre et al. 2013). Although the energy yield of denitrification is higher than that of DNRA, the stoichiometry of organic C and NO_3^- consumption for each reaction is such that high C:N environments favor DNRA over denitrification (Tiedje et al. 1982; Burgin and Hamilton 2007; Kraft et al. 2014; van den Berg et al. 2015).

Anammox contributed an average of 74% of total N loss in Shaws Bay sediments, an unusually high proportion compared to other coastal sediments (Table 6). Proportions this high

have previously been reported only in deep sea sediments and were attributed to the limitation of denitrification by low organic carbon availability (Thamdrup and Dalsgaard 2002; Dalsgaard et al. 2005; Trimmer and Nicholls 2009; Trimmer et al. 2013). While seagrass ecosystems are highly productive and contain large amounts of organic matter, there are driving factors that may function to suppress denitrification in Shaws Bay, namely the refractory nature of seagrass organic matter (Eyre et al. 2013) and competition for limited NO_3^- supply by the high rates of DNRA observed. Competition between DNRA and denitrification points to a potential mechanism that allows anammox to be the prominent N loss pathway.

Sediments in Shaws Bay were characterized by low rates of N loss that are atypical of shallow sediments (Table 6). However, rates of other microbial processes demonstrate an active microbial community in Shaws Bay that functions to recycle rather than remove N from the system. The slope of O_2 demand vs. N_2 production in Shaws Bay was an order of magnitude lower than that found across a range of Australian sand-, mud-, seagrass-, and macroalgae-dominated sediments (Eyre et al. 2013). This trend emphasizes that while the sediment microbial community is actively respiring organic matter, N loss rates are diminished in Shaws Bay relative to other coastal sediments. Several factors could contribute to the suppression of N loss in this system. Owing to the high C:N ratios of organic matter in the system, DNRA likely maintains NO_3^- limitation by outcompeting denitrifiers for substrate (Burgin and Hamilton 2007; van den Berg et al. 2015). In addition, the assimilative demand for N by heterotrophic microorganisms processing high C:N organic matter could outcompete denitrifiers for NO_3^- (Oakes et al. 2011). Furthermore, sulfide is found in seagrass systems owing to the activity of N-fixing sulfate reducers (Hemminga and Duarte 2000) and could inhibit nitrification and suppress coupled nitrification-denitrification (Joye and Hollibaugh 1995). Finally, although the organic

matter source is similar, there may be dampened microbial activity in bare sediments adjacent to seagrasses compared to sediments within the seagrass bed (Boschker et al. 2000; Jones et al. 2003; Holmer et al. 2004).

N_2O production comprised between 1.1 and 8.6% of total N loss, a typical range for aquatic sediments (Seitzinger and Kroeze 1998; McCrackin and Elser 2010). However, given that denitrification rates were markedly low, the total rate of N_2O production was ~100-fold lower than production as indicated by atmospheric emission rates measured in other coastal environments (Murray et al. 2015 and references therein). The total range of N_2O production across carbon treatments in Shaws Bay was 0.002 to 0.008 μmol N_2O m^{-2} h^{-1} (median = 0.003), whereas previous measurements in mangroves, salt marshes, and estuaries ranged from 0.1 to 6.0, -2.5 to 8.9, and 0.1 to 8.3 μmol N_2O m^{-2} h^{-1}, respectively (Murray et al. 2015 and references therein). To our knowledge, this is the first published measurement of N_2O production in sediments from a seagrass-dominated system. While this study does not address the regulation of N_2O production and atmospheric flux by seagrasses themselves, it does provide a representation of N_2O production in a coastal system that receives relatively refractory high C:N organic matter derived from seagrasses. If our results are representative of other seagrass systems, seagrass environments could have a much smaller impact on the global N_2O budget than other coastal environments. However, given that denitrification rates in Shaws Bay seem to depart from the relatively higher rates reported from other seagrass systems (reviewed in Murray et al. 2015), additional studies are needed to constrain the role of seagrass systems on the global N_2O budget.

Table 6. Nitrogen loss rates calculated by the isotope pairing technique for intact sediments and sediment slurries. ND = not detected.

Location	Details	Dentrification rate μmol N m^{-2} h^{-1}	Anammox rate μmol N m^{-2} h^{-1}	f_{amx} anammox / total N loss	Reference
Intact sediments					
Shaws Bay, Australia	Bare sediment	0.04	0.18	0.74	This study
	Sediment + seagrass	0.16	0.60	0.74	
	Sediment + phytoplankton	0.08	0.26	0.78	
12 coastal sites, Greenland	36 to 100 m depth	1.38 to 11.04	0.04 to 3.83	0.01 to 0.35	Rysgaard et al. 2004
Alsback, Gullmarsfjorden, Sweden	116 m depth	6.08	6.64	0.48	Trimmer et al. 2006
Gravesend, Thames estuary, U.K.		192.9	48.94	0.21	
Constructed wetland, Australia	Intake zone	965.9	66.1	0.06	Erler et al. 2008
	Outflow zone	651.5	199.40	0.23	
Colne Estuary, U.K.	Hythe (head)	390 to 400	ND to 157	0.00 to 0.30	Dong et al. 2009
	Alresford Creek (middle)	50 to 80	ND	0.00	
	Brightlingsea (mouth)	5 to 10	ND	0.00	
Irish Sea	Continental shelf, 50-100 m depth	3.44	1.38		Trimmer and Nicholls 2009
North Atlantic	Continental slope, 500-2000 m depth	0.42	0.61		
Mae Klong Estuary, Thailand	Salinity 0-35 PSU	3.3	ND	0.00	Dong et al. 2011
Cisadane Estuary, Indonesia	Salinity 0-35 PSU	22.5	ND	0.00	
Vunidawa-Rewa Estuary, Fiji	Salinity 0-35 PSU	0.6	ND	0.00	
St. Lawrence Estuary, Canada	345 m depth	11.3	5.5	0.33	Crowe et al. 2012
Danshuei River, Thailand	Intertidal zone	42.3	13	0.12	Hsu and Kao 2013
Skagerrak, Denmark	176 m depth	13.25	ND	0.00	Trimmer et al. 2013
	384 m depth	9.57	ND	0.00	
	610 m depth	0.61	2.01	0.77	
	688 m depth	0.3	0.77	0.72	
Great Barrier Reef, Australia	29 m depth	2.08	4.86	0.70	Erler et al. 2013
Sediment slurries					
Norsminde Fjord	1 m depth			0.00	
Randers Fjord	1 m depth	340	22	0.06	Risgaard-Petersen et al. 2003
Young Sound	36 m depth	8	2	0.19	
Skagerrak, Denmark	695 m depth	2	4	0.70	
Skagerrak, Denmark	16 m depth			0.02	Dalsgaard et al. 2005
	380 m depth			0.24	
	700 m depth			0.67	
Logan/Albert River, Australia	Upstream to river mouth transect	0.5 to 8.5	0 to 0.8	0.00 to 0.09	Meyer et al. 2005

Table 6 (cont'd)

Location	Details	Dentrification rate μmol N L^{-1} h^{-1}	Anammox rate μmol N L^{-1} h^{-1}	f_{amx} anammox / total N loss	Reference
Heron Island, Australia	1 m depth	34 to 480*	ND	0.00	Eyre et al. 2008
9 estuaries, United Kingdom				0.05 to 0.11	Nicholls and Trimmer 2009
Intact sediments					
Aarhus Bay, Denmark	16 m depth		3.46	0.02	Thamdrup and Dalsgaard 2002
Skagerrak, Denmark	380 m depth		4.13	0.24	
	695 m depth		1.25	0.67	
Thames estuary, United Kingdom	Salinity 2 PSU	100	1.5	0.015	Trimmer et al. 2003
	Salinity 10 PSU	118	9.5	0.075	
	Salinity 10 PSU	155	7	0.043	
	Salinity 26 PSU	116	3	0.025	
	Salinity 30 PSU	59	1	0.017	
	Salinity 30 PSU	36	0.5	0.014	
Sediment slurries					
East China Sea	19 m depth	14	2	0.125	Song et al. 2013
	85 m depth	2	8	0.8	

*Denitrification measured by N_2:Ar
**Unpublished data from Eyre et al. 2011b

Effect of organic carbon quality on N cycling

The addition of seagrass detritus stimulated rates of anammox, denitrification, and DNRA in Shaws Bay sediments, but low C:N phytoplankton detritus did not. This is in direct contrast to other results that suggest that labile organic matter stimulates N loss in estuarine sediments to a greater extent than relatively refractory organic matter does (Brettar and Rheinheimer 1992; Caffrey et al. 1993; Fulweiler et al. 2008; Oakes et al. 2011; Fulweiler et al. 2013). However, Babbin et al. (2014) demonstrated that N loss in the East Tropical North Pacific oxygen minimum zone was greater when water was amended with sinking particulate matter than with highly labile amino acids or sucrose. This suggests that microbial communities may be preferentially adapted to decompose and recycle organic matter that is commonly encountered. Given that this system encounters seagrass detritus to a greater extent than phytoplankton detritus, the sediment microbial community could be predisposed to utilize this refractory organic matter source.

Alternatively, because seagrass detritus includes the associated epiphytic community, the stimulation in N cycling in the first 6 h following addition of seagrass could represent selective consumption of epiphytic material (Dahllof and Karle 2005). Bacteria in seagrass sediments metabolize organic matter derived from a mix of seagrass and benthic macro- and microalgae, with a greater reliance on seagrass in more pristine sites and a mixed to algal-dominated signature in anthropogenically-impacted sites (Boschker et al. 2000; Holmer et al. 2001; Jones et al. 2003; Holmer et al. 2004; Bouillon and Boschker 2006; Williams et al. 2009). Shaws Bay is considered only slightly impacted by anthropogenic activities (Ballina Shore Council 2000), so microbial communities likely rely mainly on seagrass-derived organic matter. This relationship is expected to hold in both vegetated sediment and adjacent bare sediments (Boschker et al. 2000;

Jones et al. 2003; Holmer et al. 2004), meaning that the organic matter utilization measured in unvegetated sediments we sampled in Shaws Bay is expected to be seagrass-derived. Although we do not know whether the epiphytic component or seagrass itself enhanced N cycling in the seagrass detritus addition treatments, our results indicate that the addition of a C source common to the environment stimulates N cycling.

In this study, the proportions of anammox and denitrification contributing to N loss remained the same regardless of carbon treatment and total N loss rate. This is somewhat unexpected given that denitrification, a heterotrophic process, uses organic carbon directly, whereas anammox, an autotrophic process, does not (Jetten et al. 1999). Although the anammox reaction itself does not require carbon, a supply of carbon may be crucial to support heterotrophic nitrogen cyclers that provide substrates for anammox (Trimmer et al. 2003; Dalsgaard et al. 2005; van Hulle et al. 2012). Further, there is evidence that anammox bacteria are capable of coupling organic acid oxidation and NO_3^- reduction and compete with denitrification for both substrates (Guven et al. 2005; Kartal et al. 2007). Together, these pathways represent a means by which anammox activity can be stimulated upon addition of seagrass detritus and explain how the proportion of anammox making up total N loss can remain consistent across carbon treatments.

Conclusion

We present a revision to the isotope pairing technique (R-IPT-DNRA) that enables the simultaneous measurement of rates of anammox, denitrification, N_2O production, and DNRA in intact sediments when these processes co-occur. This approach presents a significant advance for the understanding of N processing in coastal systems, where N mitigation efforts depend on a

detailed understanding of N loss and recycling pathways. The R-IPT-DNRA model is likely to be more accurate than the traditional application of the isotope pairing technique in environments that receive inputs of carbon-rich, relatively refractory organic matter such as the seagrass ecosystem in this study. Under these conditions, DNRA is energetically favored over denitrification, and the introduction of ^{15}N into the NH_4^+ pool via DNRA can cause a substantial overestimation of denitrification rates if DNRA is not taken into account.

In Shaws Bay, a carbon-rich and N-poor seagrass-dominated coastal ecosystem, the dominance of DNRA conserves N in the system, effectively outcompeting denitrifiers for NO_3^-. In turn, the NH_4^+ production by DNRA sets the stage for anammox to dominate overall N loss. N_2O production made up a typical proportion of denitrification, yet absolute rates were markedly low compared to other coastal ecosystems owing to low overall rates of denitrification. This N cycling regime was stimulated by the addition of seagrass detritus but not by relatively labile phytoplankton detritus, suggesting that microbial communities in coastal sediments are adapted to process the organic matter that is typically encountered.

APPENDIX

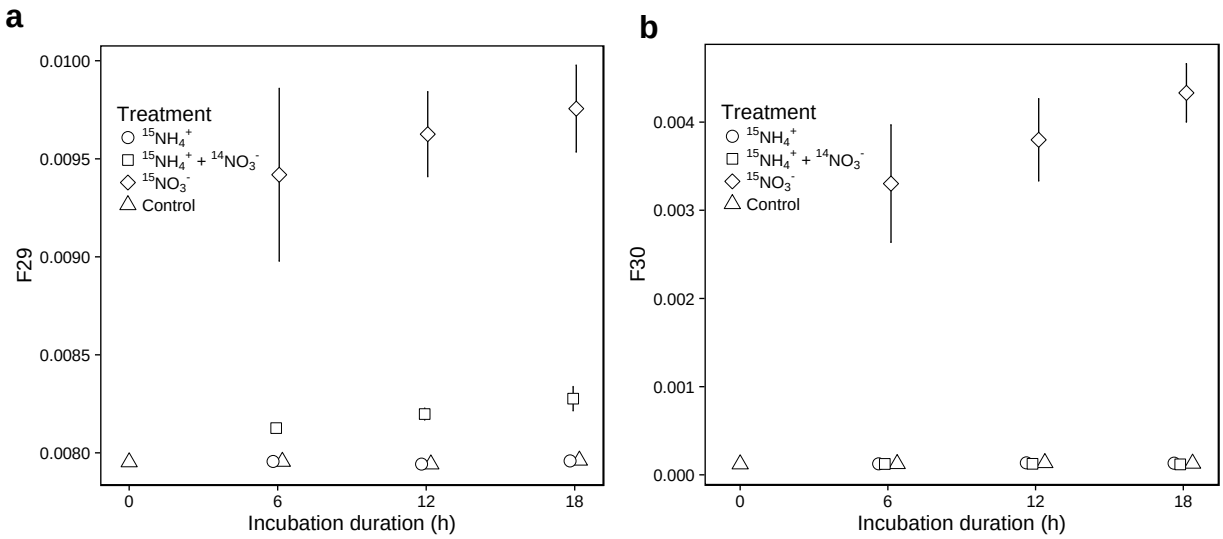

Figure A5. Isotope fraction of (a) $^{29}N_2$ and (b) $^{30}N_2$ in anoxic slurry incubations following addition of $^{15}NH_4^+$, or $^{15}NH_4^+ + {}^{14}NO_3^-$, or $^{15}NO_3^-$ over the course of 18 h. The control treatment received no amendment. An increase in F29 indicates anammox activity, whereas an increase in F30 indicates denitrification activity.

R-IPT-DNRA Derivations
Base Equations

$$x = \frac{^{14}NO_3^-}{^{14}NO_3^- + {}^{15}NO_3^-} \qquad \frac{1 - F_N}{F_N} = r_{14} = \frac{x}{y}$$

$$y = \frac{^{15}NO_3^-}{^{14}NO_3^- + {}^{15}NO_3^-} \qquad x = r_{14} \cdot y$$

$$u = \frac{^{14}NH_4^+}{^{14}NH_4^+ + {}^{15}NH_4^+} \qquad \frac{1 - F_A}{F_A} = r_{14a} = \frac{u}{v}$$

$$u = \frac{^{15}NH_4^+}{^{14}NH_4^+ + {}^{15}NH_4^+} \qquad u = r_{14a} \cdot v$$

Derivation of A_{28}

$$\frac{A_{28}}{A_{29}} = \frac{x \cdot u}{x \cdot v + u \cdot y}$$

$$A_{28}(x \cdot v + u \cdot y) = A_{29} \cdot x \cdot u$$

$$A_{28} \cdot x \cdot v = u(A_{29} \cdot x - A_{29} \cdot y)$$

$$\frac{A_{28} \cdot x \cdot v}{r_{14a} \cdot v} = A_{29} \cdot x - A_{28} \cdot y$$

$$A_{28}\left(\frac{x}{r_{14a}} + y\right) = A_{29} \cdot x$$

$$A_{28}\left(\frac{r_{14} \cdot y}{r_{14a}} + y\right) = A_{29} \cdot r_{14} \cdot y$$

$$A_{28} \cdot y\left(\frac{r_{14}}{r_{14a}} + 1\right) = A_{29} \cdot r_{14} \cdot y$$

$$A_{28} = \frac{A_{29} \cdot r_{14}}{\left(\frac{r_{14}}{r_{14a}} + 1\right)}$$

Derivation of A_{30}

$$A_{30} = \frac{v(P_{29} \cdot y - 2x \cdot P_{30})}{y \cdot u - v \cdot x}$$

$$A_{30} = \frac{v \cdot P_{29} \cdot y - v \cdot 2r_{14} \cdot y \cdot P_{30}}{y \cdot r_{14a} \cdot v - v \cdot r_{14} \cdot y}$$

$$A_{30} = \frac{v \cdot y(P_{29} - 2P_{30} \cdot r_{14})}{v \cdot y(r_{14a} - r_{14})}$$

$$A_{30} = \frac{P_{29} - 2P_{30} \cdot r_{14}}{r_{14a} - r_{14}}$$

Derivation of $A_{29\text{-}DNRA}$

$A_{29=DNRA}$: probability of pairing $^{14}NO_3^- + {}^{15}NH_4^+ = x*v$

$A_{29=ana}$: probability of pairing $^{15}NO_3^- + {}^{14}NH_4^+ = u*y$

$$A_{29-DNRA} = A_{29}(\frac{x \cdot v}{x \cdot v + u \cdot y})$$

$$\frac{A_{29}}{A_{29-DNRA}} = \frac{x \cdot v + u \cdot y}{x \cdot v}$$

$$\frac{A_{29}}{A_{29-DNRA}} = 1 + \frac{u \cdot y}{x \cdot v}$$

$$\frac{A_{29}}{A_{29-DNRA}} = 1 + \frac{r_{14a}}{r_{14}}$$

$$A_{29-DNRA} = \frac{A_{29}}{(1 + \frac{r_{14a}}{r_{14}})}$$

$$A_{29-ana} = A_{29} - A_{29-DNRA}$$

LITERATURE CITED

LITERATURE CITED

Algar CK, Vallino JJ (2014) Predicting microbial nitrate reduction pathways in coastal sediments. Aquat Microb Ecol 71:223-238. doi:10.3354/ame01678

Babbin AR, Keil RG, Devol AH, Ward BB (2014) Organic matter stoichiometry, flux, and oxygen control nitrogen loss in the ocean. Science 344:406-408. doi:10.1126/science.1248364

Ballina Shire Council (2000) Shaws Bay, East Ballina: Estuary management plan. Estuary Processes Study Report, Vol. 1. Reference no. J3320/R2147.s.

Betlach MR Tiedje JM (1981) Kinetic explanation for accumulation of nitrite, nitric oxide, and nitrous oxide during bacterial denitrification. Appl Environ Microb 42:1074-1084.

Boschker HTS, Wielemaker A, Schaub BEM, Holmer M (2000) Limited coupling of macrophyte production and bacterial carbon cycling in the sediments of Zostera spp. meadows. Mar Ecol-Prog Ser 203:181-189.

Bouillon S, Boschker HTS (2006) Bacterial carbon sources in coastal sediments: A cross-system analysis based on stable isotope data of biomarkers. Biogeosciences 3:175-185. doi:10.5194/bg-3-175-2006

Brettar I Rheinheimer G (1992) Influence of carbon availability on denitrification in the central Baltic Sea. Limnol Oceanogr 37(6):1146-1161.

Brin LD, Giblin AE, Rich JJ (2015) Effects of experimental warming and carbon addition on nitrate reduction and respiration in coastal sediments. Biogeochemistry 125:81-95. doi:10.1007/s10533-015-0113-4

Burgin AJ, Hamilton SK (2007) Have we overemphasized the role of denitrification in aquatic ecosystems? A review of nitrate removal pathways. Front Ecol Environ 5(2):89-96.

Caffrey JM, Sloth NP, Kaspar HF, Blackburn TH (1993) Effect of organic loading on nitrification and denitrification in a marine sediment microcosm. FEMS Microbiol Ecol 12:159-167.

Dahllof I, Karle I-M (2005) Effect on marine sediment nitrogen fluxes caused by organic matter enrichment with varying organic carbon structure and nitrogen content. Mar Chem 94:17-26. doi:10.1016/j.marchem.2004.07.008

Dalsgaard T, Nielsen LP, Brotas V, Viaroli P, Underwood G, Nedwell D, Sundbäck K, Rysgaard S, Miles A, Bartoli M, Dong L, Thornton DCO, Ossosen LDM, Castaldelli G, Risgaard-Petersen N (2000) Protocol handbook for NICE- Nitrogen cycling in estuaries. National Environmental Research Institute, Silkeborg, Denmark.

Dalsgaard T, Thamdrup B, Canfield DE (2005) Anaerobic ammonium oxidation (anammox) in the marine environment. Res Microbiol 156:45-464. doi:10.1016/j.resmic.2005.01.011

Davidson EA, Verchot LV (2000) Testing the hole-in-the-pipe model of nitric and nitrous oxide emissions from soils using the TRAGNET database. Global Biogeochem Cy 14(4):1035-1043. doi:10.1029/1999GB001223

Dong LF, Sobey MN, Smith CJ, Rusmana I, Phillips W, Scott A, Osborn AM, Nedwell DB (2011) Dissimilatory reduction of nitrate to ammonium, not denitrification or anammox, dominates benthic nitrate reduction in tropical estuaries. Limnol Oceanogr 56(1):279-291. doi:10.4319/lo.2011.56.1.0279

Enríquez S, Marbà N, Duarte CM, van Tussenbroek BI, Reyes-Zavala G (2001) Effects of seagrass *Thalassia testudinum* on sediment redox. Mar Ecol Prog Ser 219:149-158.

Erler DV, Trott LA, Alongi DM, Eyre BD (2013) Denitrification, anammox and nitrate reduction in the sediments of the Southern Great Barrier Reef Lagoon. Mar Ecol Prog Ser 478:57-70.

Eyre BD (2000) Regional evaluation of nutrient transformation and phytoplankton growth in nine river-dominated sub-tropical east Australian estuaries. Mar Ecol Prog Ser 205:61-83.

Eyre BD, Rysgaard S, Dalsgaard T, Christensen PB (2002) Comparison of isotope pairing and N_2:Ar methods for measuring sediment denitrification: Assumptions, modifications and implications. Estuaries 25(6A):1077-1087.

Eyre BD, Ferguson AJP, Webb A, Maher D, Oakes JM (2011a) Denitrification, N-fixation and nitrogen and phosphorus fluxes in different benthic habitats and their contribution to the nitrogen and phosphorus budgets of a shallow oligotrophic sub-tropical coastal system (southern Moreton Bay, Australia). Biogeochemistry 102:111-133. doi:10.1007/s10533-010-9425-6

Eyre BD, Maher D, Oakes JM, Erler DV, Glasby TM (2011b) Differences in benthic metabolism, nutrient fluxes, and denitrification in Caulerpa taxifolia communities compared to uninvaded bare sediment and seagrass (Zostera capricorni) habitats. Limnol Oceanogr 56(5):1737-1750. doi:10.4319/lo.2011.56.5.1737

Eyre BD, Maher DT, Squire P (2013) Quantity and quality of organic matter (detritus) drives N_2 effluxes (net denitrification) across seasons, benthic habitats, and estuaries. Global Biogeochem Cy 27:1-13. doi:10.1002/2013GB004631

Eyre B., Maher DT, Sanders C (2016) The contribution of denitrification and burial to the nitrogen budgets of three geomorphically distinct Australian estuaries: Importance of seagrass habitats. Limnol Oceanogr 61(3):1144-1156. doi:10.1002/lno.10280

Ferguson AJP, Eyre BD, Gay J (2004) Benthic nutrient fluxes in euphotic sediments along shallow sub-tropical estuaries, northern NSW, Australia. Aquat Microb Ecol 37:219-235.

Fulweiler RW, Nixon SW, Buckley BA, Granger SL (2008) Net sediment N_2 fluxes in a coastal marine system - experimental manipulations and a conceptual model. Ecosystems 11:1168−1180.

Fulweiler RW, Brown SM, Nixon SW, Jenkins BD (2013) Evidence and a conceptual model for the co-occurrence of nitrogen fixation and denitrification in heterotrophic marine sediments. Mar Ecol Prog Ser 482:57-68. doi:10.3354/meps10240

Giblin AE, Tobias CR, Song B, Weston N, Banta GT, Rivera-Monroy VH (2013) The importance of dissimilatory nitrate reduction to ammonium (DNRA) in the nitrogen cycle of coastal ecosystems. Oceanogr 26(3):124–131. doi:10.5670/oceanog.2013.54

Guven D, Dapena A, Kartal B, Schmid MC, Mass B, van de Pas-Schoonen K, Sozen S, Mendez R, Op den Camp HJM, Jetten MSM, Strous M, Schmidt I (2005) Propionate oxidation by and methanol inhibition of anaerobic ammonium-oxidizing bacteria. Appl Environ Microbiol 71(2):1066. doi:10.1128/AEM.71.2.1066-1071.2005

Hardison AK, Algar CK, Giblin AE, Rich JJ (2015) Influence of organic carbon and nitrate loading on partitioning between dissimilatory nitrate reduction to ammonium (DNRA) and N_2 production. Geochim Cosmochim Acta 164:146-160. doi:10.1016/j.gca.2015.04.049

Hemminga MA, Duarte CM (2000) Seagrass Ecology. Cambridge University Press, Cambridge.

Holmer M, Andersen FO, Nielsen SL, Boschker HTS (2001) The importance of mineralization based on sulfate reduction for nutrient regeneration in tropical seagrass sediments. Aquat Bot 71:1-17.

Holmer M, Duarte CM, Boschker HTS, Barrón C (2004) Carbon cycling and bacterial carbon sources in pristine and impacted Mediterranean seagrass sediments. Aquat Microb Ecol 36:227-237.

Howarth RW (2008) Coastal nitrogen pollution: A review of sources and trends globally and regionally. Harmful Algae 8:14-20. doi:10.1016/j.hal.2008.08.015

Hsu T-C, Kao S-J (2013) Technical note: Simultaneous measurement of sedimentary N_2 and N_2O production and new ^{15}N isotope pairing technique. Biogeosciences 10:7847-7862. doi:10.5194/bg-10-7847-2013

Hwang S, Jang K, Jang H, Song J, Bae W (2006) Factors affecting nitrous oxide production: A comparison of biological nitrogen removal processes with partial and complete nitrification. Biodegradation 17:19-29. doi:10.1007/s10532-005-2701-9

IPCC (2007) Climate Change 2007: The Physical Science Basis. In: Solomon S et al (eds) Contribution of Working Group I to the Fourth Assessment Report of the Intergovernmental Panel on Climate Change. Cambridge University Press, New York.

Jetten MSM, Strous M, van de Pas-Schoonen KT, Schalk J, van Dongen UGJM, van de Graaf AA, Logemann S, Muyzer G, van Loosdrecht MCM, Kuenen JG (1999) The anaerobic oxidation of ammonium. FEMS Microbiol Rev 22:421-437.

Jones WB, Cifuentes LA, Kaldy JE (2003) Stable carbon isotope evidence for coupling between sedimentary bacteria and seagrasses in a sub-tropical lagoon. Mar Ecol Prog Ser 255:15-25.

Joye SB, Hollibaugh JT (1995) Influence of sulphide inhibition of nitrification on nitrogen regeneration in sediments. Science 270:623-625.

Kartal B, Rattray J, van Niftrik LA, van de Vossenberg J, Schmid MC, Webb RI, Schouten S, Fuerst JA, Damsté JS, Jetten MSM, Strous M (2007) Candidatus "Anammoxoglobus propionicus" a new propionate oxidizing species of anaerobic ammonium oxidizing bacteria. Syst Appl Microbiol 30:39-49. doi:10.1016/j.syapm.2006.03.004

Kartal B, van Niftrik LA, Keltjens JT, Op den Camp HJM, Jetten MSM (2012) Anammox—growth physiology, cell biology, and metabolism. Adv Microb Physiol 60:211-262. doi:10.1016/B978-0-12-398264-3.00003-6

Khan NS, Vane CH, Horton BP (2015) Stable carbon isotope and C/N geochemistry of coastal wetland sediments as a sea-level indicator. In: Shennan I, Long AJ, Horton BP (eds) Handbook of Sea-Level Research. Wiley. pp 295-311.

Knowles R (1982) Denitrification. Microbiological Rev 46(1):43-70

Kraft B, Tegetmeyer HE, Sharma R, Klotz MG, Ferdelman TG, Hettich RL, Geelhoed JS, Strous M (2014) The environmental controls that govern the end product of bacterial nitrate respiration. Science 345:676-679. doi:10.1126/science.1254070

McCrackin ML, Elser JJ (2010) Atmospheric nitrogen deposition influences denitrification and nitrous oxide production in lakes. Ecology 91(2):528-539.

Murray RH, Erler DV, Eyre BD (2015) Nitrous oxide fluxes in estuarine environments: Response to global change. Global Change Biol 21(9):3219-3245. doi:10.1111/gcb.12923

Nielsen LP (1992) Denitrification in sediment determined from nitrogen isotope pairing. FEMS Microbiol Ecol 86:357-362.

Oakes JM, Eyre BD, Ross DJ (2011) Short-term enhancement and long-term suppression of denitrification in estuarine sediments receiving primary- and secondary-treated paper and pulp mill discharge. Environ Sci Technol 45:3400-3406. doi:10.1021/es103636d

Risgaard-Petersen N, Nielsen LP, Rysgaard S, Dalsgaard T, Meyer RL (2003) Application of the isotope pairing technique in sediments where anammox and denitrification coexist. Limnol Oceanogr Methods 1:63-73.

Schlesinger WH (2009) On the fate of anthropogenic nitrogen. Proc Natl Acad Sci USA 106:203-208. doi:10.1073pnas.0810193105

Seitzinger SP, Kroeze C (1998) Global distribution of nitrous oxide production and N inputs in freshwater and coastal marine ecosystems. Global Biogeochem Cy 12(1):93-113.

Seitzinger S, Harrison JA, Böhlke JK, Bouwman AF, Lowrance R, Peterson B, Tobias C, Van Drecht G (2006) Denitrification across landscapes and waterscapes: A synthesis. Ecol Appl 16(6):2064-2090.

Song GD, Liu SM, Marchant H, Kuypers MMM, Lavik G (2013) Anammox, denitrification, and dissimilatory nitrate reduction to ammonium in the East China Sea sediment. Biogeosciences 10:6851-6864. doi:10.5194/bg-10-6851-2013

Song GD, Liu SM, Kuypers MMM, Lavik G (2016) Application of the isotope pairing technique in sediments where anammox, denitrification, and dissimilatory nitrate reduction to ammonium coexist. Limnol Oceanogr Methods 14(12):801-815. doi:10.1002/lom3.10127

Su Y-S, Yajima M (2015) R2jags: A Package for Running jags from R. R package version 0.05-01. http://CRAN.R-project.org/package=R2jags

Thamdrup B, Dalsgaard T (2002) Production of N_2 through anaerobic ammonium oxidation coupled to nitrate reduction in marine sediments. Appl Environ Microbiol 68:1312-1318. doi:10.1128/AEM.68.3.1312-1318.2002

Tiedje JM, Sexstone AJ, Myrold DD, Robinson JA (1982) Denitrification: Ecological niches, competition and survival. Antonie van Leeuwenhoek 48:569-583.

Trimmer M, Nicholls JC, Deflandre B (2003) Anaerobic ammonium oxidation measured in sediments along the Thames Estuary, United Kingdom. Appl Environ Microbiol 69(11):6447-6454. doi:10.1128/AEM.69.11.6447–6454.2003

Trimmer M, Risgaard-Petersen N, Nicholls JC, Engström P (2006) Direct measurement of anaerobic ammonium oxidation (anammox) and denitrification in intact sediment cores. Mar Ecol Prog Ser 326:37-47.

Trimmer M, Nicholls JC (2009) Production of nitrogen gas via anammox and denitrification in intact sediment cores along a continental shelf to slope transect in the North Atlantic. Limnol Oceanogr 54(2):577-589.

Trimmer M, Engström P (2011) Distribution, activity, and ecology of anammox bacteria in aquatic environments. In Ward BB, Arp DJ, Klotz MG (eds) Nitrification. American Society of Microbiology, Washington. pp. 201-235.

Trimmer M, Engström P, Thamdrup B (2013) Stark contrast in denitrification and anammox across the deep Norwegian Trench in the Skagerrak. Appl Environ Microbiol 79(23):7381-7389. doi:10.1128/AEM.01970-13

Turner TF, Collyer ML, Krabbenhoft TJ (2010) A general hypothesis-testing framework for stable isotope ratios in ecological studies. Ecology 91(8):2227-2233.

van den Berg EM, van Dongen U, Abbas B, van Loosdrecht MCM (2015) Enrichment of DNRA bacteria in continuous culture. The ISME Journal 9:2153-2161.

van de Graaf AA, Mulder A, de Bruijn P, Jetten MSM, Robertson LA, Kuenen JG (1995) Anaerobic oxidation of ammonium is a biologically mediated process. Appl Environ Microbiol 61:1246-1251.

van Hulle SWH, Callens J, Mampaey KE, van Loosdrecht MCM, Volcke EIP (2012) N_2O and NO emissions during autotrophic nitrogen removal in a granular sludge reactor – a simulation study. Environ Technol 33:2281-2290. doi:10.1080/09593330.2012.665492

Williams CJ, Jaffé R, Anderson WT, Jochem FJ (2009) Importance of seagrass as a carbon source for heterotrophic bacteria in a subtropical estuary (Florida Bay). Estuarine Coast Shelf S 85:507-514. doi:10.1016/j.ecss.2009.09.019

Zhang L, Altabet MA, Wu T, Hadas O (2007) Sensitive measurement of NH_4^+ $^{15}N/^{14}N$ ($\delta^{15}NH_4^+$) at natural abundance levels in fresh and saltwaters. Anal Chem 79:5297-5303. doi:10.1021/ac070106d

CHAPTER 4

DRAMATIC SHIFTS IN N CYCLING DRIVE HAB FORMATION AND MITIGATION OF N LOADING IN SANDUSKY BAY, LAKE ERIE

ABSTRACT

Recent water crises in Lake Erie point to an urgent need for greater understanding of harmful algal blooms (HABs) and their drivers. While much of the focus on the control of HABs in Lake Erie is on phosphorus (P) management, nearshore areas such as Sandusky Bay become limited by nitrogen (N) in the summer and are characterized by distinct HAB compositions (i.e., *Planktothrix* over *Microcystis*). We hypothesized that microbial N removal processes drive rapid N depletion in Sandusky Bay, and N limitation stimulates N fixation that supports HAB persistence. Stable isotope tracer approaches were employed to quantify rates of denitrification, anammox, N_2O production, and N fixation. During periods of high discharge and nutrient delivery from the Sandusky River, Sandusky Bay acted as a conduit for nutrient loading into Lake Erie, which could stimulate offshore HABs. These periods were also exemplified by high N_2O emissions from the Bay, as substrates for denitrification and nitrification were abundant. As water residence time increased throughout the season, N removal processes drove marked decreases in NO_3^- and the development of N limitation. Denitrification, anammox, and N_2O production made up 84, 14, and 2 % of total N removal, respectively. N fixation was active under N limitation (maximum 2.2 μmol N L^{-1} h^{-1}), representing bioavailable N generation that could indirectly support *Planktothrix* blooms in late summer. Dramatic shifts in N availability in Sandusky Bay will likely be intensified by climate change, and the observed trends can inform management of HABs and N_2O production in Lake Erie.

INTRODUCTION

Harmful algal blooms (HABs) are increasing in frequency on a global scale and are stimulated by excessive nutrient loading to aquatic systems (Bricker et al. 2008; Heisler et al. 2008). Lake Erie, in particular, has been subject to increased incidence and expansion of cyanobacterial HABs in recent years (Michalak et al. 2013; Ho and Michalak 2015, Bullerjahn et al. 2016). These blooms are dominated by cyanobacteria that accumulate the powerful hepatotoxin, microcystin (Carmichael and Boyer 2016). cHABs are not a monoculture, and cHAB taxa often show large temporal and spatial variability (Bozarth et al. 2010; Bridgeman et al. 2012). A greater knowledge of the drivers of cHABs, including nutrient cycling, will allow for better prediction and management in Lake Erie and other ecosystems.

Phytoplankton biomass and cHABs in Lake Erie have historically been correlated with P loading from river inflows (Kane et al. 2014; Kim et al. 2014). Calls to control eutrophication in Lake Erie have proposed targets for reduced P loading but have largely ignored N (Scavia et al. 2014). However, there is a growing dialogue surrounding the dual management of N and P in lacustrine systems (Gobler at al. 2016; Paerl et al. 2016), particularly as co-limitation of phytoplankton growth by both N and P has been demonstrated in the late summer in Lake Erie (Moon and Carrick 2007; Chaffin et al. 2013; Monchamp et al. 2014; Steffen et al. 2014a; Davis et al. 2015). Further, N concentration and speciation influences toxin production by cHABs (Davis et al. 2010; Horst et al. 2014; Monchamp et al. 2014; Davis et al. 2015). Delineating the role of N in controlling HABs, therefore, involves investigation of not only total N availability but also spatial and temporal variation in multiple species of N.

Several N transformations may drive variation in N availability. Denitrification permanently removes dissolved inorganic N (DIN) through the stepwise reduction of nitrate

(NO_3^-) to dinitrogen gas (N_2; Knowles 1982). Anammox is a competing N removal process that converts nitrite (NO_2^-) and ammonium (NH_4^+) to N_2, but this process has not been extensively studied in freshwater environments (Yoshinaga et al. 2011; Zhu et al. 2013). N removal processes are expected to be particularly active in aquatic systems that receive high DIN inputs (Seitzinger et al. 2006). N removal can be accompanied by release of the potent greenhouse gas, nitrous oxide (N_2O), which is produced by both denitrification and nitrification (Wrage et al. 2001). The global warming potential of N_2O is 300 times that of carbon dioxide over a 100-year time span, and its release could exacerbate climate change (IPCC 2007). N fixation, conversely, is capable of generating bioavailable N when DIN is scarce, and its activity has been inferred in Lake Erie (MacGregor et al. 2001; Monchamp et al. 2014; Steffen et al. 2014a; Davis et al. 2015) but not quantified for several decades (Howard et al. 1970).

While the colonial cyanobacterium *Microcystis* dominates the HAB community in offshore regions of Lake Erie, filamentous *Planktothrix* has been shown to persist in N-limited bays and tributaries (Conroy et al. 2007; Davis et al. 2015). Both cHAB taxa are incapable of N fixation and require combined N for growth. *Planktothrix,* in particular, is a superior scavenger for N (Conroy et al. 2007) and responds strongly to additions of DIN (Donald et al. 2011; 2013). Under N limitation, *Planktothrix* may be able to outcompete other phytoplankton for small N inputs or rely on a commensal relationship with diazotrophs. The persistence of *Planktothrix* in nearshore zones likely operates under a fundamentally different paradigm than offshore *Microcystis* blooms, and mitigation may require attention to the distinct biogeochemical functioning of these genera in the nearshore vs. offshore.

Sandusky Bay, a south shore embayment of Lake Erie, serves as an ideal location in which to examine the relationship between N cycling and cHABs. This system is hypereutrophic

(Ostrom et al. 2005; Davis et al. 2015), with the cyanobacterium *Planktothrix* dominating phytoplankton biomass from May to October (Davis et al. 2015). Growth of *Planktothrix* in Sandusky Bay is stimulated by additions of NO_3^-, NH_4^+, and urea, indicating that formation of cHABs in this system relies on a supply of bioavailable N (Chaffin and Bridgeman 2014; Davis et al. 2015). However, Sandusky Bay experiences large variations in NO_3^- concentrations and N:P ratios throughout the summer (Davis et al. 2015), suggesting that the dynamic N cycling may influence cHAB formation in this system. Evaluating the mechanisms that promote the persistence of *Planktothrix* in this system will benefit from an examination of N removal processes and N fixation that directly influence the availability of DIN. A thorough understanding of these processes will also inform the capacity for Sandusky Bay to act as a nutrient filter, which may curtail the formation of cHABs in offshore regions of Lake Erie.

As N cycling processes have been largely ignored in lieu of P in Lake Erie, we sought to examine of the potential role of N in cHAB formation. The objectives of this study in Sandusky Bay were to (1) determine the driving factors influencing N limitation, namely denitrification, anammox, and N_2O production, (2) examine N fixation as a possible source of bioavailable N under N limitation, and (3) determine how HAB formation and persistence relate to N cycling. We hypothesized that microbial N removal processes drive rapid N depletion in Sandusky Bay, and N fixation that occurs under N limitation allows bloom persistence.

METHODS

Field sampling

Sample collection occurred weekly (water column nutrient and chlorophyll (chl) *a* concentration analyses) or monthly (water column N_2O analyses, water column and sediment N

cycling assays) from May to October, 2015 through partnership with the Ohio Department of Natural Resources (ODNR). Sampling occurred at six stations: two stations in the inner portion of Sandusky Bay (ODNR4, ODNR6), three stations in the outer portion of Sandusky Bay (ODNR2, ODNR1, and EC 1163, hereafter 1163), and one station directly outside Sandusky Bay in the western basin of Lake Erie (Bells; Figure 16). Tributary discharge data from the primary water source to Sandusky Bay, the Sandusky River, were obtained from the USGS stream monitoring station near Fremont, OH (site 04198000; Figure 16). Water residence time in Sandusky Bay was estimated by dividing the Bay volume (1.6 - 2.6 m depth, 162 km^2 area; Richards and Baker 1985) by the Sandusky River discharge rate.

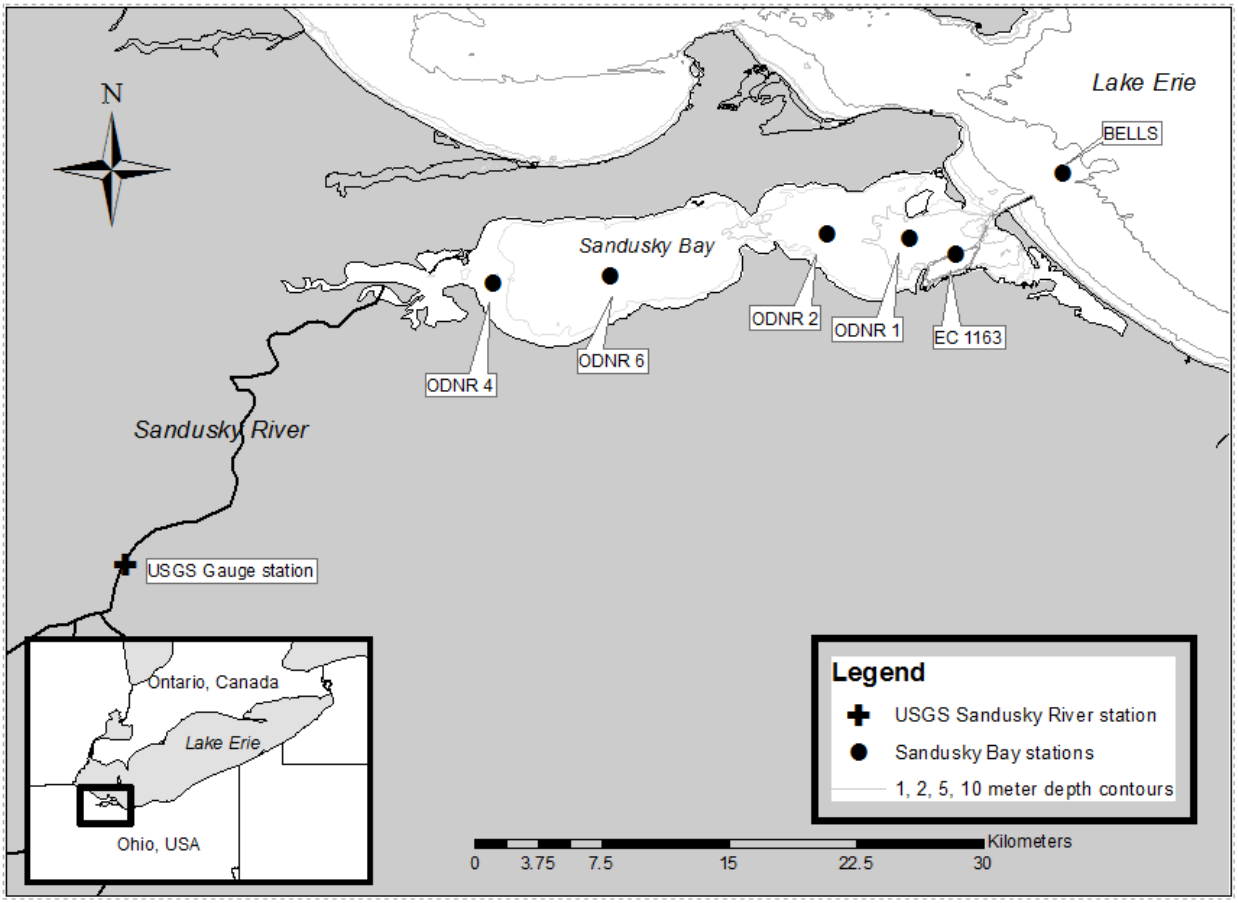

Figure 16. Sampling locations in Sandusky Bay (circles) and Sandusky River monitoring station (USGS site 04198000, cross).

At each sampling location, water column physical and chemical parameters (pH, conductivity, temperature, dissolved oxygen) were measured and recorded using a YSI 600QS sonde (YSI Inc., Yellow Springs, OH). Water samples were collected by Van Dorn bottle at 1 m depth for analysis of N_2O, NO_3^-, NH_4^+, phosphate (PO_4^{3-}), and chl *a* concentrations. Samples for N_2O concentrations and isotopic analysis were transferred into 60 and 250 mL glass serum bottles, respectively, by filling from the bottom to overflowing and sealing with no headspace with butyl rubber septa. Biological activity was halted by adding saturated $HgCl_2$ solution to a final concentration of 0.4 % by volume. Samples for dissolved nutrient analysis were filtered (0.2 μm) and frozen upon return to lab. Samples for determination of chl *a* concentrations were collected on 0.2 μm polycarbonate membrane filters and frozen. Station 1163 has an extensive monitoring history and was chosen for additional water and sediment assays. An additional 20 L carboy was filled with surface water from station 1163 for N fixation assays and sediment incubations.

Sediment cores for the evaluation of denitrification, anammox, and N_2O production rates by the isotope pairing technique (IPT) were collected at station 1163 using a modified piston corer as described by Davis and Steinman (1998). Intact sediment cores were collected in polycarbonate tubes (7 cm i.d.) to a depth of 25 cm. Water (1 cm) was maintained overlying the sediment during transport to preserve redox gradients. Upon return to the lab, water from station 1163 was gently added to cores to a depth of 20 cm. Cores were pre-incubated for 12 h in the dark at *in situ* temperature under gentle aeration to maintain oxic conditions in the overlying water.

Isotope tracer assays

Following pre-incubation of sediment cores, a sample was taken from the overlying water for DIN concentration analysis (NO_3^-, NO_2^- and NH_4^+), filtered through a precombusted GF/F filter and frozen until analysis. ^{15}N-NO_3^- (100 µmol L^{-1}) was then added to the overlying water in each core. Cores were then capped and gently stirred throughout the duration of the experiment. An initial equilibration period was employed to allow homogenization of NO_3^- between the overlying water and the NO_3^- reduction zone in the sediment porewater (Dalsgaard et al. 2000). Cores were sacrificed in triplicate or quadruplicate at intervals of 0, 3 or 4, and 6 h. Dissolved O_2 in the overlying water was monitored to evaluate the maintenance of oxic conditions throughout the incubation using a YSI 600QS sonde (YSI Inc., Yellow Springs, OH). A final sample for DIN analysis was collected when each core was sacrificed and processed as described above.

Samples for the determination of $\delta^{15}N_2$ were collected according to Hamilton and Ostrom (2007); briefly, dissolved gases were equilibrated with a He atmosphere, and the headspace was transferred into a pre-evacuated 12 mL Exetainer. Samples for analysis of dissolved N_2 concentrations were siphoned into 12 mL Exetainers to overflowing and amended with 200 µL of saturated $ZnCl_2$ solution to halt biological activity. All Exetainers were stored underwater at room temperature to minimize diffusion of atmospheric N_2 during storage. Samples for analysis of the $\delta^{15}N_2O$ and N_2O concentrations were siphoned into 250 and 60 mL serum bottles, respectively, to overflowing and sealed without a headspace with a butyl rubber septum. Biological activity was halted by adding saturated $HgCl_2$ solution to a final concentration of 0.4 % by volume.

N fixation assays were conducted by the dissolution method, which involves the addition of $^{15}N_2$-equilibrated water to a water sample rather than a $^{15}N_2$ bubble (Großkopf et al. 2012).

Preparation of $^{15}N_2$-equilibrated water involved sparging water in a serum bottle equipped with a butyl rubber septum with He to remove ambient N_2, followed by injection of $^{15}N_2$ (98 % atom fraction, Sigma-Aldrich Lot #MBBB0968V) while maintaining atmospheric pressure with a vent needle. Water from station 1163 was transferred into 1.18 L serum bottles and amended with $^{15}N_2$-equilibrated water to a final dissolved atom fraction of 1.14 - 2.33 %. Bottles were inverted 100 times to ensure uniform mixing and then incubated at *in situ* light and temperature conditions for 24 h. Samples were then vacuum filtered through precombusted GF/F filters. Filters were then dried at 60° C, acidified with 10 % HCl to remove carbonates, and dried again.

To evaluate the potential contamination of $^{15}N_2$ gas with $^{15}NO_3^-$ or $^{15}NH_4^+$ (Dabundo et al. 2014), a mass scan of the isotopically enriched gas was performed on an Isoprime isotope ratio mass spectrometer (IRMS; Elementar Americas, Inc., Mount Laurel, NJ). The mass scan revealed that potential impurities made up < 1 % of the enriched gas, and maximum contamination reported by Dabundo et al. (2014) could have made up less than 5 % of measured N fixation rates if all available $^{15}NO_3^-$ and $^{15}NH_4^+$ was assimilated.

Analyses

Concentrations of $NO_3^- + NO_2^-$, NO_2^-, NH_4^+, and PO_4^{3-} were measured on field-filtered sample water using standard U.S. EPA methods (353.1, 353.2, 350.1, and 365.1, respectively) on a SEAL Analytical QuAAttro continuous segmented flow analyzer (SEAL Analytical Inc., Mequon, WI). NO_3^- concentration was determined as the difference between $NO_3^- + NO_2^-$ and NO_2^-. Seven known concentration standard solutions (including 0) were used for the standard curve ($R^2 > 0.999$), and every-tenth sample was spiked with a known amount of analyte to ensure high accuracy and precision throughout the analysis (> 95 % recovery). Samples with

concentrations exceeding the highest standard were diluted and reanalyzed. Values were averaged over two or three replicates. Method detection limits were 0.165, 0.044, 0.558, and 0.044 µmol L^{-1} for NO_3^- + NO_2^-, NO_2^-, NH_4^+, and PO_4^{3-}, respectively. Extractive chl *a* concentration was measured following Welschmeyer (1994). Filters containing phytoplankton seston were extracted with 90% aqueous acetone overnight at -20 °C followed by measurement of the clarified extract by fluorometry (model TD-700, Turner Designs, Sunnyvale, CA).

Prior to N_2O concentration analysis, a headspace of 20 mL He at atmospheric pressure was created in each 60 mL bottle by removing 20 mL water by syringe while simultaneously adding He. Serum bottles were allowed to equilibrate under gentle shaking for at least 12 h prior to analysis. The headspace was then analyzed by GC-ECD (Shimadzu Greenhouse Gas Analyzer GC-2014, Shimadzu Scientific Instruments, Columbia, MD) for N_2O concentration. The dissolved concentration was calculated based on the headspace equilibrium concentration (Hamilton and Ostrom 2007). Diffusive atmospheric emissions of N_2O (F) were calculated by equations 19 and 20:

$$F = k_w(C_w - C_a) \quad (19)$$

where C_w is the dissolved N_2O concentration at the surface (measured at 1 m depth) and C_a is the calculated dissolved N_2O concentration in equilibrium with the atmosphere (Wanninkhof 1992; Walker et al. 2010). The gas transfer coefficient (k_w, in m s^{-1}) is calculated as:

$$k_w = 0.31U_{10}^2(Sc/600)^{-1/2} \quad (20)$$

where Sc is the Schmidt number for N_2O determined by the kinematic viscosity of freshwater divided by the diffusion coefficient of N_2O (Wanninkhof 1992) and U_{10} is the wind speed 10 m above the surface determined using the measured wind speed 1 m above the surface and the

power law relationship outlined in Walker et al. (2010). Wind speed data were collected from Erie-Ottawa International Airport (KPCW), located 2 km north of ODNR6.

The isotopic composition of N_2O was analyzed upon introduction of sample water into an enclosed 0.75 L glass vessel that was previously purged of atmospheric air using a gentle flow of He. Dissolved gases were subsequently stripped from the water by sparging the sample with He (Sansone et al. 1997), which carried sample gases into a Trace Gas sample introduction system interfaced to an IRMS. The relative abundance of a stable isotope within a particular material or reservoir is reported in standard delta notation:

$$\delta = \frac{R_{sam} - R_{std}}{R_{std}} \times 1000 \quad (21)$$

where R_{sam} is the isotope ratio of the sample, R_{std} is the isotope ratio of the standard, and δ is reported as per mil (‰). The isotopic composition of the N atom in the central position (α) and the N atom in the outer position (β) was analyzed separately. The difference between $\delta^{15}N^{\alpha}$ and $\delta^{15}N^{\beta}$ in N_2O, referred to as site preference (SP), was also calculated. SP is a conservative tracer of N_2O production mechanism and can be used to quantitatively apportion N_2O production sources, primarily through isotope mixing models that consider denitrification (SP = -10 to 0 ‰) and nitrification via hydroxylamine oxidation (SP = 33 to 37 ‰) as end members (Toyoda et al. 2005; Sutka et al. 2006; Frame and Casciotti 2010). Analytical reproducibility for replicate samples was 0.5 ‰ for bulk $\delta^{15}N$ and $\delta^{18}O$, 0.75 ‰ for $\delta^{15}N^{\alpha}$ and $\delta^{15}N^{\beta}$, and 1.3 ‰ for SP.

Concentrations of dissolved N_2 were analyzed by membrane inlet mass spectrometry (MIMS; Eyre et al. 2002). The isotopic composition of N_2 was analyzed by introducing the sample to an evacuated 800 µL sampling loop and then onto a packed molecular sieve (5 Å) column (Alltech, Inc., Deerfield, IL) using He carrier gas within a gas chromatograph (HP-5980,

Hewlett Packard, Ramsey, MN) interfaced to an Isoprime IRMS. Analytical reproducibility of standards was 0.3 ‰.

The concentration and isotopic composition of particulate organic matter (POM) from N fixation assays was analyzed by scraping the contents of dried and acidified filters into tin cups and introducing samples to an elemental analyzer interfaced to an Isoprime IRMS. Analytical reproducibility of standards was 0.2 ‰.

Modeling

Denitrification, anammox, and N_2O production rates were calculated by the IPT_{anaN2O} (Hsu and Kao 2013), which builds on the R-IPT (Risgaard-Petersen et al. 2003) by enabling quantification of N_2O production simultaneously with denitrification and anammox. N fixation rates were calculated according to Montoya et al. (1996).

Statistical modeling was carried out in R (version 3.2.4). Correlations between nutrient concentrations and discharge as well as N_2O isotopes by date were analyzed by linear regression. Potential differences in denitrification, N_2O production, and N fixation by date were analyzed by one-way ANOVA.

RESULTS

NO_3^- concentrations ranged from below detection to > 600 µmol L^{-1} across sites during the sampling period (Figure 17a). The greatest NO_3^- concentrations occurred in June and July, followed by a decline to non-detectable levels in late August that continued through October. The magnitude of these shifts was greater for the inner bay stations (ODNR4, ODNR6) than the outer bay and coastal Lake Erie stations (ODNR1, ODNR2, 1163, Bells). NO_3^- concentration

was positively correlated with Sandusky River discharge (Fig. 2f; df = 81, $R^2 = 0.18$, $p < 0.0001$). NH_4^+ concentration ranged from below detection to 17.5 µmol L^{-1} across sites during the sampling period (Figure 17b). The greatest NH_4^+ concentrations occurred in the inner bay, but these spikes occurred episodically throughout the sampling season and were not correlated with Sandusky River discharge or with NO_3^- concentration. PO_4^{3-} concentrations ranged from below detection to 4.25 µmol L^{-1} across sites during the sampling period (Figure 17c). Higher PO_4^{3-} concentrations generally occurred in the inner bay, and overall concentrations were correlated with Sandusky River discharge (df = 81, $R^2 = 0.06$, $p = 0.01$). The ratio of DIN to dissolved inorganic P (N:P; $NO_3^- + NH_4^+$ to PO_4^{3-}) was variable throughout the sampling period, exceeding 10,000 in July and falling to values below Redfield stoichiometry (16) in late August and September (Figure 17d). Chl *a* concentrations ranged from 3.5 to nearly 150 µg L^{-1} across sites during the sampling period (Figure 17e). Maximum chl *a* concentrations occurred in late August to early September, approximately one month after the peak in NO_3^- and PO_4^{3-} concentrations. Water residence time was as low as eight days when discharge from the Sandusky River was greatest in June and Early July (Figure 17f). As discharge decreased in late July and remained low for the remainder of the summer and early fall, water residence time increased to several months.

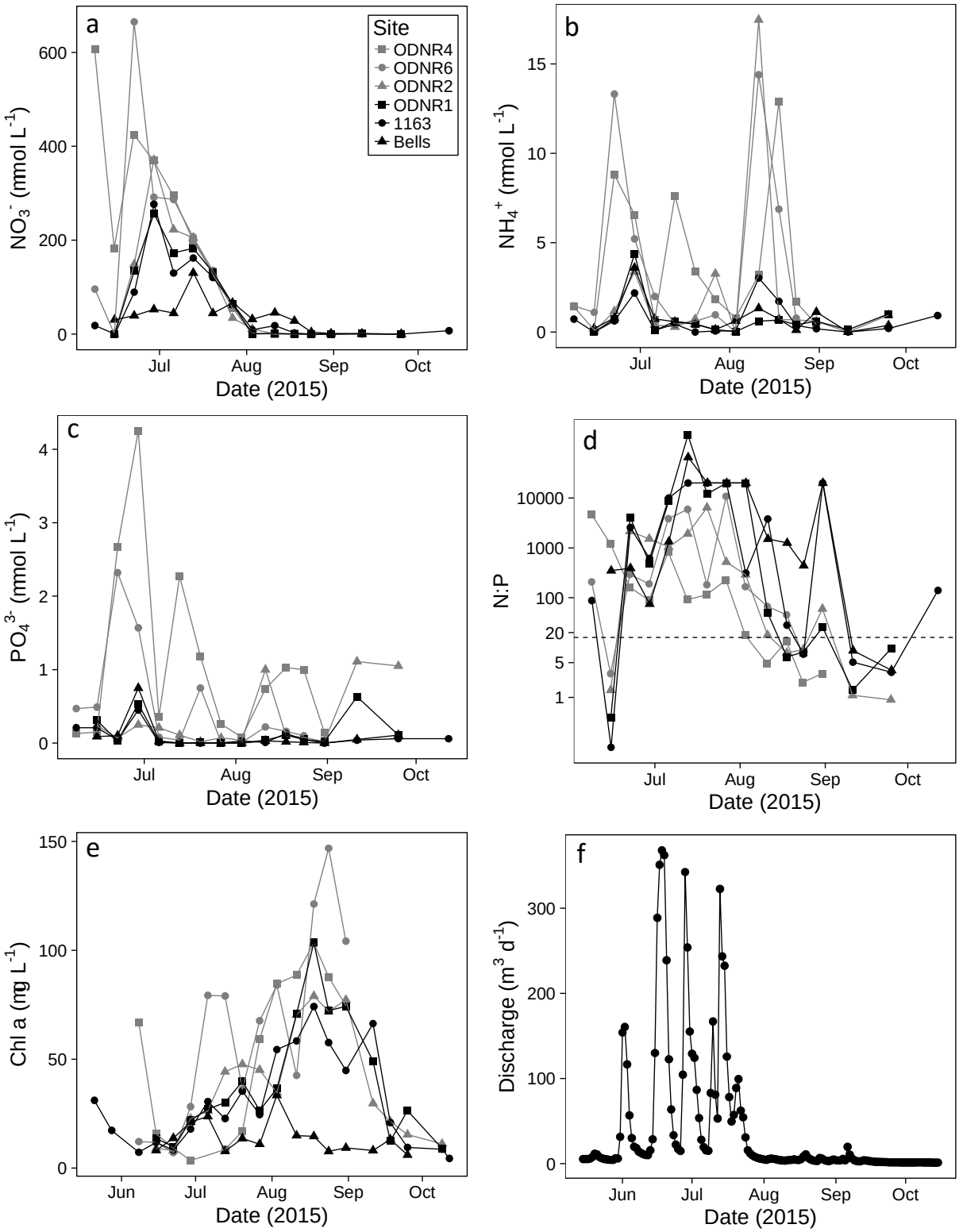

Figure 17. (a) NO_3^-, (b) NH_4^+, (c) PO_4^{3-}, (d) N:P (NO_3^- + NH_4^+ : PO_4^{3-}) ratio, and (e) chlorophyll *a* concentration in six sites in Sandusky Bay in 2015. (f) Discharge of the Sandusky River at Fremont obtained from USGS monitoring station 04198000. The dotted line in (d) indicates a N:P ratio of 16 (note log scale on y axis).

Sediment denitrification rates at station 1163 ranged from 10.02 - 64.81 μmol N m^{-2} h^{-1} over all sampled dates, decreasing over time (Figure 18a). Denitrification rates varied significantly by date (ANOVA, $F = 6.53$, $df = 24$, $p < 0.01$), and rates on June 22 were significantly higher than other dates (Tukey HSD post-hoc test). Sediment anammox activity was detected on all sampling dates but not in all replicate sediment cores. Anammox rates at station 1163 ranged from 0.52 - 8.10 μmol N m^{-2} h^{-1} across sampled dates, displaying no clear temporal trend (Figure 18b). The majority of measured anammox rates were less than 7 μmol N m^{-2} h^{-1}, with the exception of two cores on July 27 that displayed anammox rates of 15.15 and 30.75 μmol N m^{-2} h^{-1}. Owing to high variability among replicates, anammox rates did not vary significantly by date (ANOVA, $F = 2.60$, $df = 24$, $p = 0.08$). N_2O production rates at station 1163 ranged from 0.09 - 2.34 μmol N m^{-2} h^{-1} across sampled dates, decreasing over time (Figure 18c). N_2O production rates varied significantly by date (ANOVA, $F = 6.85$, $df = 24$, $p < 0.01$), and rates on June 22 were significantly higher than other dates (Tukey HSD post-hoc test). Denitrification, anammox, and N_2O production made up an average of 84 %, 14 %, and 2 % of total N removal, respectively.

N_2O was supersaturated in the surface water by more than 10 % in all sites on June 22 and July 27 and for three sites (ODNR4, 1163, Bells) on August 31 (Figure 19a). The greatest degree of N_2O supersaturation (up to 676 %) occurred on June 22, corresponding to the date with the greatest measured N_2O production rate. N_2O saturation was positively correlated with NO_3^- concentration ($df = 16$, $R^2 = 0.42$, $p < 0.01$). N_2O fluxes to the atmosphere were positive at all sites on all sampled dates except ODNR6 and ONDR2 on August 31, with highest fluxes occurring on June 22 (Figure 19b).

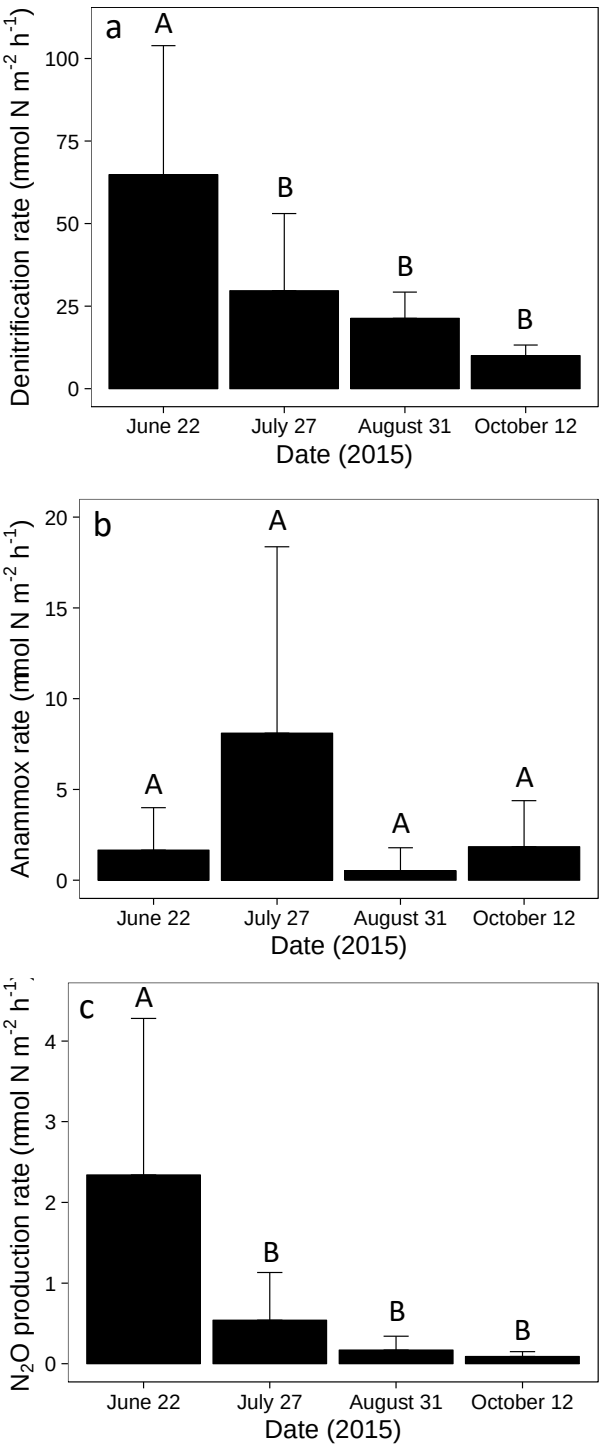

Figure 18. (a) Denitrification, (b) anammox, and (c) N_2O production at Sandusky Bay station 1163 in 2015. Rates were measured by the isotope pairing technique. Error bars represent +1 SD. Letters indicate groupings of statistically significant differences at $p < 0.05$.

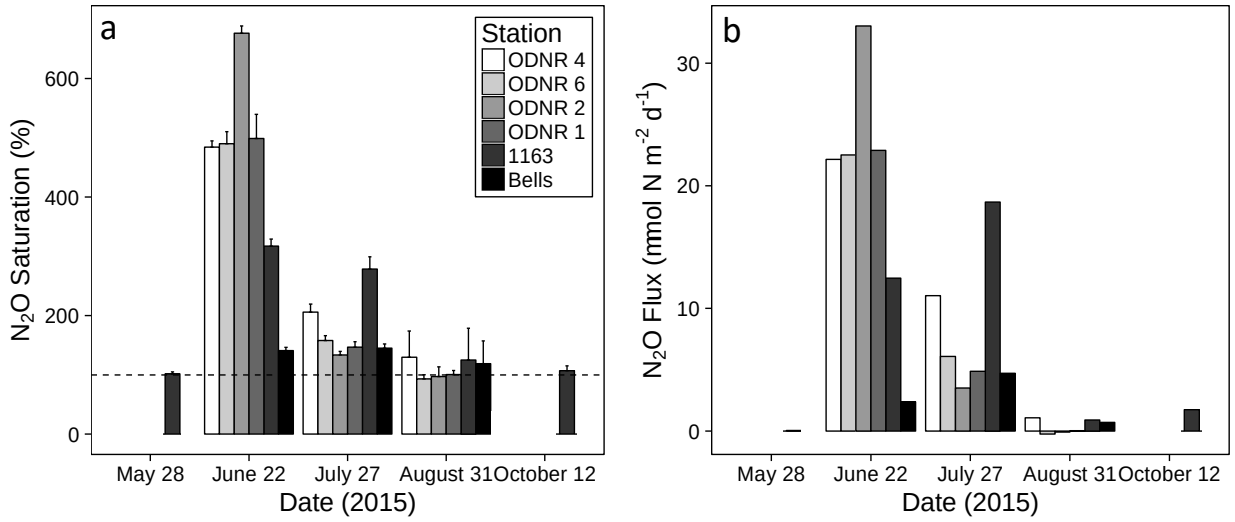

Figure 19. (a) N_2O saturation and (b) diffusive emissions of N_2O to or from the atmosphere at six stations in Sandusky Bay. A saturation of 100% is represented by the horizontal dotted line in (a). Data on May 28 and October 12 were available only for station 1163. Error bars represent +1 SD.

The $\delta^{15}N$ and $\delta^{18}O$ of N_2O did not exhibit variation as a function of date or station (Figure 20a). N_2O SP data clustered within two distinct groups: (a) four samples from ODNR4 and ODNR1 with values > 45 ‰ and (b) the majority of samples with values ranging within 7.0 to 34.3 ‰ (Figure 20b). N_2O samples in the former group were not associated with anomalous $\delta^{15}N$ or $\delta^{18}O$ values (Figure 20a) but were associated with the highest $\delta^{15}N^{\alpha}$ and lowest $\delta^{15}N^{\beta}$ values of the dataset (Figure 20c). SP values in the latter group increased throughout the sampling period (linear regression, df = 14, $R^2 = 0.20$, $p = 0.048$), but this increase was not accompanied by an increase in $\delta^{15}N$, $\delta^{18}O$, $\delta^{15}N^{\alpha}$, or $\delta^{15}N^{\beta}$ (Figure 20).

Water column N fixation rates at station 1163 ranged from 0.74 – 2.16 µmol N L^{-1} h^{-1} over all sampled dates (Figure 21). N fixation rates varied significantly by date (ANOVA, $F = 48.81$, df = 8, $p < 0.0001$), and rates on June 22 and October 12 were significantly higher than those on July 27 and August 31 (Tukey HSD post-hoc test).

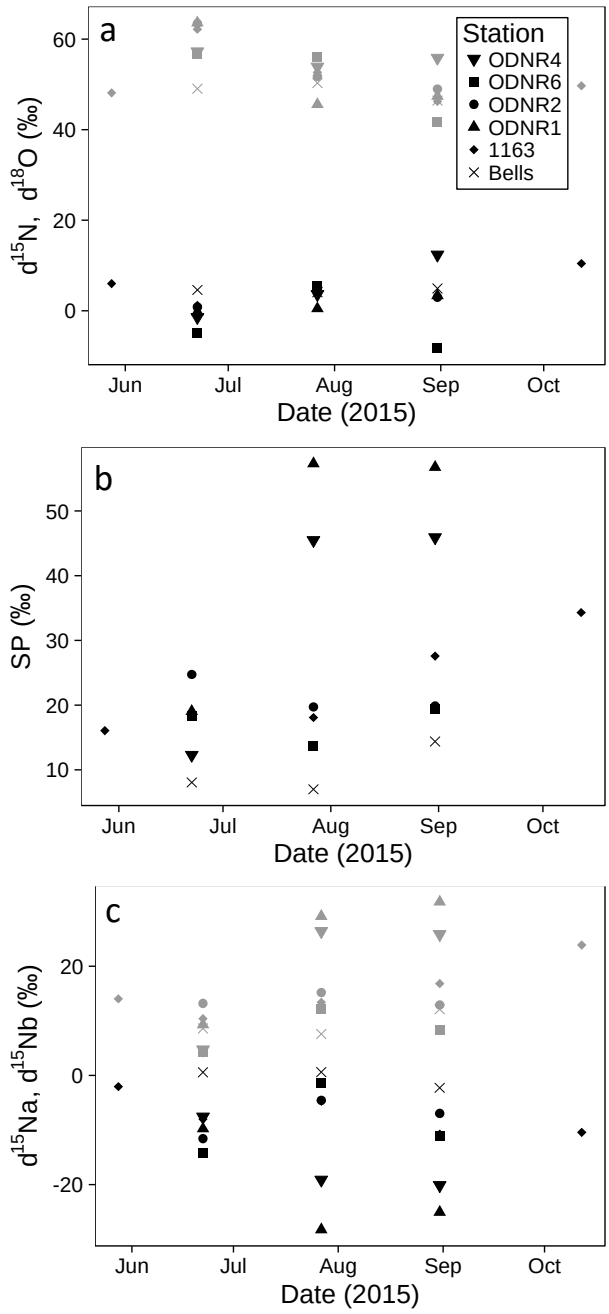

Figure 20. N_2O isotopomers in Sandusky Bay. (a) $\delta^{15}N$ and $\delta^{18}O$ in black and gray, respectively, (b) SP values, and (c) $\delta^{15}N^{\alpha}$ and $\delta^{15}N^{\beta}$ in gray and black, respectively.

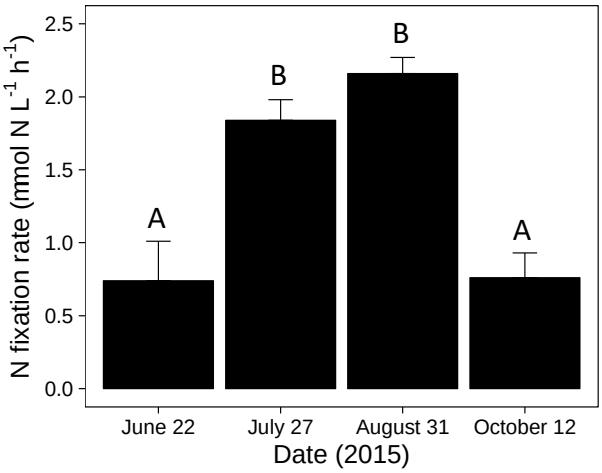

Figure 21. N fixation rates at Sandusky Bay station 1163 in 2015. Error bars represent +1 SD. Letters indicate groupings of statistically significant differences at $p < 0.05$.

DISCUSSION

Nutrient stoichiometry

Sandusky Bay displayed considerable shifts in nutrient concentrations, N:P ratios, and chl *a* concentrations, indicative of a system characterized by dynamic changes in hydrology and biogeochemical activity. Maximum chl *a* concentrations (> 100 µg L^{-1}) were similar to other hypereutrophic systems (Zhang et al. 2011; Wheeler et al. 2012; Steffen et al. 2014b), as were large swings in NO_3^- concentrations (Xu et al. 2010; McCarthy et al. 2016). As discharge from the Sandusky River decreased throughout the summer, N:P ratios fell from a maximum of over 10,000 to below 16, the threshold for N limitation. This decline was largely driven by decreases in NO_3^- concentration, as the range in PO_4^{3-} and NH_4^+ concentration was comparatively narrow (Figure 17). Depletion of NO_3^- can be attributed to both assimilatory and dissimilatory NO_3^- reduction. If phytoplankton were solely responsible for the decline in NO_3^-, nutrients would be expected to be drawn down in molar proportions of approximately 16N:1P (Redfield 1934; Sterner and Elser 2002). However, N:P ratios in Sandusky Bay fell sharply throughout the summer, while PO_4^{3-} concentrations were relatively constant by comparison. Although this trend

could be influenced by luxury uptake of N by phytoplankton and internal P loading from sediments (Filbrun et al. 2013; McCarthy et al. 2016), the dramatic depletion in DIN compels an examination of microbial N removal processes as a major mechanism for N drawdown in Sandusky Bay.

N removal processes

Denitrification and anammox were evaluated as processes likely responsible for consuming appreciable quantities of NO_3^- in Sandusky Bay. The primary N removal mechanism in Sandusky Bay was denitrification, which made up an average of 84 % of total N removal across sampling dates. Denitrification rates were positively associated with N availability, which has also been observed in estuaries, lakes, and continental shelves (Seitzinger et al. 2006). Denitrification rates measured in Sandusky Bay are among the highest rates reported for the Laurentian Great Lakes (McCarthy et al. 2007; Small et al. 2014; 2016), reinforcing the capacity for Sandusky Bay and other shallow embayments and river mouths to act as hotspots of N removal in the Great Lakes system.

Anammox activity in Sandusky Bay was highly variable, even among replicate sediment cores from the same site and date. The range of observed anammox rates (0 - 30.75 μmol N m^{-2} h^{-1}) is similar to those reported for shallow estuarine environments (Dong et al. 2009; 2011; Hsu and Kao 2013). Consequently, marked variability may be characteristic of anammox activity in freshwater environments, even across small spatial and temporal scales (Yoshinaga et al. 2011; Zhu et al. 2013; 2015). Anammox made up an average of 14 % of total N removal across the sampling period, indicating anammox activity in Sandusky Bay, with a mean depth of 1.6 - 2.6 m (Richards and Baker 1985), may be typical of shallow estuarine (Thamdrup and Dalsgaard 2002;

Dalsgaard et al. 2005) and freshwater systems (Schubert et al. 2006; McCarthy et al. 2016). A recent study using 16s RNA showed that anammox genera were active across western and central basins of Lake Erie (Small et al. 2016). Together, anammox rate and genomic data demonstrate that although denitrification is generally the dominant N removal mechanism, there is potential for anammox to be an significant N removal pathway in Sandusky Bay and other nearshore regions within the Great Lakes.

While denitrification and anammox were the primary drivers of N depletion in Sandusky Bay, water residence time was evaluated as an additional contributing factor. Estimates of water residence time when discharge was greatest in June and early July was as low as eight days. By late July, however, water residence time increased to several months and continued to increase as discharge remained low for the remainder of the summer and early fall. Although N removal rates were greatest in late June when NO_3^- concentrations were highest, the capacity for N removal to substantially deplete NO_3^- was hindered by the short residence time within the Bay. N removal rates in late June were capable of consuming approximately 2 % of ambient NO_3^- daily, so water residence times of 1 - 2 weeks would allow for the removal of only ~1/4 of NO_3^- from Sandusky Bay prior to release into Lake Erie. Export of nutrients from Sandusky Bay to Lake Erie is exemplified by increases in NO_3^- concentrations at the Lake Erie Bells station concomitant with increases in NO_3^- in the Bay (Figure 17a). The development of N limitation in mid-July through August occurred when water residence time lengthened to several months, which provided the opportunity for N removal processes to extensively consume NO_3^-. Thus, Sandusky Bay acts as a conduit for N delivery from the Sandusky River to Lake Erie under short water residence time but acts as a sink for NO_3^- under long water residence time. This pattern is

consistent with observations in other river mouths and coastal embayments of the Great Lakes (McCarthy et al. 2007; Larson et al. 2013).

N_2O production and emissions

N_2O displayed a wide range in production rate, concentration, and atmospheric flux on a seasonal basis (Figure 18c, 19). The greatest degree of N_2O saturation and highest N_2O production rate occurred when NO_3^- concentrations were highest, suggesting that nutrient delivery from the Sandusky River drives N_2O production in Sandusky Bay. The range of observed N_2O fluxes are typical of other inland lakes (Whitfield et al. 2011; Yang et al. 2015 and references therein). However, the maximum observed atmospheric emissions of N_2O from Sandusky Bay were remarkably high, considering the highest published global emissions from lacustrine environments occur in littoral zones dominated by emergent macrophytes (Wang et al. 2006) and in stratified systems that develop hypoxia or anoxia (Salk et al. 2016; Wenk et al. 2016). The influx of NO_3^- from the Sandusky River coupled with a shallow water column and high rates of N cycling drives substantial benthic N_2O production and release (Figure 17a, 18c, 19). Moreover, active N cycling in this and other shallow embayments in the Great Lakes (McCarthy et al. 2007; Small et al. 2016) suggests that emissions from these locations may make up the majority of N_2O emissions from the Great Lakes.

The isotopic composition of N_2O in Sandusky Bay provided insight into its microbial production pathways. With the exception of four samples that were characterized by remarkably high SP values (> 45 ‰), N_2O produced in Sandusky Bay appeared to be derived from a mixture of denitrification (SP = -10 to 0 ‰) and nitrification (SP = 33 to 37 ‰) pathways (Toyoda et al. 2005; Sutka et al. 2006; Frame and Casciotti 2010), with SP values ranging from 7 to 34 ‰. SP

values increased throughout the sampling period, indicating either a greater proportional contribution of nitrification to N_2O production or reduction of N_2O to N_2 by denitrification. Concomitant increases in $\delta^{15}N$ and $\delta^{18}O$ with SP are expected when N_2O reduction occurs (Westley et al. 2006; Jinuntuya-Nortman et al. 2008; Well et al. 2012; Wenk et al. 2016), but this trend was not apparent in Sandusky Bay (Figure 20). Consequently, we conclude that increasing SP is associated with an increased contribution of nitrification to N_2O production, which ranged from approximately 50 % up to 100 % of N_2O production from the beginning to the end of the sampling season. This pattern can be attributed to a decrease in overall denitrification activity throughout the sampling season combined with a small proportion of denitrification end-product released as N_2O (2 % of total N removal, on average). N_2O production in Sandusky Bay is thus governed by variation in denitrification activity, which allows production from nitrification to dominate when denitrification rates are low. Nitrification has previously been observed as the primary N_2O production mechanism in Muskegon Lake, another lake in the Great Lakes basin (Salk et al. 2016) as well as several ocean environments (Charpentier et al. 2007; Fujii et al. 2013), illustrating the importance of nitrification as a source of N_2O fluxes from aquatic systems.

The high SP values (> 45 ‰) observed in four N_2O samples could result from N_2O reduction or an unusual production signal. Because these samples were not associated with elevated $\delta^{15}N$ or $\delta^{18}O$ and reduction is associated with substantial fractionation in the isotopic ratios of SP, N, and O (Lewicka-Szczebak et al 2015 and references therein), reduction was unlikely to have appreciably influenced N_2O SP in these samples. High SP, on the other hand, was associated with high $\delta^{15}N^{\alpha}$ and low $\delta^{15}N^{\beta}$. This observation is consistent with Breider et al. (2015), who found that N_2O produced in the oxygen minimum layer in the western North Pacific was characterized by higher SP values than in the oxic layer. This increase in SP was

accompanied by a shift toward higher $\delta^{15}N^{\alpha}$ and lower $\delta^{15}N^{\beta}$ values with no overall change in $\delta^{15}N$. Similarly, a pattern of increasing SP, increasing $\delta^{15}N^{\alpha}$, and decreasing $\delta^{15}N^{\beta}$ has also been observed in purified fungal nitric oxide reductase despite observations of constant SP in fungal cultures (Sutka et al. 2008; Yang et al. 2014). These authors proposed that SP generally does not isotopically fractionate under *in situ* conditions because the internal concentration of the substrate, nitric oxide, is held constant in cells. If, however, the substrate concentration within cells is not held constant, as in enzyme cultures, SP could vary. It is possible that during periods of hydrologic and biogeochemical transition in Sandusky Bay, the capacity for denitrifiers and nitrifiers to produce N_2O changes and intracellular concentrations of hydroxylamine and/or nitric oxide fluctuate. Therefore, changes in intracellular substrate concentrations could result in the unusually high SP values observed at ODNR4 and ODNR1 in August and September.

N fixation

N fixation in the water column of Sandusky Bay was an active process not only during periods of N limitation but also when bioavailable N was replete. The greatest rates of N fixation occurred in July and August as N limitation developed in Sandusky Bay. *Planktothrix* made up the majority of phytoplankton biomass during this period, suggesting that N fixation may generate bioavailable N that is utilized by non-diazotrophs. Additionally, N fixation was detected when NO_3^- and NH_4^+ was abundant in June, an unusual observation considering high NO_3^- concentrations are expected to inhibit N fixation (Holl and Montoya 2005). Trace metal co-limitation has been proposed as a mechanism for the inhibition of NO_3^- uptake in offshore Lake Erie (North et al. 2007; Havens et al. 2012), although common metal cofactors between nitrate reductase and nitrogenase render the simultaneous suppression of NO_3^- uptake and stimulation of

N fixation unlikely (Romero et al. 2013). However, alleviation of trace metal colimitation by iron addition has been shown to influence NO_3^- uptake and N fixation differently between nearshore and offshore zones in Lake Victoria (Guildford et al. 2003), and a similar mechanism may operate in Sandusky Bay. The data in this study offer a contemporary depiction of N fixation in an area of Lake Erie exemplified by active N cycling, establishing that N fixation is active not only under N limitation but also under N-replete conditions. The occurrence of N fixation also signals a mechanism for the generation of bioavailable N that could allow *Planktothrix* to thrive under N limitation.

Harmful algal blooms

Blooms of *Planktothrix* were evident in Sandusky Bay, particularly during August and early September (Figure 17e; T. Tuttle, personal communication). Sandusky River discharge decreased in the mid-summer, leading to an increase in the water residence time in the Bay that allowed N removal and N uptake processes to deplete nutrient concentrations. Chl *a*, a proxy for total phytoplankton abundance (Becker et al. 2009, Millie et al., 2009, Davis et al. 2012), reached maximum levels approximately one month after maximum NO_3^- and PO_4^{3-} concentrations were observed (Figure 17). This pattern suggests that low flushing rates play a positive role in the production of phytoplankton biomass, perhaps by creating a stable physical environment in which phytoplankton can prosper (Michalak et al. 2013). Further, low nutrient availability during this period coupled with highest measured N fixation rates indicates that N fixation is integral to phytoplankton growth and also cHAB persistence. Analysis of nitrogenase (*nifH)* transcripts in metatranscriptomic datasets from Sandusky Bay reveals that the pelagic N-fixing population was comprised largely of N-fixing *Aphanizomenon* and *Dolichospermum* (T.

Tuttle, personal communication). However, these diazotrophs were minor components of the cyanobacterial assemblage, while *Planktothrix* was the major component of phytoplankton in the summer, even during periods of DIN scarcity (Davis et al. 2015; T. Tuttle, personal communication). The persistence of *Planktothrix* blooms in Sandusky Bay when DIN is low may be supported by uptake of small inputs of N (Chaffin and Bridgeman 2014; Donald et al. 2011; 2013; Davis et al. 2015), perhaps from sediment NH_4^+ regeneration (Paerl et al. 2011; McCarthy et al. 2106), and/or a commensal relationship with diazotrophs that are active during this period.

Conclusions

In 2015, Sandusky Bay underwent a rapid and dramatic transition from excess N abundance to N limitation by mid-summer, a pattern that has been observed in other years (Conroy et al. 2007; Davis et al. 2015). During periods of short water residence time, Sandusky Bay acted as a conduit for nutrient loading into the central basin of Lake Erie despite high N removal rates. This period was also exemplified by high N_2O emissions from the Bay, owing to the abundance of N substrates for denitrification and nitrification. As water residence time increased, N removal (mainly via denitrification) drove marked decreases in NO_3^- concentrations and the development of N limitation. N fixation was active during periods of N limitation, representing a mechanism for bioavailable N generation that could indirectly support blooms of *Planktothrix* that reached their maximum during this period. Discharge of nutrients from Sandusky Bay into Lake Erie in the early summer could stimulate the formation of blooms offshore, whereas filtering of nutrients later in the season could limit nutrient export.

Climate change-induced shifts in precipitation have the capacity to intensify the strong transitions in N cycling in Sandusky Bay. Overall precipitation in the summer is decreasing in

the Lake Erie catchment, whereas incidences of extreme precipitation are increasing (Prein et al. 2016). Thus, discharge into Sandusky Bay is expected to become more episodic in the future, with the hydrology of the Bay dominated by periods of long water residence time but punctuated by pulses of high discharge and nutrient loading. These changing hydrologic patterns have implications for N cycling and cHAB formation in Lake Erie. High N loading has the potential to drive brief yet substantial N_2O emissions from Sandusky Bay. Periods of low discharge will likely stimulate cHAB formation in Sandusky Bay, while episodic high discharge events will favor delivery of nutrients that may support cHABs in the central basin of Lake Erie and exacerbate water quality issues downstream, such as hypoxia in the St. Lawrence Estuary (Lehmann et al. 2009; Michalak et al. 2013).

LITERATURE CITED

LITERATURE CITED

Becker RH, Sultan MI, Boyer GL, Twiss MR, Konopko E (2009) Mapping cyanobacterial blooms in the Great Lakes using MODIS. J Great Lakes Res 35(3):447–453. doi:10.1016/j.jglr.2009.05.007

Bozarth CS, Schwartz AD, Shaparson JW, Colwell FS, Dreher TW (2010) Population turnover in a *Microcystis* bloom results in predominately nontoxigenic variants late in the season. Appl Environ Microbiol 76:5207-5213.

Breider F, Yoshikawa C, Abe H, Toyoda S, Yoshida N (2015) Origin and fluxes of nitrous oxide along a latitudinal transect in western North Pacific: Controls and regional significance. Global Biogeochem Cy 29:1014-1027. doi:10.1002/ 2014GB004977

Bricker SB, Longstaff B, Dennison W, Jones A, Boicourt K, Wicks C, Woerner J (2008) Effects of nutrient enrichment in the nation's estuaries: A decade of change. Harmful Algae 8:21-32. doi:10.1016/j.hal.2008.08.028

Bridgeman TB, Chaffin JD, Kane DD, Conroy JD, Panek SE, Armenio PM (2012) From river to lake: phosphorus partitioning and algal community compositional changes in western Lake Erie. J Great Lakes Res 38:90-97.

Bullerjahn GS, McKay RM, Davis TW, Baker DB, Boyer GL, D'Anglada LV, Doucette GJ, Ho JC, Irwin EG, Kling CL, Kudela RM, Kurmayer R, Michalak AM, Ortiz JD, Otten TG, Paerl HW, Qin B, Sohngen BL, Stumpf RP, Visser PM, Wilhelm SW (2016) Global solutions to regional problems: Collecting global expertise to address the problem of harmful cyanobacterial blooms. A Lake Erie case study. Harmful Algae 54:223-238. doi: 10.1016/j.hal.2016.01.003

Carmichael WW, Boyer, GL (2016) Health impacts from cyanobacteria harmful algae blooms: Implications for the North American Great Lakes. Harmful Algae 54:194-212.

Chaffin JD, Bridgeman TB, Bade DL (2013) Nitrogen constrains the growth of late summer cyanobacterial blooms in Lake Erie. Advances Microbiol 3(6A):16-26. doi:10.4236/aim.2013.36A003

Chaffin JD, Bridgeman TB (2014) Organic and inorganic nitrogen utilization by nitrogen-stressed cyanobacteria during bloom conditions. J Appl Phycol 26:299-309. doi:10.1007/s10811-013-0118-0

Charpentier J, Farias L, Yoshida N, Boontanon N, Raimbault P (2007) Nitrous oxide distribution and its origin in the central and eastern South Pacific Subtropical Gyre. Biogeosciences 4:729-741.

Conroy JD, Quinlan EL, Kane DD, Culver DA (2007) *Cylindrospermopsis* in Lake Erie: Testing its association with other cyanobacterial genera and major limnological parameters. J Great Lakes Res 33(3):519-535. doi:10.3394/0380-1330(2007)33[519:CILETI]2.0.CO;2

Dabundo R, Lehmann MF, Treibergs L, Tobias CR, Altabet MA, Molsander PH, Granger J (2014) The contamination of commercial $^{15}N_2$ gas stocks with ^{15}N-labeled nitrate and ammonium and consequences for nitrogen fixation measurements. PLoS ONE 9(10): e110335. doi:10.1371/journal.pone.0110335

Dalsgaard T, Nielsen LP, Brotas V, Viaroli P, Underwood G, Nedwell D, Sundbäck K, Rysgaard S, Miles A, Bartoli M, Dong L, Thornton DCO, Ossosen LDM, Castaldelli G, Risgaard-Petersen N (2000) Protocol handbook for NICE- Nitrogen cycling in estuaries. National Environmental Research Institute, Silkeborg, Denmark.

Dalsgaard T, Thamdrup B, Canfield, DE (2005) Anaerobic ammonium oxidation (anammox) in the marine environment. Res Microbiol 156:45-464. doi:10.1016/j.resmic.2005.01.011

Davis WP, Steinman AD (1998) A lightweight, inexpensive benthic core sampler for use in shallow water. J. Freshwater Ecology 13:475-479.

Davis TW, Harke MJ, Marcoval MA, Goleski J, Orano- Dawson C, Berry DL, Gobler CJ (2010) Effects of nitrogenous compounds and phosphorus on the growth of toxic and non-toxic strains of *Microcystis* during cyanobacterial blooms. Aquat Microb Ecol 61:149−162.

Davis TW, Koch F, Marcoval MA, Wilhelm SW, Gobler CJ (2012) Mesozooplankton and microzooplankton grazing during cyanobacterial blooms in the western basin of Lake Erie. Harmful Algae 15:26–35. doi:10.1016/j.hal.2011.11.002

Davis TW, Bullerjahn GS, Tuttle T, McKay RM, Watson SB (2015) Effects of increasing nitrogen and phosphorus concentrations on phytoplankton community growth and toxicity during *Planktothrix* blooms in Sandusky Bay, Lake Erie. Environ Sci Tech 49:7197-7207. doi:10.1021/acs.est.5b00799

Donald DB, Bogard MJ, Finlay K, Leavitt PR (2011) Comparative effects of urea, ammonium, and nitrate on phytoplankton abundance, community composition, and toxicity in hypereutrophic freshwaters. Limnol Oceanogr 56(6):2161-2175. doi:10.4319/lo.2011.56.6.2161

Donald DB, Bogard MJ, Finlay K, Bunting L, Leavitt PR (2013) Phytoplankton-specific response to enrichment of phosphorus-rich surface waters with ammonium, nitrate, and urea. PLoS ONE 8(1):E53277. doi:10.1371/journal.pone.0053277

Dong LF, Smith CJ, Papaspyrou S, Stott A, Osborn AM, Nedwell DB (2009) Changes in benthic denitrification, nitrate ammonification, and anammox process rates and nitrate reductase gene abundances along an estuarine nutrient gradient (the Colne Estuary, United Kingdom). Appl Environ Microbiol 75(10):3171-3179, doi:10.1128/AEM.02511-08

Dong LF, Sobey MN, Smith CJ, Rusmana I, Phillips W, Scott A, Osborn AM, Nedwell DB (2011) Dissimilatory reduction of nitrate to ammonium, not denitrification or anammox, dominates benthic nitrate reduction in tropical estuaries. Limnol Oceanogr 56(1):279-291. doi:10.4319/lo.2011.56.1.0279

Eyre BD, Rysgaard S, Dalsgaard T, Christensen PB (2002) Comparison of isotope pairing and N_2:Ar methods for measuring sediment denitrification: Assumptions, modifications and implications. Estuaries 25(6A):1077-1087.

Filbrun JE, Conroy JD, Culver DA (2013) Understanding seasonal phosphorus dynamics to guide effective management of shallow, hypereutrophic Grand Lake St. Marys, Ohio. Lake Reservoir Manage 29:165-178.

Frame CH, Casciotti KL (2010) Biogeochemical controls and isotopic signatures of nitrous oxide production by a marine ammonia-oxidizing bacterium. Biogeosciences 7:2695-2709. doi:10.5194/bg-7-2695-2010

Fujii A, Toyoda S, Yoshida O, Watanabe S, Sasaki K, Yoshida N (2013) Distribution of nitrous oxide dissolved in water masses in the eastern subtropical North Pacific and its origin inferred from isotopomers analysis. J Oceanogr 69:147-157. doi: 10.1007/s10872-012-0162-4

Gobler CJ, Burkholder JM, Davis TW, Harke MJ, Johengen T, Stow CA, Van de Waal DB (2016) The dual role of nitrogen supply in controlling the growth and toxicity of cyanobacterial blooms. Harmful Algae 54:87-97.

Großkopf T, Mohr W, Baustian T, Schunck H, Gill D, Kuypers MMM, Lavik G, Schmitz RA, Wallace DWR, La Roche J (2012) Doubling of marine dinitrogen-fixation rates based on direct measurements. Nature 488:361-364. doi:10.1038/nature11338

Guildford SJ, Hecky RE, Taylor WD, Mugidde R, Bootsma HA (2003) Nutrient enrichment experiments in tropical great lakes Malawi and Victoria. J Great Lakes Res 29:89-106. doi:10.1016/S0380-1330(03)70541-3

Hamilton SK, Ostrom NE (2007) Measurements of the stable isotope ratio of dissolved N_2 in ^{15}N tracer experiments. Limnol Oceanogr Methods 5:233-240.

Havens SM, Hassler CS, North RL, Guildford SJ, Silsbe G, Wilhelm SW, Twiss MR (2012) Iron plays a role in nitrate drawdown by phytoplankton in Lake Erie surface waers as observed in lake-wide assessments. Can J Fish Aquat Sci 69:369-381. doi:10.1139/F2011-157

Heisler J, Glibert P, Burkholder J, Anderson D, Cochlan W, Dennison W, Gobler C, Dortch Q, Heil C, Humphries E, Lewitus A, Magnien R, Marshall H, Sellner K, Stockwell D, Stoecker D, Suddleson M (2008) Eutrophication and harmful algal blooms: A scientific consensus. Harmful Algae 8:3–13. doi:10.1016/j.hal.2008.08.006

Ho JC, Michalak AM (2015) Challenges in tracking harmful algal blooms: A synthesis of evidence from Lake Erie. J Great Lakes Res 41(2):317-325. doi:10.1016/j.jglr.2015.01.001

Holl CM, Montoya JP (2005) Interactions between nitrate uptake and nitrogen fixation in continuous cultures of the marine diazotroph Trichodesmium (Cyanobacteria). J Phycoloby 41(6):1178-1183. doi: 10.1111/j.1529-8817.2005.00146.x

Horst GP, Sarnelle O, White JD, Hamilton SK, Kaul RB, Bressie JD (2014) Nitrogen availability increases the toxin quota of a harmful cyanobacterium, *Microcystis aeruginosa*. Water Res 54:188-198. doi: 10.1016/j.watres.2014.01.063

Howard DL, Frea JI, Pfister RM, Dugan PR (1970) Biological nitrogen fixation in Lake Erie. Science 169(3940):61-62.

Hsu T-C, Kao S-J (2013) Technical note: Simultaneous measurement of sedimentary N_2 and N_2O production and new ^{15}N isotope pairing technique. Biogeosciences 10:7847-7862. doi:10.5194/bg-10-7847-2013

Jinuntuya-Nortman M, Sutka RL, Ostrom PH, Gandhi H, Ostrom NE (2008) Isotopologue fractionation during microbial reduction of N_2O within soil mesocosms as a function of water-filled pore space. Soil Biol Biochem 40:2273-2280. doi:10.1016/j.soilbio.20 08.05.016

Kane DD, Conroy JD, Richards RP, Baker DB, Culver DA (2014) Re-eutrophication of Lake Erie: Correlations between tributary nutrient loads and phytoplankton biomass. J Great Lakes Res 40:496-501. doi:10.1016/j.jglr.2014.02.004

Kim D-K, Zhang W, Watson S, Arhonditsis GB (2014) A commentary on the modeling of the causal links among nutrient loading, harmful algal blooms, and hypoxia patterns in Lake Erie. J Great Lakes Res 40:117-129. doi:10.1016/j.jglr.2014.02.014

Knowles R (1982) Denitrification. Microbiol Rev 46(1):43-70.

Lehmann MF, Barnett B, Gélinas Y, Gilbert D, Maranger RJ, Mucci A, Sundby B, Thibodeau B (2009) Aerobic respiration and hypoxia in the Lower St. Lawrence Estuary: Stable isotope ratios of dissolved oxygen constrain oxygen sink partitioning. Limnol Oceanogr 54(6):2157-2169.

Lewicka-Szczebak D, Well R, Bol R, Gregory AS, Matthews GP, Misselbrook T, Whalley WR, Cardenas LM (2015) Isotope fractionation factors controlling isotopocule signatures of soil-emited N_2O produced by denitrification processes of various rates. Rapid Commun Mass Spectrom 29:269-282. doi:10.1002/rcm.7102

Larson JH, Trebitz AS, Steinman AD, Wiley MJ, Mazur MC, Pebbles V, Braun HA, Seelbach PW (2013) Great Lakes rivermouth ecosystems: Scientific synthesis and management implications. J Great Lakes Res 39:513-524. doi:10.1016/j.jglr.2013.06.002

MacGregor BJ, Van Mooy B, Baker BJ, Mellon M, Moisander PH, Paerl HW, Zehr J, Hollander D, Stahl DA (2001) Microbiological, molecular biological and stable isotopic evidence for nitrogen fixation in the open waters of Lake Michigan. Environ Microbiol 3(3):205-219.

McCarthy MJ, Gardner WS, Lehmann MF, Guindon A, Bird DF (2016) Benthic nitrogen regeneration, fixation, and denitrification in a temperate, eutrophic lake: Effects on the nitrogen budget and cyanobacteria blooms. Limnol Oceanogr 61(4):1406-1423. doi: 10.1002/lno.10306

McCarthy MJ, Gardner WS, Lavrentyev PJ, Moats KM, Jochem FJ, Klarer DM (2007) Effects of hydrological flow regime on sediment-water interface and water column nitrogen dynamics in a Great Lakes coastal wetland (Old Woman Creek, Lake Erie). J Great Lakes Res 33(1):219-231.

Michalak AM, Anderson EJ, Beletsky D, Bolans S, Bosch NS, Bridgeman TB, Chaffin JD, Cho K, Confesor R, Daloglu I, DePinto JV, Evans MA, Fahnenstiel GL, He L, Ho JC, Jenkins L, Johengen TH, Kuo KC, LaPorte E, Liu X, McWilliams MR, Moore MR, Posselt DJ, Richards RP, Scavia D, Steiner AL, Verhamme E, Wright DM, Zagorski MA (2013) Record-setting algal bloom in Lake Erie caused by agricultural and meterological trends consistent with expected future conditions. P Natl Acad Sci USA 110(16):6448-6452. doi:10.1073/pnas.1216006110

Millie DF, Fahnenstiel GL, Bressie JD, Pigg RJ, Rediske RR, Klarer DM, Tester PA, Litaker RW (2009) Late-summer phytoplankton in western Lake Erie (Laurentian Great Lakes): bloom distributions, toxicity, and environmental influences. Aquat Ecol 434:915–934. doi:10.1007/s10452-009-9238-7

Monchamp M-E, Pick FR, Beisner BE, Maraner R (2014) Nitrogen forms influence microcystinconcentration and composition via changes in cyanobacterial community structure. PLoS ONE 9(1):e85573. doi:10.1371/journal.pone.0085573

Montoya JP, Voss M, Kähler P, Capone DG (1996) A simple, high-precision, high-sensitivity tracer assay for N_2 fixation. Applied Environ Microbiol 62(3):986-993.

Moon JB, Carrick HJ (2007) Seasonal variation of phytoplankton nutrient limitation in Lake Erie. Aquat Microb Ecol 48:61-71.

North RL, Guildford SJ, Smith REH, Havens SM, Twiss MR (2007) Evidence for phosphorus, nitrogen, and iron colimitation of phytoplankton communities in Lake Erie. Limnol Oceanogr 52(1):315-328. doi:10.4319/lo.2007.52.1.0315

Ostrom NE, Carrick HJ, Twiss MR, Piwinski L (2005) Evaluation of primary production in Lake Erie by multiple proxies. Oecologia 144:115-124.

Paerl HW, Xu H, McCarthy MJ, Zhu G, Qin B, Li Y, Gardner WS (2011) Controlling harmful cyanobacterial blooms in a hyper-eutrophic lake (Lake Taihu, China): The need for a dual nutrient (N & P) management strategy. Water Res 45(5):1973-1983. doi:10.1016/j.watres.2010.09.018

Paerl HW, Scott JT, McCarthy MJ, Newell SE, Gardner WS, Havens KE, Hoffman DK, Wilhelm SW, Wurtsbaugh WA (2016) It takes two to tango: When and where dual nutrient (N & P) reductions are needed to protect lakes and downstream ecosystems. Environ Sci Technol 50(20):10805-10813. doi:10.1021/acs.est.6b02575

Prein AF, Rasmussen RM, Ikeda K, Liu C, Clark MP, Holland GJ (2016) The future intensification of hourly precipitation extremes. Nature Climate Change doi:10.1038/nclimate3168

Redfield A (1934) On the proportions of organic derivatives in sea water and their relation to the composition of plankton. In Daniel, R.J. (ed James Johnstone Memorial Volume). University Press of Liverpool 177–192.

Richards RP, Baker DB (1985) Assimilation and flux of sediments and pollutants in the Sandusky River Estuary, Sandusky Bay, and the adjacent nearshore zone of Lake Erie. Final Report, Grant NA80RAD00038.

Risgaard-Petersen N, Nielsen LP, Rysgaard S, Dalsgaard T, Meyer RL (2003) Application of the isotope pairing technique in sediments where anammox and denitrification coexist. Limnol Oceanogr Methods 1:63-73.

Romero IC, Klein NJ, Sañudo-Wilhelmy SA, Capone DG (2013) Potential trace metal co-limitation controls on N_2 fixation and NO_3^- uptake in lakes with varying trophic status. Frontiers Microbiol 4:54. doi:10.3389/fmicb.2013.00054

Salk KR, Ostrom PH, Biddanda BA, Weinke AD, Kendall ST, Osrom NE (2016) Ecosystem metabolism and greenhouse gas production in a mesotrophic northern temperate lake experiencing seasonal hypoxia. Biogeochemistry 131:303-319. doi:10.1007/s10533-016-0280-y

Sansone FJ, Popp BN, Rust TM (1997) Stable carbon isotopic analysis of low-level methane in water and gas. Anal Chem 69(1):40-44. doi:10.1021/ac960241i

Scavia D, Allan JD, Arend KK, Bartell S, Beletsky D, Bosch NS, Brandt SB, Briland RD, Daloglu I, DePinto JV, Dolan DM, Evans MA, Farmer TM, Goto D, Han H, Hook TO, Knight R, Ludsin SA, Mason D, Michalak AM, Richards RP, Roberts JJ, Rucinski DK, Rutherford E, Schwab DJ, Sesterhenn TM, Zhang H, Zhou Y (2014) Assessing and addressing the re-eutrophication of Lake Erie: Central basin hypoxia. J Great Lakes Res 40:226-246. doi:10.1016/j.jglr.2014.02.004

Schubert CJ, Durisch-Kaiser E, Wehrli B, Thamdrup B, Lam P, Kuypers MMM (2006) Anaerobic ammonium oxidation in a tropical freshwater system (Lake Tanganyika). Environ Microbiol 8(10):1857-1863. doi:10.1111/j.1462-2920.2006.001074.x

Seitzinger S, Harrison JA, Böhlke JK, Bouwman AF, Lowrance R, Peterson B, Tobias C, Van Drecht G (2006) Denitrification across landscapes and waterscapes: A synthesis. Ecol Appl 16(6):2064-2090.

Small GE, Cotner JB, Finlay JC, Stark RA, Sterner RW (2014) Nitrogen transformations at the sediment-water interface across redox gradients in the Laurentian Great Lakes. Hydrobiologia 731:95-108. doi:10.1007/s10750-013-1569-7

Small GE, Finlay JC, McKay RML, Rozmarynowycz MJ, Brovold S, Bullerjahn GS, Spokas K, Sterner RW (2016) Large differences in potential denitrification and sediment microbial communities across the Laurentian great lakes. Biogeochemistry 128: 353-368. doi:10.1007/s10533-016-0212-x

Steffen MM, Belisle BS, Watson SB, Boyer GL, Wilhelm SW (2014a) Status, causes and controls of cyanobacterial blooms in Lake Erie. J Great Lakes Res 40:215-225. doi:10.1016/j.jglr.2013.12.012

Steffen MM, Zhu Z, McKay RML, Wilhelm SW, Bullerjahn GS (2014b) Taxonomic assessment of a toxic cyanobacteria shift in hypereutrophic Grand Lake St. Marys (Ohio, USA). Harmful Algae 33:12-18.

Sterner RW, Elser JJ (2002) Ecological Stoichiometry: The Biology of Elements from Molecules to the Biosphere. Princeton University Press, New Jersey.

Sutka RL, Ostrom NE, Ostrom PH, Breznak JA, Gandhi H, Pitt AJ, Li F (2006) Distinguishing nitrous oxide production from nitrification and denitrification on the basis of isotopomer abundances. Appl Environ Microb 72(1):638-644. doi:10.1128/AEM.72.1.638-644.2006

Sutka RL, Adams GC, Ostrom NE, Ostrom PH (2008) Isotopologue fractionation during N_2O production by fungal denitrification. Rapid Comm Mass Spec 22:3989-3996. doi:10.1002/rcm.3820

Thamdrup B, Dalsgaard T (2002) Production of N_2 through anaerobic ammonium oxidation coupled to nitrate reduction in marine sediments. Appl Environ Microbiol 68:1312-1318. doi:10.1128/AEM.68.3.1312-1318.2002

Toyoda S, Mutobe H, Yamagishi H, Yoshida N, Tanji Y (2005) Fractionation of N_2O isotopomers during production by denitrifier. Soil Biol Biochem 37(8):1535-1545. doi:10.1016/j.soilbio.2005.01.009

Walker JT, Stow CA, Geron C (2010) Nitrous oxide emissions from the Gulf of Mexico hypoxic zone. Environ Sci Technol 44(5):1617-1623. doi:10.1021/es902058t

Wang H, Wang W, Yin C, Wang Y, Lu J (2006) Littoral zones as the "hotspots" of nitrous oxide (N_2O) emission in a hyper-eutrophic lake in China. Atmos Environ 40:5522-5527. doi:10.1016/j.atmosenv.2006.05.032

Wanninkhof R (1992) Relationship between wind speed and gas exchange over the ocean. J Geophys Res 97(C5):7373-7382. doi:10.1029/92JC00188

Well R, Eschenbach, Flessa H, von der Heide C, Weymann D (2012) Are dual isotope and isotopomers ratios of N_2O useful indicators for N_2O turnover during denitrification in nitrate-contaminated aquifers? Geochim Cosmochim Ac 90:265-282. doi:10.1016/j.gca.2012.04.045

Welschmeyer NA (1994) Fluorometric analysis of chlorophyll a in the presence of chlorophyll b and pheopigments. Limnology and Oceanography 39(8):1985-1992.

Wenk CB, Frame CH, Koba K, Casciotti KL, Veronesi M, Niemann H, Schubert CJ, Yoshida N, Toyoda S, Makabe A, Zopfi J, Lehmann MF (2016) Differential N_2O dynamics in two oxygen-deficient lake basins revealed by stable isotope and isotopomer distributions. Limnol Oceanogr 61:1735-1749. doi:10.1002/lno.10329

Westley MB, Yamagishi H, Popp BN, Yoshida N (2006) Nitrous oxide cycling in the Black Sea inferred from stable isotope and isotopomers distributions. Deep-Sea Res Pt II 53:1802-1816. doi:10.1016/j.dsr2.2006.03.012

Wheeler SM, Morrissey LA, Levine SN, Livingston GP, Vincent WF (2012) Mapping cyanobacterial blooms in Lake Champlain's Missisquoi Bay using QuickBird and MERIS satellite data. J Great Lakes Res 38:68-75.

Whitfield CJ, Aherne J, Baulch HM (2011) Controls on greenhouse gas concentrations in polymictic headwater lakes in Ireland. Sci Total Environ 410-411:217-225. doi:10.1016/j.scitotenv.2011.09.045

Wrage N, Velthof GL, van Beusichem ML, Oenema O (2001) Role of nitrifier denitrification in the production of nitrous oxide. Soil Biol Biochem 33(12-13):1723-1732.

Xu H, Paerl HW, Qin B, Zhu G, Gao G (2010) Nitrogen and phosphorus inputs control phytoplankton growth in eutrophic Lake Taihu, China. Limnol Oceanogr 55(1):420-432.

Yang H, Andersen T, Dörsch P, Tominaga K, Thrane J-E, Hessen DO (2015) Greenhouse gas metabolism in Nordic boreal lakes. Biogeochemistry 126:211-225. doi:10.1007/s10533-015-0154-8

Yang H, Gandhi H, Ostrom NE, Hegg EL (2014) Isotopic fractionation by a fungal P450 nitric oxide reductase during the production of N_2O. Environ Sci Technol 48:10707-10715. doi:10.1021/es501912d

Yoshinaga I, Amano T, Yamagishi T, Okada K, Ueda S, Sako Y, Suwa Y (2011) Distribution and diversity of anaerobic ammonium oxidation (anammox) bacteria in the sediment of a eutrophic freshwater lake, Lake Kiraura, Japan. Microbes Environ 26(3):189-197. doi:10.1264/jsme2.ME10184

Zhang Y, Lin S, Qian X, Wang Q, Qian Y, Liu J, Ge Y (2011) Temporal and spatial variability of chlorophyll *a* concentration in Lake Taihu using MODIS time-series data. Hydrobiologia 661(1):235-250. doi:10.1007/s10750-010-0528-9

Zhu G, Wang S, Wang W, Wang Y, Zhou L, Jian B, Op den Camp HJM, Risgaard-Petersen N, Schwark L, Peng Y, Hefting MM, Jetten MSM, Yin C (2013) Hotspots of anaerobic ammonium oxidation at land-freshwater interfaces. Nature Geoscience 6:103-107. doi:10.1038/NGEO1683

Zhu G, Wang S, Zhou L, Wang Y, Zhao S, Xia C, Wang W, Zhou R, Wang C, Jetten MSM, Hefting MM, Yin C, Qu J (2015) Ubiquitous anaerobic ammonium oxidation in inland waters of China: An overlooked nitrous oxide mitigation process. Nature Scientific Reports 5:17306. doi:10.1038/srep17306